

B cell Tolerance Mechanisms Following ABO-incompatible Infant Heart Transplant:
A Potential Role for CD22

by

Kimberly Marie Biffis

A thesis submitted in partial fulfillment of the requirements for the degree of

Master of Science
in
Medical Sciences - Pediatrics

University of Alberta

© Kimberly Marie Biffis, 2015

ABSTRACT

Due to presumed immune immaturity, infants are able to accept heart transplants across the ABO barrier, a procedure that would result in catastrophic consequences if performed in adults. Our group has demonstrated that following ABO-incompatible heart transplantation (ABOi HTx), infants develop specific B cell tolerance to the A/B antigens of their new graft. (1) A precise understanding of ABO-immunobiology in this setting, including elucidating mechanisms of B cell tolerance to donor A/B antigens, is essential to efforts to expand ABOi HTx beyond the immature immune period and thus reduce organ transplant waitlists, as well as to explore human neonatal tolerance to non-ABO antigens.

One of many potential mechanisms of B cell tolerance may involve the B cell surface molecule CD22. CD22 has been recognized as an inhibitory molecule of the B cell. (2-4) Interaction of CD22 with its ligand has been reported to play a role in down-regulation of B cell responses and subsequent B cell tolerance *in vivo* in animal studies. (2) In this thesis we began to investigate the role of CD22 in B cell tolerance in human infants. We examined expression levels of CD22 on human B cell subsets across the lifespan and found increased expression of CD22 on the splenic CD27⁺IgM⁺ B cell subset in infants. To further study the role of CD22 in B cell tolerance, we then developed a FACS protocol to isolate the CD27⁺IgM⁺ and CD27⁻IgM⁺ B cell subsets. Isolated B cells were then analyzed by ELISPOT to assess whether this fraction contained ABO antibody-secreting B cells (ASC), the cells presumably tolerized in the setting of infant ABOi HTx. Results indicated that the majority of the ABO ASC were derived from the CD27⁺IgM⁺ B cell subset from infant and adult samples. Lastly, we optimized a Phospho-specific flow cytometry assay using Ramos cells to measure B cell signaling upon engagement of the B cell receptor (BCR) and CD22. Future plans are to use this assay to investigate isolated primary B

cells of infants and older individuals and compare signaling profiles upon engagement of BCR and CD22. Understanding inhibitory signaling pathways in B cells from infants and those beyond infancy may allow us to manipulate the immune system and expand the timeframe in which ABOi HTx can be safely performed.

PREFACE

This thesis is an original work by Kimberly Biffis. The research project, of which this thesis is a part, received research ethics approval from the University of Alberta Health Research Ethics Board, Project Name “Cardiac Transplantation in Infancy”, Project number 00001408, November 23, 2005.

As mentioned herein, some of the research conducted for this thesis forms part of a research collaboration of the Glyconanotechnology in Transplantation CIHR Team at the University of Alberta. The Glyconanotechnology in Transplantation Team includes the labs of Drs. Lori West, Chris Cairo, Todd Lowary and Jillian Buriak.

ACKNOWLEDGMENTS

Many people have made this project possible and for this I am very grateful.

First, I would like to thank Dr. Lori West for giving me the opportunity to be a part of her team. Her mentorship, support and expertise guided me through this exciting scientific journey. Dr. West's passion for research has instilled in me a joy for learning and has motivated me to work hard to reach my goals. I'd especially like to thank her for all of the time she's invested in me and in this project. Lastly, I'd like to thank Dr. West for always making herself available, even if she happened to be halfway across the world!

I would like to thank the members of my supervisory committee, Dr. Colin Anderson, Dr. Robert Ingham and Dr. Simon Urschel, for their invaluable intellectual input, for their time in many committee meetings and in the review of my thesis and thesis defense.

I would like to thank our collaborators from the University of Alberta, Dr. Buriak, Dr. Burshtyn, Dr. Cairo and Dr. Lowary for their time, support and contributions to my project.

I would like to thank Dr. Esmé Dijke for taking me under her wing, for her guidance and the many hours and efforts she put forth into my project. Her unending support, encouragement and friendship will always be remembered. I have learned so much from her and I am so thankful that our paths have crossed.

I would like to thank all past and present members of the West laboratory for their efforts in this project. It was a pleasure to work with and learn from so many intelligent, caring and hard-working people. I would especially like to acknowledge Dr. Bruce Motyka, for his unending intellectual and technical support and for his time in reviewing my thesis, Ingrid Larsen, for her hard work in coordinating patients, data and sample collections and Carrie Andrewes, for her continuous administrative and emotional support.

I would like to thank all of my wonderful family and friends for their encouragement, love and support. For always listening, listening and... listening. It was a relief to know that there was always someone who I could call! Thank you all.

Last and certainly not least, I would like to thank my best friend and husband, Kristopher Biffis. For his love, selfless support, extreme patience, encouragement and repeated calendar reminders throughout this time. Thank you for always holding down the fort at home and allowing me to wholeheartedly pursue my studies. Kris, thank you for being my rock. I love you very much!

TABLE OF CONTENTS

CHAPTER ONE: INTRODUCTION	1
1.1 HEART TRANSPLANTATION IN INFANCY	1
1.2 ABO-INCOMPATIBLE TRANSPLANTATION	1
1.2.1 ABO Blood Group System	2
1.2.2 History of ABO-incompatible Organ Transplantation	3
1.3 ABO-INCOMPATIBLE HEART TRANSPLANTATION IN INFANCY	4
1.3.1 Neonatal Tolerance Induction	5
1.3.2 B cell Tolerance following ABOi HTx in Infants	6
1.4 B LYMPHOCYTES	7
1.4.1 B cell Development in the Bone Marrow	7
1.4.2 Human B cell Subsets in the Periphery	7
1.4.3 B cell Subsets from Infancy to Adulthood	9
1.4.4 B cell Activation and Signaling	10
1.4.5 B cell Regulation	11
1.5 CD22	12
1.5.1 Siglecs: CD22 and Siglec-G	12
1.5.2 CD22 Ligands	13
1.5.3 CD22 and B cell Inhibition	14
1.5.4 CD22, B cell Tolerance and Autoimmunity	15
1.6 RATIONALE OF THESIS	16
1.7 HYPOTHESIS OF THESIS	16
1.8 RESEARCH AIMS OF THESIS	17
1.9 TABLES & FIGURES	18
CHAPTER TWO: MATERIALS AND METHODS	21
2.1 CELL SOURCES	21
2.1.1 Human Samples	21
2.1.2 Ramos Cells	21
2.2 PREPARATION OF CELLS	22
2.2.1 Isolation and Cryopreservation of Cells	22
2.2.1.1 PBMCs	22
2.2.1.2 Splenocytes	22
2.2.2 Thawing of PBMCs and Splenocytes	22
2.2.3 Cryopreservation and Culture of Ramos Cells	23

2.3 SURFACE STAINING	23
2.3.1 Surface Staining Protocol	23
2.3.2 Identification of Various B cell Subsets	24
2.3.2.1 Quantification of CD22 Expression on the B cell Surface	24
2.3.3 Ramos Cell Phenotyping	25
2.4 PROTOCOL OPTIMIZATION: B CELL ISOLATIONS FROM TOTAL SPLENOCYTES	25
2.4.1 Protocols to isolate CD19 ⁺ B cells	25
2.4.1.1 Isolation Method 1: Magnetic Separation of CD19 ⁺ B cells	25
2.4.1.2 Isolation Method 2: Automated Magnetic Separation of CD19 ⁺ B cells	26
2.4.2 Protocols to Isolate Memory B cell Subsets	26
2.4.2.1 Isolation Method 1: Based on Positive Selection of IgM	26
2.4.2.2 Isolation Method 2: Based on Positive Selection of CD27	27
2.4.2.3 Isolation Method 3: Based on Positive Selection of CD27-PE	27
2.4.2.4 Isolation Method 4: Based on Depletion of IgA/IgG Expressing B cells and Positive Selection of CD27	27
2.4.2.5 Isolation Method 5: Based on Positive Selection of CD27 and IgM	28
2.4.3 Evaluation of B cell Isolations	28
2.5 ANALYSIS OF B CELL PROLIFERATION AND CD22, CD27 AND IGM SURFACE EXPRESSION	28
2.5.1 Labeling with Cell Proliferation Dye	28
2.5.1.1 Proliferation Assay: Isolated CD27 ⁺ IgM ⁺ and CD27 ⁻ IgM ⁺ B cells	29
2.5.1.2 Analysis of proliferation and surface expression of CD22, CD27 and IgM	29
2.6 ENZYME-LINKED IMMUNOSPOT ASSAYS: DETECTION OF A/B ANTIGEN-SPECIFIC B CELLS	29
2.6.1 Cell Isolation	29
2.6.2 Cell Culture	29
2.6.3 Preparation of ELISPOT Plates	30
2.6.4 Cell Culture in ELISPOT Plates	30
2.6.5 Detection of Secreted Antibody	31
2.6.6 Image Acquisition and Analysis of Spots	31
2.7 PROTOCOL OPTIMIZATION: PHOSPHO-SPECIFIC FLOW CYTOMETRY	31
2.7.1 Stimulations & Treatments Used in Phospho-specific Flow Cytometry (PPF) Assay	31
2.7.2 PPF Assay	32
2.7.3 Quantification of Intracellular Signals PLC γ 2 (pY759) and CD22 (pY822) After PPF Assay	33
2.8 NEURAMINIDASE TREATMENT OF CELLS	33

2.8.1 Neuraminidase (from <i>Arthrobacter ureafaciens</i>) Treatment of Ramos Cells	33
2.8.2 Analysis of Neuraminidase Treatment	34
2.9 SYNTHESIZING ANTI-IGM COATED MICROSPHERES	34
2.9.1 Attaching Anti-IgM to Streptavidin Microspheres	34
2.9.2 Detection of Anti-IgM on Microspheres	35
2.10 STATISTICAL ANALYSES	35
2.10.1 CD22 Expression on B cell Subsets of PBMCs	35
2.10.2 CD22 Expression on B cell Subsets of splenocytes	35
2.10.3 CD22 Expression and age correlation on B cell Subsets of splenocytes and PBMCs	36
2.10.4 Differences in CD22 Expression of CD27 ⁺ IgM ⁺ B cell Subsets	36
2.11 TABLES & FIGURES	37
CHAPTER THREE: RESULTS - ANALYSIS OF PRIMARY B CELLS: CD22 EXPRESSION, B CELL ISOLATIONS AND ELISPOT ANALYSIS	44
3.1 INTRODUCTION	44
3.2 FREQUENCIES OF VARIOUS B CELL SUBSETS FROM INFANCY TO ELDERLY	44
3.3 CD22 EXPRESSION ON B CELL SUBSETS THROUGHOUT THE LIFETIME	45
3.3.1 Differential expression of CD22 on spleen and peripheral blood B cell subsets	45
3.3.2 Levels of CD22 expression correlate with age in the CD27 ⁺ IgM ⁺ B cells	46
3.4 PROTOCOL OPTIMIZATION: B CELL ISOLATION OF CD27⁺IgM⁺ B CELLS	46
3.4.1 Negative selection of CD19 ⁺ B cells was performed prior to B cell isolation	46
3.4.2 Various protocols used to isolate the CD27 ⁺ IgM ⁺ B cell population from total splenocytes	47
3.4.2.1 A commercially available IgM ⁺ memory B cell isolation kit was ineffective in isolating CD27 ⁺ IgM ⁺ B cells	47
3.4.2.2 PE conjugated anti-CD27 antibody and anti-PE antibody microbeads by MACS was a successful method for isolating CD27 ⁺ B cells	47
3.4.2.3 Enrichment of IgM ⁺ B cells followed by PE-conjugated anti-CD27 antibody and anti-PE antibody microbeads and MACS isolation did not result in an enriched CD27 ⁺ IgM ⁺ B cell population	48
3.4.2.4 Isolation by FACS resulted in high purities of CD27 ⁺ IgM ⁺ and CD27 ⁻ IgM ⁺ B cells	48
3.5 B CELL ELISPOT ASSAY	48

3.5.1 Stimulation with CpG, IL-2, IL-10 and IL-15 results in B cell proliferation and changes in surface expression of CD22 in adult CD27 ⁺ IgM ⁺ and CD27 ⁻ IgM ⁺ B cells	49
3.5.2 A/B antibody-secreting B cells are primarily derived from the CD27 ⁺ IgM ⁺ B cells of infant and adult spleen	50
3.6 SUMMARY	51
3.7 TABLES & FIGURES	52
CHAPTER FOUR: RESULTS - PHOSPHO-SPECIFIC FLOW CYTOMETRY (PPF) ASSAYS TO STUDY INFANT B CELL SIGNALING	74
4.1 INTRODUCTION	74
4.2 RESULTS: PROTOCOL OPTIMIZATION OF PPF ASSAYS	74
4.2.1 Ramos cells express CD19, CD22, CD27 and IgM cell surface markers	74
4.2.2 BCR stimulation with anti-IgM Ab initiates distinct signaling kinetics in Ramos cells	74
4.2.3 Ramos cells can be stimulated with anti-IgM Ab bound to SaV-coated microspheres	76
4.2.4 The TLR9 pathway did not affect the signaling kinetics of PLC γ 2 (pY759) and CD22 (pY822)	76
4.2.5 Approaches to study the effect of CD22 binding on downstream signaling	76
4.3 SUMMARY	78
4.4 FIGURES	79
CHAPTER FIVE: DISCUSSION	92
5.1 ANALYSIS OF PRIMARY B CELLS: CD22 EXPRESSION, B CELL ISOLATIONS AND ELISPOT ANALYSIS	92
5.2 PPF ASSAYS TO STUDY INFANT B CELL SIGNALING	95
5.3 FUTURE DIRECTIONS	96
5.4 SIGNIFICANCE	99
CHAPTER SIX: REFERENCES	100
APPENDIX A	116
APPENDIX B	118

LIST OF TABLES

Table 1-1. ABO blood group in humans	18
Table 2-1. Listing of staining antibodies used in this project	37
Table 2-2. B cell subsets based on expression of the cell surface markers CD19, IgM, CD27, IgD and CD38	38
Table 3-1. Frequency of peripheral blood B cell subsets in different age groups	52
Table 3-2. Frequency of splenic B cell subsets in different age groups	53
Table 3-3. Outline of ELISPOT experiments	54

LIST OF FIGURES

Figure 1-1. CD22-CD22L engagement.	19
Figure 1-2. Project Hypothesis.	20
Figure 2-1. Gating strategy for characterizing B cell subsets in both splenocyte and PBMC samples.	39
Figure 2-2. Optimization of B cell isolation of CD27 ⁺ IgM ⁺ B cells from total splenocytes.	40
Figure 2-3. Outline of the B cell ELISPOT assay.	41
Figure 2-4. Phosphorylated intracellular signaling proteins PLC γ 2 (pY759) and CD22 (pY822) upon anti-IgM stimulation in the PPF assay.	43
Figure 3-1. CD19 ⁺ B cells within this study expressed the surface molecule CD22.	55
Figure 3-2. CD22 expressed amongst the peripheral B cell subsets.	56
Figure 3-3. CD22 expression was highest on splenic CD27 ⁺ IgM ⁺ B cells and lowest on splenic CD27 ⁻ IgM ⁻ IgD ⁻ B cells.	57
Figure 3-4. CD22 expression of splenic CD27 ⁺ IgM ⁺ B cells, but not of peripheral blood CD27 ⁺ IgM ⁺ B cells, was correlated with age.	58
Figure 3-5. CD22 expression on infant CD27 ⁺ IgM ⁺ splenic B cells was significantly higher than on CD27 ⁺ IgM ⁺ B cells of older individuals.	59
Figure 3-6. CD19 ⁺ B cell isolation purities were similar between magnetic sort and automated MACS.	60
Figure 3-7. IgM ⁺ Memory B cell isolation using an isolation kit was ineffective at sorting the IgM ⁺ Memory B cells.	61
Figure 3-8. CD27 ⁺ Memory B cell isolation using an isolation kit was ineffective at sorting the CD27 ⁺ B cells.	62
Figure 3-9. CD27 ⁺ Memory B cell isolation, with CD27-PE antibody + anti-PE magnetic microbeads and MACS, was effective at sorting the CD27 ⁺ B cells.	63
Figure 3-10. CD27 ⁺ IgM ⁺ B cell isolation, using anti-CD27-PE, anti-PE magnetic microbeads and anti-IgA/anti-IgG antibodies and MACS, was ineffective at sorting the CD27 ⁺ IgM ⁺ B cells.	64

Figure 3-11. FACS resulted in high purities of CD27 ⁺ IgM ⁺ and CD27 ⁻ IgM ⁺ B cells.	65
Figure 3-12. CpG, IL-2, IL-10 and IL-15 stimulation resulted in proliferation of CD27 ⁺ IgM ⁺ and CD27 ⁻ IgM ⁺ B cells (adult).	66
Figure 3-13. CD22 expression decreases on proliferating B cells (adult).	67
Figure 3-14. A percentage of proliferating CD27 ⁻ B cells became CD27 ⁺ after culture with CpG, IL-2, IL-10 and IL-15.	68
Figure 3-15. ELISPOT of CD27 ⁻ IgM ⁺ and CD27 ⁺ IgM ⁺ B cells isolated from splenocytes from a blood type O individual (18 years of age) by MACS.	69
Figure 3-16. B cell ELISPOT of CD27 ⁻ IgM ⁺ and CD27 ⁺ IgM ⁺ B cells isolated from splenocytes from a blood type A individual (66 years of age) by MACS.	72
Figure 3-17. B cell ELISPOT of CD27 ⁻ IgM ⁺ and CD27 ⁺ IgM ⁺ B cells isolated from splenocytes from a blood type A individual (21 years of age) by FACS.	73
Figure 4-1. Ramos cells expressed surface markers CD19, CD22, CD27 and IgM.	79
Figure 4-2. 10µg/ml anti-IgM Ab was optimal stimulation of Ramos cells in the Phospho-specific flow (PPF) assay.	80
Figure 4-3. PLCγ2 (pY759) signaling kinetics of Ramos cells upon anti-IgM Ab stimulation.	81
Figure 4-4. CD22 (pY822) signaling kinetics of Ramos cells upon anti-IgM Ab stimulation.	82
Figure 4-5. Anti-IgM Ab (Fab') ₂ stimulation alone was optimal in inducing PLCγ2 (pY759) and CD22 (pY822) signaling kinetics in PPF assay of Ramos cells.	84
Figure 4-6. Bound biotinylated anti-IgM Ab could be detected on SaV microspheres.	85
Figure 4-7. Stimulation with anti-IgM Ab bound to SaV microspheres led to the phosphorylation of PLCγ2 (pY759).	86
Figure 4-8. PLCγ2 (pY759) and CD22 (pY822) signaling kinetics in Ramos cells not due to activation through the CpG-TLR signaling cascade.	87

Figure 4-9. Neuraminidase treatment resulted in cleaving the CD22L on the surface of Ramos cells.	88
Figure 4-10. Neuraminidase treatment did not affect PLC γ 2 (pY759) and CD22 (pY822) signaling kinetics in Ramos cells.	89
Figure 4-11. Stimulation with CD22L-BLG conjugates did not affect PLC γ 2 (pY759) and CD22 (pY822) phosphorylation in Ramos cells.	91
Figure A-1. PPF assay in primary CD27 ⁺ IgM ⁺ and CD27 ⁻ IgM ⁺ B cells.	117
Figure B-1. A proposed model for the inhibition of the B cell signal by the engagement of CD22L and anti-IgM coated microspheres.	118

GLOSSARY OF TERMS

Ab	Antibody
ABOc	ABO-compatible
ABOi	ABO-incompatible
AF	Alexa Fluor
AP-1	Activator Protein 1
APC	Antigen presenting cell
BCR	B cell receptor
BLG	Beta (β)-lactoglobulin
Blnk	B cell linker protein
BM	Bone marrow
Btk	Bruton's tyrosine kinase
CD22L	CD22 ligand
CIHR	Canadian Institutes of Health Research
CSR	Class-switch recombination
DAG	Diacyl-glycerol
dH ₂ O	Distilled water
DMSO	Dimethyl sulfoxide
DPBS	Dulbecco's Phosphate Buffered Saline
ELISPOT	Enzyme-Linked Immuno Spot
EtOH	Ethanol
FACS	Fluorescence-activated cell sorting
FBS	Fetal bovine serum
FO	Follicular B cells
FSB	FACS staining buffer
FSC	Forward scatter
GNT	Glyconanotechnology in Transplantation
HRP	Horseradish peroxidase
HTx	Heart transplant/transplantation
IFN	Interferon
IP ₃	Inositol triphosphate
ISHLT	International Society for Heart & Lung Transplantation
ITAM	Immuno receptor tyrosine activation motif
ITIM	Immuno receptor tyrosine inhibitory motif
IU	International Units
KT	Kidney transplantation
LPS	Lipopolysaccharide
MACS	Magnetic activated cell sorting
mIg	Membrane-bound immunoglobulin

MZ	Marginal zone
Neu5Ac	N-acetylneuraminic acid
Neu5Gc	M-glycolyneuraminic acid
NFAT	Nuclear Factor of Activated T cells
NFκB	Nuclear Factor kappa B
PA	Polyacrylamide
PBMCs	Peripheral blood mononuclear cells
PHTS	Pediatric Heart Transplantation Study
PIP ₂	Phosphatidylinositol 4,5-bisphosphate
PLCγ2	Phospholipase C Gamma 2
PPF	Phospho-specific flow cytometry
RBE	Recent bone marrow emigrants
r _s	Spearman's correlation
RT	Room temperature
SaV	Streptavidin
SFK	Src family kinase
SH	Somatic hypermutation
SH2	Src-homology 2
sIg	Surface immunoglobulin
SLC	Surrogate light chain
SSC	Sideward scatter
Syk	Spleen tyrosine kinase
TD	T cell-dependent
T _h	Helper T cell
TI	T cell-independent
TLR	Toll-like receptors
Tx	Transplant/transplantation
UAH	University of Alberta Hospital
UNOS	United Network for Organ Sharing
α-gal	Galα1-3Galβ1-4GlcNAc-R

CHAPTER ONE: INTRODUCTION

1.1 Heart Transplantation in Infancy

Heart transplantation (HTx) in infancy is a successful therapy for end-stage heart diseases, the most common indication for transplantation being congenital heart disease (CHD) (54%) followed by cardiomyopathies (41%). (5) CHD includes a spectrum of abnormalities in the structure of the heart or intra-thoracic great vessels, ranging from very mild to very severe. (6, 7) Cardiomyopathies are a group of diseases of the myocardium that are associated with the mechanical and/or electrical dysfunction of the heart. They are either confined to the heart or are part of generalized systemic disorders, often leading to cardiovascular death or progressive heart failure. (8)

The first successful infant heart transplant was performed in 1985 by Dr. Leonard Bailey and colleagues. (9) According to the Sixteenth Official Pediatric Heart Transplant Report issued by the International Society of Heart and Lung Transplantation (ISHLT), there have been 11,000 reported transplants in children. (5)

Infants, as defined in the study by Dipchand *et al.* (5) as < 1 year in age, have better long-term transplant outcomes when compared to individuals of any other age group, with the longest median survival at 19.7 years old. For infant recipients surviving their first year post-transplant, their median conditional survival is >21 years. (5) However, donor organ shortages leading to long transplant waitlists, and the necessity for lifelong immunosuppression therapy associated with multiple side effects, remain major limitations to transplantation.

1.2 ABO-incompatible Transplantation

One possible solution to increase the number of organs available for transplantation is the use of organs from ABO-incompatible (ABOi) donors. ABO-incompatibility is generally considered an insurmountable immunological barrier for heart transplantation due to the presence of pre-formed circulating anti-A/B antibodies, which are known to initiate graft damage, as discussed below. (10)

1.2.1 ABO Blood Group System

Karl Landsteiner discovered the A, B, and O blood groups in the early 1900's. The A/B antigens are carbohydrate structures expressed on red blood cells, platelets and tissues of embryonic mesodermal origin, including vascular endothelium. (11-14) ABO polymorphisms result from the A and B genes thought to be responsible for encoding the A- and B-specific glycosyltransferases, respectively. Specificities in the glycosyltransferases differ due to differences in amino acid base substitutions. (15) The A and B glycosyltransferases transfer terminal trisaccharides to the H chain to form A, B, or both A and B antigens. Expression of the A/B antigens defines the individuals of blood type of A, B or AB. The O gene is thought to be silent or thought to give rise to an inactive glycosyltransferase (16) incapable of modifying the H antigen and therefore individuals of blood type O express only the H antigen. (15)

Additional polymorphisms in the ABO blood group system can be found within the subgroups of the blood types. For example, subgroups A1 and A2 are based on differences in A transferase activity, resulting in qualitative and quantitative differences in the A carbohydrate antigen expression. (11)

Individuals normally produce 'natural' anti-A and/or anti-B antibodies, which is thought to be due to an immune response to non-pathogenic gut flora, to the A/B antigens in which they do not express. (17, 18) For example, blood-type A individuals express A antigens on the surfaces of their red cells and tissues and develop anti-B antibodies; blood-type B individuals express B antigens on the surfaces of their red cells and tissues and develop anti-A antibodies; blood-type O individuals do not express A or B antigens on the surfaces of their red blood cells and tissues and develop both anti-A/B antibodies. Lastly, blood type AB individuals express both A/B antigens on their red cells and tissues and do not develop any anti-A/B antibodies. (Table 1-1) During normal infancy, antibodies directed to ABO antigens are not produced until the first 5-6 months after birth, and slowly rise thereafter. (17, 19)

1.2.2 History of ABO-incompatible Organ Transplantation

ABOi transplantation involves exposure of the immune system to foreign, non-self antigens. Pre-formed A/B antibodies secreted by A/B-specific B cells of the recipient will bind to A/B antigens expressed on the donor graft endothelium, initiating a cascade of complement activation and widespread vascular thrombosis. (20-22) ABOi transplantation carries a ‘high risk’ of hyperacute graft rejection if clinical maneuvers to remove antibodies are not undertaken.

Intentional efforts to cross the ABO blood-group barrier in transplantation began in adults in both kidney and liver transplantation in the late 1980’s due to donor organ shortages. Initial reports of ABOi liver transplants showed the 1-year survival rate of recipients was 66%. The authors suggested the use of ABOi grafts was justifiable in emergencies “when no other donor was available”. (23) The first ABOi kidney transplantation was successfully performed in 1987 along with plasmapheresis and splenectomy to reduce the anti-donor A/B antibodies and minimize the risks of hyperacute rejection. (24) Since, with the availability of more effective antibody removal techniques and therapies directed at B cells and plasma cells, ABOi kidney transplantation has become well-established therapy, (25) especially in countries like Japan where deceased organ donation is rare due to cultural and religious reasons. (26, 27) With improved clinical interventions, the overall graft survival rates of ABOi kidney transplant have become equivalent to those of ABO-compatible (ABOc) transplants. (25)

Decision-making regarding risk/benefit of heart transplantation is different than kidney transplantation because loss of a heart graft due to immune or other injury typically results in patient death, whereas if the patient loses a kidney, renal dialysis may be an option. Therefore intentional ABOi heart transplantation was generally thought to be absolutely contraindicated. In a global survey conducted in 1990 at 66 centers worldwide regarding experience with ABOi HTx, of 8 patients who received ABOi heart transplants (all accidentally performed due to errors in determining or reporting the donor blood type), 5 of the hearts were hyperacutely rejected: 4 within the first 24 hours post-transplant and 1 at 13 days post-transplant. Of the 3 ABOi heart transplants that were not hyperacutely rejected, 2 patients remained alive at 12 and 26 months later and the third patient died of unrelated

causes. Given these results after accidental ABOi HTx, the reported cases of catastrophic consequences reinforced strict adherence to blood group compatibility between donor and recipient. (28)

1.3 ABO-incompatible Heart Transplantation in Infancy

In the 1990's critical shortages of donor organs and high wait-list mortalities in infants and young children, coupled with the knowledge of delayed ABO-antibody production during normal infancy, led Dr. West and colleagues to the introduction of intentional ABOi infant HTx. (29) The surgical procedure of ABOi infant HTx involved standard orthotopic HTx. The initial study by West *et al.* (29) measured serum isohemagglutinin titres before and after transplant and performed plasma exchange during cardiopulmonary bypass to eliminate circulating antibodies directed against blood-group antigens; no further procedures were used to remove antibodies. All infant recipients received intravenous methylprednisolone during the operation, and immediately after the operation. Until renal function stabilized, infants received induction therapy with rabbit polyclonal anti-thymocyte antibody. Following transplantation, the standard immunosuppression regimen consisted of cyclosporine, azathioprine and prednisone for the first 2 ABOi recipients. Due to newly available immunosuppressive drugs, subsequent ABOi recipients received tacrolimus, mycophenolate mofetil and prednisone. Graft rejection (acute cellular and humoral) was monitored by endomyocardial biopsy.

The first cohort comprising 10 infants was a success: 8 of the 10 infants survived ABOi HTx and there was no hyperacute rejection. The 2 deaths were unrelated to blood group incompatibility. The results of this study contributed to a decreased mortality rate among infants on the institutional waiting list from 58 percent to 7 percent.

Since the first successful cohort ABOi infant HTx, (29) many centers around the world have integrated ABOi infant HTx as a general protocol to improve organ availability and usage in pediatric transplantation. (30-32) A number of published reports confirm that the medium and long-term graft survival rates are similar to ABOc HTx. According to Henderson *et al.*, (32) data obtained from the Pediatric Heart Transplant Study (PHTS) indicate that over a 12 year time period (January 1996 – December 2008) there were a total

of 85 ABOi heart transplants (median age at HTx: 3.2 months) out of 502 (17%) total heart transplants (median age at HTx: 4.6 months) performed at 20 PHTS centers. The authors concluded that young children who received an ABOi transplant had equivalent 1-year survival and freedom from rejection compared to ABOc transplant. The authors suggested the re-examination of current policies of United Network for Organ Sharing (UNOS) that gives priority to ABOc over ABOi transplantation in the United States. In addition, a recent study by Urschel *et al.* (30) suggested standardizing organ allocation strategies after examining data from 58 ABOi infant heart transplants (median age at HTx: 6.8 months) performed at 6 centers across North America and Europe. The authors concluded that successful ABOi HTx could be performed safely in children of “older ages”, with higher anti-donor antibody titres than initially assumed, all while maintaining immunosuppressive regimens similar to ABOc HTx and rare reports of rejection and graft vasculopathy.

Generally speaking, following ABOi infant HTx, most infants remain deficient in antibodies directed against the graft donor blood type. The unexpected success of ABOi HTx during infancy is associated with development of immunological tolerance to the donor antigens on the graft, (1) as discussed below.

1.3.1 Neonatal Tolerance Induction

Neonatal tolerance induction occurs when foreign antigens are introduced during the naïve stages of early immune development and results in the elimination of antigen-specific immunity, a process well documented in animal models. (33-37) Owen described the natural setting of alloantigen exposure during the period of immunologic immaturity in fetal calves. (33) Later, skin grafting experiments in twin cattle demonstrated that shared placental circulation resulted in dizygotic twin calves’ ability to accept skin grafts transplanted from their non-identical twin. In contrast, twin calves with a separate placental circulation *in utero* did not accept transplanted skin grafts. (38) Based in part on this work, Burnet first proposed the idea of the susceptibility of the immature animal to tolerance induction (34) and linked it to the immunologic discrimination of self vs. non-self antigens. A decade later, Lederberg alternatively proposed that tolerance induction was due to the immaturity of the immune system. (39) He defined maturity as “the progression of a cell from sensitivity to reactivity”

and theorized that “the immature antibody-forming cell is hypersensitive to antigen-antibody combination: it will be suppressed if it encounters the homologous antigen at this time.” Lederberg further predicted that tolerance induction should be possible in adult animals through exposure of “initial” antibody-forming cells to a given antigen. Lederberg’s work was expanded by Medawar *et al.*; (40) intentional exposure of newborn mice to alloantigens demonstrated acceptance of allo-specific skin transplants in adult mice and specific abrogation of immune responses to the antigens encountered during immaturity. Decades of subsequent work have demonstrated cellular mechanisms of tolerance induction in this setting to include anergy or inactivation, deletion or suppression and receptor editing in B cells. (36, 41-46)

1.3.2 B cell Tolerance following ABOi HTx in Infants

Immunological immaturity and Medawar’s model of neonatal tolerance induction are valuable in attempting to understand B cell tolerance that ensues following ABOi infant HTx. Over time, infant recipients of ABOi HTx spontaneously develop B cell tolerance to the graft A/B antigens. (47) This can be defined as a persistent and selective deficiency in the production of antibody specific to the donor blood type following transplantation. Serum samples from infant recipients of ABOi heart transplants were serially diluted and assessed for presence of isohemagglutinins (antibody) by ELISA and agglutination assays. (1) Results from the initial cohort confirmed that most children who received an ABOi graft remained largely deficient in production of IgM antibodies specific to the donor blood group, while still producing antibodies to non-self A/B antigens not present in the donor graft. As a specific example, patients of blood type O who received heart transplants from blood type B donors generally failed to produce anti-B antibodies, however, the production of anti-A antibodies proceeded relatively normally.

In contrast to recipients of ABOi heart grafts, ABOc transplant recipients of the same age receiving similar immunosuppressive medications developed anti-A/B antibodies normally. The pattern of normal antibody production to non-self non-donor ABO antigens in ABOi graft recipients, together with normal isohemagglutinin development in ABOc recipients, indicates that the deficiency of antibodies to donor A/B antigens in ABOi

recipients cannot be attributed to immunosuppressive therapy. Instead, this suggests that specific B cell tolerance has occurred, induced by exposure to the blood group antigens of the donor during a time of immunologic immaturity. Interest in defining precise mechanisms of tolerance in this setting was initiated after this first report of acquired neonatal tolerance in humans. In particular, we were interested in B lymphocytes (B cells) and their particular involvement in mechanisms of tolerance to donor ABO antigens.

1.4 B lymphocytes

1.4.1 B cell Development in the Bone Marrow

B cells and the antibodies they produce are crucial components of the humoral immune response and exert protection as part of the adaptive immune system. (48) In humans and mice, B cells develop in the bone marrow (BM) from hematopoietic precursor cells. During embryonic life, the fetal liver supplies the BM with hematopoietic stem cells. Early B cell development is BM-dependent and involves rearrangement of the immunoglobulin gene segments. (49) V_H , D_H and J_H rearrangements of the heavy chain (H-chain) gene segments, together with the V_L - J_L rearrangements of the light chain (L-chain) segments, (50) results in an extensive repertoire of functional VDJ_H and VJ_L combinations that encode B cell receptors (BCR) capable of recognizing more than 5×10^{13} different antigens. (51) Three developmental stages are defined in the rearrangement of the H- and L-chains. First, pro-B cells rearrange the D and J segments of the H-chain. A second rearrangement joins the V gene segment to the already existing DJ segment. (51) In the pro-B stage, signal-transducing components, $Ig\alpha$ (CD79a) and $Ig\beta$ (CD79b), are expressed at the cell surface. (52, 53) After μ -H-chain recombination and further assembly with surrogate light chains (SLCs) the pre-BCR is formed. (51) Signaling through the pre-BCR causes rearrangement of V and J gene segments of the L-chain resulting in mature BCR surface expression and delineation of the immature B cell. (53)

1.4.2 Human B cell Subsets in the Periphery

Transitional or immature B cells emigrate from the BM and circulate as naïve B cells

through the secondary lymphoid tissues (lymph nodes and spleen). They form two distinct populations of 'B2' B cells including follicular (FO) B cells and marginal zone (MZ) B cells. After antigen encounter in the follicles of the secondary lymphoid tissues, FO B cells move toward the T cell areas to present antigen to helper T (T_H) cells. Following the interaction, the FO B cell either (1) becomes a short-lived extra-follicular plasmablast or (2) enters the germinal center and undergoes proliferation and differentiation into plasma cells and memory cells. (54)

Maturation of antibody affinity occurs through somatic hypermutation (SHM) of the V region and results in high-affinity antigen binding sites. (55, 56) SHM involves point mutations to diversify the V region of the BCR. (57) Heavy-chain V regions encoding the antigen binding sites are rearranged through a process called class switch recombination (CSR). CSR involves replacement of the constant μ region (C_μ) with C_γ , C_α or C_ϵ segments to produce isotypes of IgG, IgA, or IgE, respectively, resulting in increased functional diversity of the B cell. (58, 59)

Plasmablasts secrete antibodies yet continue to divide and interact with T cells. After a few days, they stop dividing and die or undergo terminal differentiation into plasma cells. Plasma cells secrete antibodies at high rates but can no longer respond to antigen or T_H cells due to their low levels of surface immunoglobulin (sIg) and lack of MHC II molecules. (60-62) Some plasma cells remain in the lymphoid organs and are short-lived while others move to the BM where they continue producing antibodies. Plasma cells play an important role in ABOi transplantation, as they are responsible for the production of antibodies directed against A/B blood-group antigens. These plasma cells are known as A/B antibody-secreting cells (ASC). There is limited knowledge about the origin and location of these cells.

Memory B cells populate the blood, lymph nodes and spleen. They persist in the absence of the original antigen that induced them. With an extensive lifetime, memory B cells respond quickly upon re-encounter of antigen and therefore play a prominent role in the maintenance of immunity for extended periods. (63) In humans, the surface marker defining memory B cells is CD27, (64) a member of the tumor necrosis factor receptor family that binds to CD27 ligand (CD70). CD27-CD70 is an important interaction in the differentiation of CD27⁺ memory B cells to plasma cells. (65)

MZ B cells function as innate-like lymphocytes that can mount rapid antibody

responses. Upon interaction with antigen presented on neutrophils, macrophages or dendritic cells, MZ B cells quickly differentiate into plasmablasts to produce vast amounts of IgM. (66) MZ B cells are found in the splenic MZ as well in other MZ-like areas such as the inner wall of the subcapsular sinus of lymph nodes and the epithelium of tonsil crypts. (66) IgM⁺IgD⁺CD27⁺ B cells present in human peripheral blood have been shown to share markers specific to MZ B cells (including CD21, CD23 and CD1c) suggesting that human MZ B cells recirculate. In contrast to rodents, the human MZ B cells have been reported to account for 10-30% of the B cell population in the blood and spleen. (67)

An additional subset of mature B cells, B-1 cells, has been described in mice, having a distinct lineage from conventional 'B-2' cells discussed above. B-1 cells are the first to appear in fetal development and are primarily found in the peritoneal and the pleural cavity fluid. B-1 cells are thought to be important in early phases of the adaptive immune response to pathogens and are thought to contribute strongly to responses against carbohydrate antigens. They secrete 'natural antibodies' which have broad specificity and bind with low-affinity to both microbial and self-antigens. (68) Whether or not human B-1 cells exist is controversial in the literature. (69) CD5⁺ B cells have been detected in human fetal tissues (70) and also in adult tissues. (71) But because CD5 is not a restricted B-1 B cell marker, evidence that this population exists remains unknown. Recent work by Griffin *et al.* (72) screened defined populations of cells obtained from human cord and peripheral blood and tested the samples for properties that resemble murine B-1 cells. They identified the CD20⁺CD27⁺CD43⁺CD70⁻ B cell subset in humans with characteristics consistent with B-1 cells in mice.

1.4.3 B cell Subsets from Infancy to Adulthood

Van Gent *et al.* (73) characterized the reference values of pediatric B cell compartments in healthy children aged 0-18 years. The authors concluded the following: the naïve B cell population, defined as constituting the CD27⁺IgM⁺IgD⁺ population, minus the CD19⁺CD27⁻IgM⁺IgD⁺CD10⁺CD38^{bright} recent bone marrow emigrants [RBE] (these were defined as progenitors to naïve B cells), constituted the largest peripheral B cell subset throughout childhood; RBE constituted the second largest B cell subset until the age of 4

years. The absolute numbers and percentages of recent bone marrow emigrants (RBE) reached peak levels in the first 0-6 months while naïve B cells reached peak levels from 6-12 months, with numbers decreasing gradually during childhood and stabilizing during puberty (numbers similar to adults). The authors concluded that this temporal difference between RBE and naïve B cells was due to an increased B cell output from BM directly after birth followed by differentiation of RBE into naïve cells 6-12 months later. Further they found that the majority of memory B cells during childhood constituted non-class-switched memory B cells CD27⁺IgM⁺IgD⁺. The percentages of CD27⁺ class-switched memory B cells (defined as CD27⁺IgM⁻IgD⁻ B cells, consisting of CD27⁺IgA⁺ and CD27⁺IgG⁺ memory B cells) slowly increased with age.

1.4.4 B cell Activation and Signaling

B cell activation is generally considered to be T cell-dependent (TD) or T cell-independent (TI), depending on the antigen. TD antigens require the help of T cells to initiate a secondary signal for B cell activation. (74) T cells recognize antigen peptides bound in the MHC class II molecules presented by the B cell or other antigen-presenting cell (APC). In contrast, TI antigens can induce antibody responses in the absence of T cell help. TI antigens can be classified into Type 1 or Type 2 (TI-1 or TI-2) antigens. TI-1 antigens contain molecules that trigger B cells to proliferate and differentiate regardless of antigen specificity, known as polyclonal activation. Examples of TI-1 antigens are bacterial DNA or lipopolysaccharide (LPS). These structures are thought to stimulate the B cell through its surface toll-like receptors (TLRs). These antigens can activate both immature and mature B cells. TI-2 antigens have highly repetitive epitopes and a minimal molecular weight of 100,000MW. (75) In an immune response to TI-2 antigens, cross-linking and clustering of the BCR is necessary for B cell stimulation. (76)

Each mature B cell displays a membrane bound molecule called the B cell receptor (BCR). The BCR is multimeric complex composed of proteins including the surface immunoglobulin (Ig) molecule and a heterodimer composed of CD79a (Ig α) and CD79b (Ig β). (77-79) The B cell becomes activated when the B cell receptor (BCR) binds its antigen; the outcome depends on the affinity of the BCR for the antigen as well as co-

activating or co-inhibitory signals. The Ig α and Ig β heterodimers have intrinsic signaling capacity, unlike the Ig portion. (80) Upon ligation and/or crosslinking of the BCR with an antigen, a signal is transduced across the plasma membrane of the B cell leading to phosphorylation of the immune-receptor tyrosine-based activation motifs (ITAMs) contained within the cytoplasmic tails of Ig α and Ig β . A signaling cascade is then initiated involving phosphorylation of phospholipase C-gamma 2 (PLC γ 2). (81) PLC γ 2 cleaves phosphatidylinositol 4,5-bisphosphate (PIP $_2$) to generate inositol triphosphate (IP $_3$) and diacyl-glycerol (DAG). (82, 83) IP $_3$ binds to the IP $_3$ receptor, located in the membrane of the endoplasmic reticulum, and results in release of stores of intracellular Ca $^{2+}$ ions. The reduction in Ca $^{2+}$ activates calcium-release-activated channels and results in an influx of extracellular calcium ions. (84, 85) The other by-product DAG binds to protein kinase C (PKC). The BCR signal further propagates to include translocation of the transcription factors Nuclear Factor of Activated T cells (NFAT), Nuclear Factor kappa B (NF κ B) and Activator Protein 1 (AP-1). The net results of these processes drive B cell proliferation and differentiation. (48)

B cells express additional co-receptors that lower the threshold of B cell activation. CD19 is a co-receptor with multiple tyrosines present in its cytoplasmic region that may be phosphorylated by SFK leading to increased activation. In addition, CD21 associates with CD19 to amplify the BCR signal via binding to the C3d component of complement. (86, 87)

1.4.5 B cell Regulation

Though it is necessary for the immune system to initiate responses against pathologic antigens for protection, it is also necessary that it avoid auto-reactivity to self ('self' tolerance). B cell regulation is essential in balancing immune responses. Central tolerance mechanisms eliminate self-reactive B cells during B cell development in the BM. (88) These mechanisms include B cell deletion and receptor editing. (89, 90) High avidity interactions with self-antigens result in an arrest of the B cell at the immature stage. (89) Reactivation of recombinant activating genes results in alteration of the auto-reactive BCR. (90) Tolerance mechanisms are also in place in the periphery that regulate immature B cells that encounter self-antigens not present in the BM. High avidity interactions with these antigens result in

rapid deletion of transitional B cells. In contrast, low avidity interactions of transitional B cells with self-antigens have been shown to result in B cell anergy. Anergy is characterized by decreased responsiveness in antibody production capabilities of the B cell. (91)

Extrinsic factors contribute to B cell regulation including interactions with cytokines, complement and T cells. (92-95) In addition, molecules on the B cell surface such as the co-inhibitory molecule CD22 are known to negatively regulate B cell signaling. (2, 3) This molecule is of particular interest to us because it has been shown to induce B cell tolerance to TI-2 antigens. (2) TI-2 antigens are thought to include ABO carbohydrate structures. (96, 97)

1.5 CD22

CD22 is a B cell surface molecule known to associate with the BCR and regulate its activity. Other proposed functions of CD22 include a role in B cell migration (98) and B cell development. (99) For the purposes of this project we will focus on CD22 and its function as an inhibitory co-receptor of the BCR and its role in B cell regulation.

1.5.1 Siglecs: CD22 and Siglec-G

CD22 is a member of the sialic acid-binding immunoglobulin-like lectin (Siglec) family. Siglecs are transmembrane surface proteins (100) expressed on most cell types in the human immune system. (101) While siglecs bind exclusively to sialylated carbohydrates, some show strict ligand requirements while others recognize a broader range of sialic acids. (102, 103)

CD22 is initially expressed in the cytoplasm of B cells in the pro-B to pre-B stage; it relocates to the cell surface as B cells mature to express IgD. (104, 105) CD22 is expressed by MZ B cells and follicular mantle B cells but only weakly expressed by germinal center B cells. (106) As activated B cells differentiate into antibody-secreting plasma cells, CD22 expression is lost. (107-109)

Siglec-G is another siglec known to associate with the BCR and negatively regulate B cell signaling in mice. (110) Siglec-G is found predominantly on the surface of B cells as well as other cell types including dendritic cells. (111, 112) In humans the homolog of Siglec-G is Siglec-10. A recent study by Pfrengle *et al.* (113) demonstrated that Siglec-G was

able to inhibit B cell activation in a manner similar to CD22. However, further studies will be necessary to determine if Siglec-10 and CD22 work collectively to inhibit human BCR signaling.

1.5.2 CD22 Ligands

The extracellular domain of CD22 contains seven immunoglobulin domains. The outermost domain binds sialic acids in an α 2,6-linkage to galactose, the preferred ligand of CD22 (CD22L). (114) In general, sialic acids attach to glycans via α 2,3, α 2,6 and α 2,8 linkages. Human CD22 binds to sialic acids containing N-acetylneuraminic acid (Neu5Ac) whereas murine CD22 binds to sialic acids containing N-glycolyneuraminic acid (Neu5Gc). (115-117) The α 2,6-linkage is found on various plasma proteins, such as soluble IgM or haptoglobin. (118, 119) They are also abundantly expressed on the surface of T-cells, (120) cytokine activated endothelial cells, (121) monocytes (122) and erythrocytes. (123) Several proteins on B cells also carry sialic acid residues, such as CD22 itself, and IgM. Though CD22 can engage its ligand on many surfaces, including different cell types, it is highly probable that not all interactions have physiological relevance. (4)

ST6Gal I sialyltransferase is the unique enzyme resulting in production of CD22L (124), found in hematopoietic cells and the liver. (4) Further evidence demonstrated that the STN6 gene, encoding the ST6Gal I sialyltransferase, was found in human fetal and adult tissues including the heart. (125)

CD22 may interact in *cis* orientation with CD22L on the same cell surface or in *trans* with ligands presented on adjacent surfaces of other cells or soluble glycoproteins (Figure 1-1). Due to a high concentration of α 2-6 sialic acids on the B cell surface, most CD22 molecules are thought to interact in *cis* with glycoprotein ligands on the same cell. (126) Unmasking of CD22 by sialidase or periodate is required if CD22 is to bind to lower-affinity probes. In contrast, binding to higher affinity multivalent probes does not require previous unmasking of CD22. (127) Certain B cell subsets, including transitional B cells and MZ B cells, have been described to have a higher proportion of unmasked CD22 in the spleen. (128) Courtney *et al.* (129) demonstrated that CD22 could engage multivalent antigens in *trans* to inhibit B cell activation. Moreover, they showed that the level of ligand substitution

on the antigen could influence the activation level of the B cell: antigens with no CD22L were strong activators of B cells, antigens with moderate CD22L were weak activators and those substituted with high levels of CD22L were most effective at inhibiting B cell activity. These results indicate that it is possible to alter the immunogenicity of an antigen or cell via manipulation of sialylation on the antigen/cell surface.

1.5.3 CD22 and B cell Inhibition

Studies using CD22-deficient mice demonstrated that CD22 functions predominantly as a co-inhibitory receptor *in vivo*. (130-133) CD22 deficiency resulted in increased Ca^{2+} mobilization and subsequent increased signaling in response to BCR stimulation. Described as a “dominant inhibitor” of conventional B cells, (4) CD22 becomes tyrosine phosphorylated less than one minute after BCR cross-linking. (134) Simultaneous presentation of the BCR antigen and CD22L results in additional CD22 molecules being recruited to the vicinity of the BCR, resulting in an even stronger inhibition of the BCR signal. (135)

The cytoplasmic domain of CD22 contains negative regulatory elements that diminish B cell signaling. (114) The inhibitory properties of CD22 can be attributed to its three immune-receptor tyrosine-based inhibitory motifs (ITIMs) and additional ITIM-like motifs found within this region. (130) Upon BCR crosslinking, tyrosine residues located within the ITIMS of CD22 are rapidly phosphorylated by the Src kinase, Lyn. (136) Lyn is thought to be responsible for this phosphorylation as Lyn-deficient mice demonstrate defective CD22 tyrosine phosphorylation. (135) SHP-1 is believed to be the central signaling molecule involved in mediating CD22 inhibition. (4) This molecule is recruited to phosphorylated CD22 ITIMs and requires at least two of three tyrosine motifs be phosphorylated to be most effective. (137) SHP-1 acts to dephosphorylate components of the BCR signaling cascade leading to a decrease in BCR signal. (127)

1.5.4 CD22, B cell Tolerance and Autoimmunity

B cells play an important role in protecting the host from pathogens through production of antibodies specific to pathogenic antigens. However, in order to prevent autoimmunity, B cells must be regulated upon encountering self-antigen.

The differential expression of CD22L between host and microbe has led to the suggestion that the inhibitory co-receptor, CD22, has a role in self vs. non-self discrimination. CD22Ls are ubiquitously expressed in higher eukaryotes (138, 139) but absent in most microbes, with the exception of those pathogenic strains that have evolved to express these ligands to evade immune responses. (139, 140)

A study by Duong *et al.* (2) examined the involvement of siglecs (CD22 and Siglec-G) in B cell tolerance to synthetic “self-like” TI-2 antigens *in vivo*. Their study design consisted of polyacrylamide (PA) as the core backbone for sialic acid and non-sialic acid TI-2 antigen conjugates. To test the hypothesis that self TI-2 antigens induce B cell tolerance via CD22 and Siglec-G, they used hapten nitrophenol (NP) and conjugated it to synthetic TI-2 antigens. (The authors reported that haptens appropriately displayed on high molecular weight PA should behave as TI-2 antigens. (75)) The conjugates included PA alone (NP-PA), NP-PA-NeuGc (NeuGc is a natural sialoside for mice) and a high affinity ligand, NP-PA-bNeuGc. They measured hapten-specific IgM and IgG3 immune responses to TI-2 antigens (NP responses) in mice after immunization and 7-day incubation period. Results included robust immune responses for NP-PA, significantly reduced responses for NP-PA-NeuGc and negligible responses for NP-PA-bNeuGc. NP-PA-bNeuGc most effectively inhibited humoral immune responses and this was attributed to its role as a high affinity ligand. Additional experiments examined whether TI-2 antigen conjugates would induce B cell tolerance *in vivo*. Results of the study demonstrated that decorating a TI-2 antigen with ligands for siglecs not only prevented its immunogenicity, but also tolerized B cells to subsequent challenges with the un-sialylated form of the antigen.

The role of CD22 in autoimmunity has been studied in gene-targeted mice. Loss of CD22 alone is not sufficient for development of spontaneous autoimmune diseases in mice. (130, 132, 133) However, when CD22-deficient mice are crossed to strains prone to autoimmunity, such as Yaa (Y-linked autoimmune accelerator) mice, CD22 deficiency can

contribute to increased autoimmunity. (141, 142) At least three alleles of the CD22 gene have been identified: CD22^a, CD22^b and CD22^c. CD22 polymorphisms exist in mouse strains that are susceptible to autoimmunity (142, 143); for example, Lupus-prone strains such as NSW express the CD22^a allele. (142, 144) Most of the polymorphisms in these alleles occur in the ligand-binding domain of CD22 and suggest that alterations in this domain may contribute to autoimmunity. Mice deficient in molecules associated with CD22 signaling, namely SHP-1 and Lyn, also show signs of autoimmunity. (145)

Sialic acid acetyltransferase (SIAE) is an additional factor linking B cell siglecs to autoimmunity. SIAE modifies sialic acids by removing an inhibitory acetyl group from the 9-OH position enabling CD22 binding. (146, 147) Mice lacking SIAE demonstrate a 9-O-acetylation of sialic acid, which limits accessibility to CD22. SIAE-deficient mice develop Lupus-like autoimmune disease with high titres of antibodies. (146)

1.6 Rationale of Thesis

Mechanisms of B cell tolerance to donor A/B antigens in ABOi infant HTx are not well understood. ABO antigens are carbohydrate antigens that are thought to initiate a TI-2 immune response under normal conditions. In mice, the B cell surface molecule CD22 has been described as having an important role in the development of B cell tolerance to TI-2 antigens. The overall goal of this thesis was to investigate a possible role for CD22 in ABO tolerance in infants following ABOi HTx.

1.7 Hypothesis of Thesis

We hypothesize that CD22 is involved in the down-regulation or inhibition of B cell responses to ABO antigens following ABOi infant heart transplantation. CD22 present on host B cells may bind to CD22L on donor heart tissue and inhibit B cell activation. This, together with ligation of the ABO-specific B cell receptor to donor A/B antigens present on graft tissue, may contribute to induction of donor-specific tolerance to donor A/B antigens and enable long-term acceptance of an ABOi graft. (Figure 1-2)

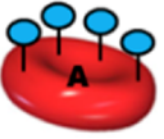
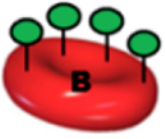
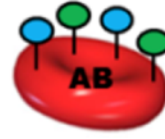






1.8 Research Aims of Thesis

The specific experiments described in this thesis represent a part of the overarching work of elucidating mechanisms of B cell tolerance to donor A/B antigens in the setting of ABOi infant heart transplantation. Specifically, these experiments were important preliminary steps towards determining whether CD22 plays a role in the inhibition of human B cell responses in donor-specific ABO tolerance. To study this we focused on:

1. Defining differences in the surface expression of CD22 in human B cells across the lifespan.
2. Isolation of CD27⁺IgM⁺ B cell subsets from infants (defined in these experiments as < 2 years in age) and older individuals for further functional studies (the CD27⁺IgM⁺ B cell subset was found to have increased expression of CD22 during infancy – Aim 1).
3. Determination of the A/B antigen-specific B cells capable of becoming antibody-secreting cells.
4. Use of the Ramos human B cell line to develop protocols to study signaling in CD27⁺IgM⁺ B cells following BCR and/or CD22 stimulation.

1.9 Tables & Figures

Table 1-1. ABO blood group in humans

	Type A	Type B	Type AB	Type O
A/B antigens (present on RBC surface, vascular endothelium)				
Plasma Antibodies Anti-A Ab  Anti-B Ab 			NONE	

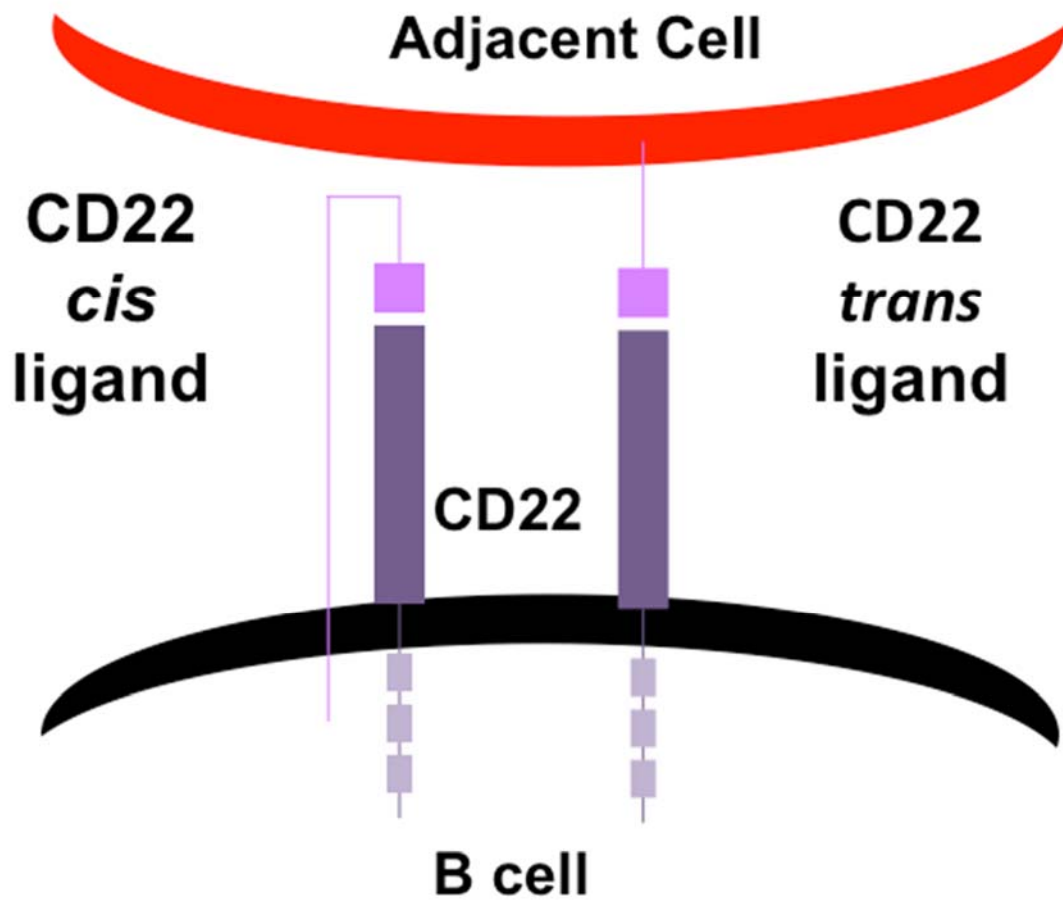


Figure 1-1. CD22-CD22L engagement. CD22 is capable of engaging its ligand (CD22L; α 2,6-linked sialic acid) in *cis* conformation, with a ligand present on the B cell surface, or in *trans* conformation, with a ligand present on an adjacent cell or plasma protein.

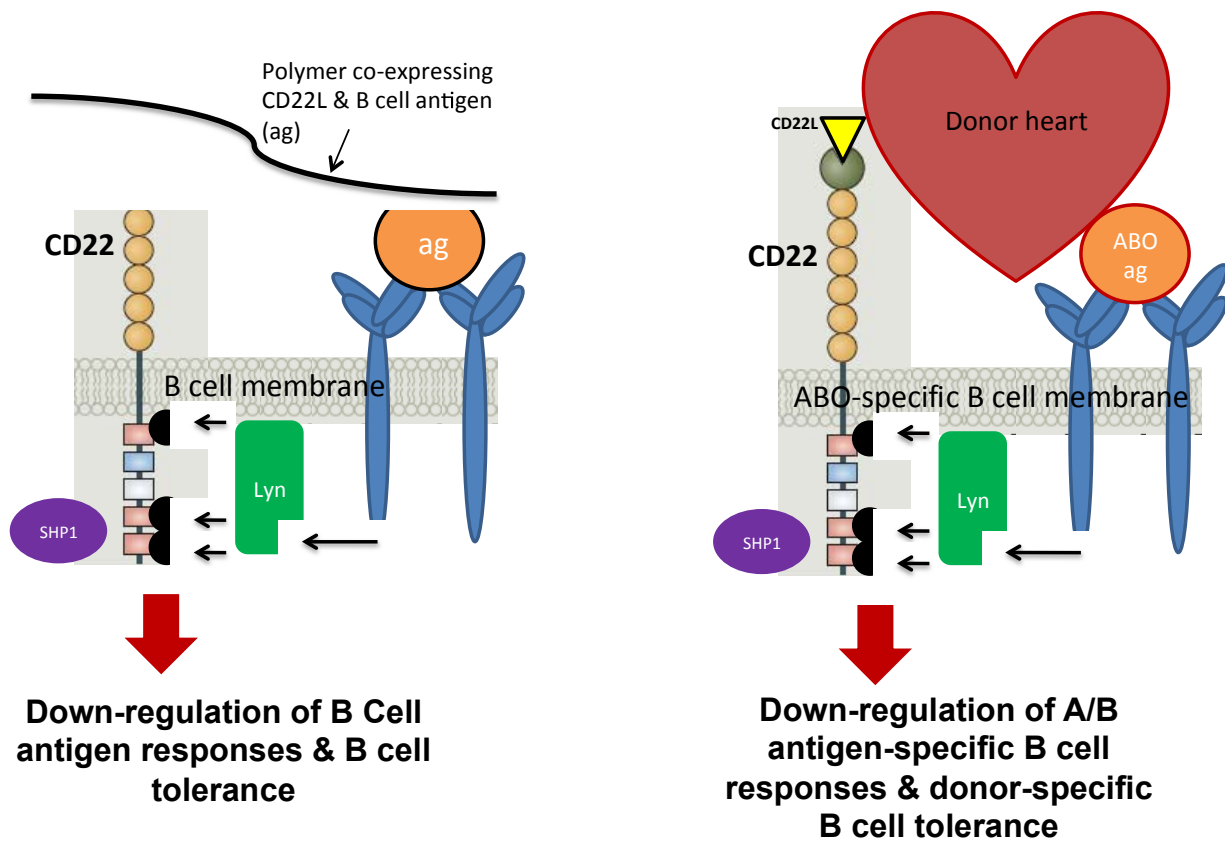


Figure 1-2. Project Hypothesis. (A) A study by Duong et al. has reported CD22 to be involved in the down-regulation of B cell antigen responses and subsequent B cell tolerance upon exposure to polymers co-expressing CD22L & the B cell antigen (ag). (B) The hypothesis of my project states that ABO antigens together with CD22L present on the vascular endothelium of the donor heart, may be involved in enabling similar responses (as seen in the study by Duong et al.) following ABOi infant HTx leading to the down regulation of A/B antigen specific B cell responses and subsequent B cell tolerance. (Image Modified from: Crocker et al. 2007, Nat Rev Immunol)

CHAPTER TWO: MATERIALS AND METHODS

2.1 Cell Sources

2.1.1 Human Samples

Peripheral blood mononuclear cells (PBMCs) were derived from whole blood of healthy adult volunteers, and pediatric cardiac patients (including cardiac surgery and aged matched controls). Patient samples were collected at the Stollery Children's Hospital in Edmonton, Alberta, as part of the ongoing Cardiac Transplantation in Infancy Study. Splenocytes were isolated from spleens of deceased organ donors. All samples were collected in accordance with the regulations of the Health Research Ethics Board at the University of Alberta together with the operational approval from Northern Alberta Clinical Trials and Research Center for Alberta Health Services. Spleen tissue was obtained from deceased organ donors through the Human Organ Procurement Program (HOPE) of Alberta Health Services, University of Alberta Hospital (UAH). No transplant patient samples were included in any of these studies. Samples were selected based on age at time of collection and included all blood types.

2.1.2 Ramos Cells

Dr. Burshtyn from the department of Medical Microbiology and Immunology at the University of Alberta generously donated the Ramos cell line. It is an EBV-negative cell line derived from American Burkitt's Lymphoma in humans. (148, 149)

2.2 Preparation of Cells

2.2.1 Isolation and Cryopreservation of Cells

2.2.1.1 PBMCs

Whole blood was collected in sterile sodium-heparin vacutainer tubes (BD Biosciences, Mississauga, ON) and stored at room temperature (RT) until processed. PBMCs were isolated from whole blood via standard ficoll (GE Health Care Life Sciences, Baie d'Urfe, Quebec) gradient centrifugation. Cells were washed in R-10 media (500 ml RPMI [Invitrogen, Burlington, ON], 5 ml (1%) penicillin/streptomycin [Invitrogen], 50 ml (10%) heat-inactivated fetal bovine serum (FBS) [Invitrogen]) and counted using the MACSQuant flow cytometer (Miltenyi Biotec Inc., San Diego, CA). Cells were stored at $5-10 \times 10^6$ cells/ml in 20% dimethyl sulfoxide (DMSO) (Sigma-Aldrich, Oakville, ON) in heat-inactivated FBS. Isolated PBMCs were transferred into cryovials (Corning - Life Sciences, Tewksbury, MA) and into the -80°C freezer overnight. PBMCs were then moved into liquid nitrogen storage for cryopreservation.

2.2.1.2 Splenocytes

Spleen tissue samples were collected from donors in the operating room at UAH and stored in saline solution at 4°C until processed. Upon retrieval, spleen tissue was disassociated using the gentleMACS tissue dissociator (Miltenyi Biotec Inc.) and red blood cell lysis was performed using Ammonium Chloride Solution (red blood cell lysis buffer) (StemCell Technologies, Vancouver, BC). Cells were washed in R-10 media and counted using the MACSQuant flow cytometer. Cells were then transferred into cryovials at 5×10^7 cells/ml in 20% DMSO in FBS and into the -80°C freezer overnight. The following day the cells were placed in liquid nitrogen to be cryopreserved and stored for future use.

2.2.2 Thawing of PBMCs and Splenocytes

For both PBMC and splenocyte samples, cells were thawed in a 37°C water bath with

gentle hand mixing. Upon thaw the samples were washed 2x with 9ml R-10 media and 1ml FBS. Samples were then washed in 10ml fluorescent activated cell sorting (FACS) Staining Buffer (FSB) (970ml 1x Phosphate Buffered Saline (PBS), 10ml of 10% Sodium Azide, 20ml heat inactivated FBS), counted using the MACSQuant flow cytometer, and resuspended as per protocol.

2.2.3 Cryopreservation and Culture of Ramos Cells

Ramos cells were stored in liquid nitrogen at $5-10 \times 10^6$ cells/ml in 20% DMSO (Sigma-Aldrich) in heat-inactivated FBS (Invitrogen). Upon use cells were thawed, washed 2x in 9ml R-10/1ml FBS, and counted on the MACSQuant flow cytometer. Cells were cultured at 5×10^5 cells/ml in R-10 media using a sterile 12-well polystyrene plate. R-10 culture media was refreshed every 2 days by removing 1ml of the media in use and replacing with 1ml fresh media. Cells were split on day 4 of culture, counted on the MACSQuant flow cytometer on day 7 and re-seeded to the concentration above. Ramos cells were given a minimum of 1 week to culture before use in experiments.

2.3 Surface Staining

2.3.1 Surface Staining Protocol

For PBMC and splenocyte samples, cells were thawed as per *section 2.2.2*. For surface staining cells were resuspended to 5×10^5 cells in 100 μ l FSB (PBMCs) or 1.0×10^6 cells in 100 μ l (splenocytes) FSB.

Ramos cells were collected from cell culture (37°C), washed 1x in R-10 media, counted using the MACSQuant flow cytometer and resuspended to 0.5×10^6 cells in 100 μ l FSB.

Cells were then incubated with relevant antibodies (Table 2-1) for 30 minutes at 4°C in the dark. The amount of antibody/isotype used was based on the manufacturer's suggestions and/or titration experiments to optimize staining. Following incubation the cells were washed 2x in FSB and immediately run on the MACSQuant flow cytometer. Unstained cells and compensation beads (Affymetrix eBioscience, San Diego, CA) were used as

fluorescence controls. Data acquired were subsequently analyzed using FlowJo software, Version 7 or Version 10 (Treestar Inc., Ashland, OR).

2.3.2 Identification of Various B cell Subsets

In order to identify the six B cell subsets of interest (Table 2-2), all samples were stained using a 6-color antibody panel as per *section 2.3.1*. Refer to Table 2-1 for a listing of antibodies used in these experiments: CD19-eFluor 450 (clone: SJ25C1; Affymetrix eBioscience) or CD19-eFluor 780 (clone: HIB19; Affymetrix eBioscience), IgM-PE (clone: G20-127; BD Pharmingen, Mississauga, ON), CD27-APC-Cy7 (clone: O323, Biolegend; San Diego, CA) or CD27-PerCP-eFluor 710 (Clone: O323; Affymetrix eBioscience), CD38-PE-Cy7 (clone: HIT2; BD Pharmingen) and IgD-APC-H7 (clone: IA6-2; BD Pharmingen). B cells were initially identified as CD19⁺ on a histogram. Further gating was performed to separate CD27⁺ B cells from the CD27⁻ B cells using a histogram. Within the CD27⁺ B cell subset we examined the expression of IgM, using a histogram, to identify non-class-switched CD27⁺IgM⁺ memory B cells and class-switched CD27⁺IgM⁻ memory B cells. (73) The CD27⁻ B cell subset was subdivided using a quadrant to distinguish the co-expression of IgM and IgD; giving rise to CD27⁻IgM⁻IgD⁻ B cells and the CD27⁻IgM⁻IgD⁺ and CD27⁻IgM⁺IgD⁺ naïve B cells. (150) The CD27⁻IgM⁺IgD⁺ naïve B cells were further analyzed to examine CD38 expression; CD27⁻IgM⁺IgD⁺CD38^{high} B cells are the recent bone marrow emigrants (151) (Figure 2-1).

2.3.2.1 Quantification of CD22 Expression on the B cell Surface

In addition to identifying the various B cell subsets, we examined CD22 expression on each subset, and thus the antibody panel was comprised of seven antibodies; six antibodies previously mentioned in *2.3.1* and also CD22-FITC (clone: S-HCL-1; BD Pharmingen). CD22 expression was identified as the MFI of the fluorochrome FITC for each of the B cell subsets in each sample. Any sample with <300 events per gate was excluded from the analysis.

2.3.3 Ramos Cell Phenotyping

Ramos cells were collected and stained as per *section 2.3.1*. To identify cell surface markers on cell surface, we stained the cells with the following antibodies: CD22-APC (clone: S-HCL-1; BD Pharmingen) or CD22-FITC (BD Pharmingen), CD19-eFluor 450 (clone: SJ25C1; Affymetrix eBioscience), CD27-PerCP-eFluor 710 (Affymetrix eBioscience) and IgM-PE (clone: G20-127; BD Pharmingen). The total cell population for Ramos cells was identified based on forward scatter (FSC) and side scatter (SSC). Histograms were used to identify the surface expression of CD19, CD22, CD27 and IgM.

2.4 Protocol Optimization: B cell Isolations from Total Splenocytes

Human splenocytes were thawed and prepared as per *section 2.2.2*. Various commercial kits described below consisted of antibody cocktails and magnetic microparticles designed for magnetic activated cell sorting (MACS) B cell separation using the autoMACS Pro Separator (Miltenyi Biotec Inc.) magnetic cell separator or the manual EasySep Magnet (StemCell Technologies). Additional protocols involved the use of fluorescent-labeled antibodies and FACS cell sorting with the Influx Flow Cytometer (Cytocopia-BD Biosciences, Mississauga, ON) or the FACS Aria III (BD Biosciences) (Figure 2-2).

2.4.1 Protocols to isolate CD19⁺ B cells

2.4.1.1 Isolation Method 1: Magnetic Separation of CD19⁺ B cells

The isolation of CD19⁺ B cells was performed using the Human B cell enrichment kit (StemCell Technologies) and EasySep Magnet (StemCell Technologies). Using this negative selection method, non-B cells are labeled with dextran-coated magnetic particles using specific antibody complexes. Non-B cells were identified and bound by antibody complexes recognizing surface antigens CD2, CD3, CD14, CD16, CD36, CD43, CD56, CD66b, and CD235a (Glycophorin A). As per the company's protocol, cells were washed in Recommended Media (2.5ml FBS + 122.5ml 1xPBS), filtered through a 40µm filter and transferred into a 5ml polystyrene tube. The non-B cells were labeled with the human B cell

enrichment cocktail with antibodies recognizing surface markers as specified above followed by labeling with EasySep D Magnetic particles. After a 5-minute incubation in the EasySep magnet, the sample tube and magnet were inverted to pour off the unlabeled B cells into a new 5ml tube. The labeled non-B cells were subsequently depleted from the sample, as they remained bound inside the original tube.

2.4.1.2 Isolation Method 2: Automated Magnetic Separation of CD19⁺ B cells

The isolation of CD19⁺ B cells was performed using the B cell isolation kit II (Miltenyi Biotec Inc.), in which human B cells are isolated by negative selection. Cells were washed in autoMACS buffer (1L 1x PBS, 0.5% bovine serum albumin (VWR International, Edmonton, AB) 2mM Ethylenediaminetetraacetic acid (EDTA) (Sigma-Aldrich). The non-B cells were labeled with a cocktail of biotin-conjugated monoclonal antibodies against CD2, CD14, CD16, CD36, CD43, and CD235a as primary labeling reagent followed by anti-biotin monoclonal antibodies conjugated to magnetic Microbeads as secondary labeling reagent. The samples were subsequently subject to magnetic separation by the autoMACS Pro Separator. This method will be referred to as MACS. The unlabeled B cells were eluted as the negatively selected cell fraction.

2.4.2 Protocols to Isolate Memory B cell Subsets

2.4.2.1 Isolation Method 1: Based on Positive Selection of IgM

The isolation of memory B cells was performed using the IgM⁺ Memory B cell isolation kit using positive selection (Miltenyi Biotec Inc.). Cells were washed in autoMACS buffer and the non-memory B cells were labeled with a cocktail of biotin-conjugated monoclonal antibodies, followed by anti-biotin magnetic microbeads (as per *section 2.4.1.2*). B cells were then washed in autoMACS buffer and labeled with anti-IgM magnetic microbeads and isolated from the pre-enriched B cell fraction. The magnetically labeled IgM⁺ memory B cells were eluted as the positively selected cell fraction after MACS.

2.4.2.2 Isolation Method 2: Based on Positive Selection of CD27

The isolation of memory B cells was performed using the Memory B cell isolation kit by positive selection (Miltenyi Biotec Inc.). Non-B cells were labeled with a cocktail of biotin-conjugated monoclonal antibodies and anti-biotin magnetic microbeads (as per *section 2.4.1.2*). B cells were then washed in autoMACS buffer and labeled with CD27 magnetic microbeads and isolated by positive selection from the pre-enriched B cell fraction. The magnetically labeled CD27⁺ memory B cells were eluted as the positively selected cell fraction after MACS.

2.4.2.3 Isolation Method 3: Based on Positive Selection of CD27-PE

The isolation of memory B cells was performed using both positive and negative selection processes. B cells were initially isolated by negative selection by MACS (as per *section 2.4.1.2*). Subsequently, the pre-enriched B cells were washed in autoMACS buffer and were labeled with CD27-PE antibody (clone: M-T271; Miltenyi Biotec Inc.) followed by labeling with anti-PE magnetic microbeads (Miltenyi Biotec Inc.). The cells were then subjected to MACS again. The magnetically labeled CD27⁺ memory B cells were eluted as the positively selected cell fraction.

2.4.2.4 Isolation Method 4: Based on Depletion of IgA/IgG Expressing B cells and Positive Selection of CD27

B cells were isolated by negative selection via MACS (as per *section 2.4.1.2*). In addition to the cocktail of biotin-conjugated monoclonal antibodies as the primary labeling reagent, we also included biotinylated anti-IgA (clone: IS11-8E10; Miltenyi Biotec Inc.) and anti-IgG (clone: IS11-3B2.2.3; Miltenyi Biotec Inc.) antibodies to simultaneously deplete IgG⁺ and IgA⁺ B cells. In the second step, the CD27⁺ B cells were positively selected as per *section 2.4.2.2 or 2.4.2.3*.

2.4.2.5 Isolation Method 5: Based on Positive Selection of CD27 and IgM

B cells were isolated by negative selection as per *section 2.4.1.1 or 2.4.1.2*. The enriched B cells were further labeled with CD27-PE or CD27-PerCP-eFluor 710 and IgM-APC antibodies (as per *section 2.3.1*) and sorted using the FACS Aria III cell sorter. This method will be referred to as FACS.

2.4.3 Evaluation of B cell Isolations

In order to evaluate the automated cell separations, the MACS and FACS methods of cell sorting, we assessed the purity of the isolated B cells by examining the expression of CD19-eFluor 450. Specific B cell populations were identified by the surface expression of IgM-PE or IgM-APC (clone: PJ2-22H3; Miltenyi Biotec Inc.) and/or CD27-PerCP-eFluor 710 or CD27-PE or CD27-APC (clone: M-T271; Miltenyi Biotec Inc.) antibodies within the CD19⁺ B cells. Cell surface staining, quantification and analysis were performed as per *section 2.3.1*.

2.5 Analysis of B cell Proliferation and CD22, CD27 and IgM Surface Expression

2.5.1 Labeling with Cell Proliferation Dye

Cell proliferation dye eFluor 450 (Affymetrix eBioscience) was reconstituted to a stock concentration of 10mM with anhydrous DMSO. Once reconstituted the dye was stored in the dark at -20°C. Cells were washed 2x in PBS and resuspended at 2x the desired final concentration in PBS. A 20uM solution of the cell proliferation dye in pre-warmed PBS was prepared and mixed in a 1:1 volume ratio with the 2x cell suspension while vortexing. The cells were incubated with the proliferation dye for 10 minutes at 37°C in the dark. At the end of the incubation, the dye was quenched with 4-5x the volume of cold complete media and the cells were put on ice for 5 minutes. Cells were washed 3x with complete media and counted on the MACSQuant flow cytometer.

2.5.1.1 Proliferation Assay: Isolated CD27⁺IgM⁺ and CD27⁻IgM⁺ B cells

Splenocytes were stained with cell proliferation dye eFluor 450 as per *section 2.5.1*. Following labeling with proliferation dye, CD27⁺IgM⁺ and CD27⁻IgM⁺ B cells were isolated from total splenocytes as per *section 2.4.2.5* (with added biotinylated anti-IgA and anti-IgG antibodies in the first step of B cell isolation the isolation). Cells were plated in a 96-well U bottom plate (BD Biosciences) at 100,000 cells/well in 200µl total volume of R-10 media plus various combinations of stimulators including affiniPure F(ab')₂ fragment goat anti-human IgM (10µg/ml; Jackson ImmunoResearch, West Grove, PA), affiniPure F(ab')₂ fragment donkey anti-goat IgG [H+L] (IgM-cross-linker; 10µg/ml; Jackson ImmunoResearch), CD40 ligand (1µg/ml; Enzo Life Sciences, Brockville, ON), CD40L enhancer (1µg/ml; Enzo Life Sciences), ODN2006 CpG (2µg/ml; Invivogen, San Diego, CA), IL-2 (40 international units (IU)/ml; R&D Systems, Minneapolis, MN), IL-10 (50ng/ml; R&D Systems) and IL-15 (10ng/ml; R&D Systems). Cells were cultured for 7 days, collected, washed 1x in FSB and stained with fluorescent antibodies as per *section 2.3.1* and quantified on the MACSQuant flow cytometer.

2.5.1.2 Analysis of proliferation and surface expression of CD22, CD27 and IgM

Data acquired were subsequently analyzed using FlowJo software. The surface expression of CD22, CD27 and IgM was evaluated together with B cell proliferation.

2.6 Enzyme-linked Immunospot Assays: Detection of A/B Antigen-Specific B cells

2.6.1 Cell Isolation

CD27⁺IgM⁺ and CD27⁻IgM⁺ B cells were isolated from total splenocytes as per *section 2.4.2.4 and 2.4.2.5*. Purity of isolated B cells was evaluated as per *section 2.4.3*.

2.6.2 Cell Culture

Isolated B cells were cultured at 37°C in 96-well flat-bottom plates (BD Falcon) at 1-5x10⁵ cells/well in AIM-V media (research grade; Invitrogen)/2.5% human AB serum

(Sigma-Aldrich) with ODN2006 CpG (4 µg/ml; Invivogen), IL-2 (40 IU/ml; R&D Systems), IL-10 (50ng/ml; R&D Systems), and IL-15 (10ng/ml; R&D Systems) according to established protocols for differentiation of B cells to antibody-secreting cells (ASC). (152, 153) On day 4 and 5 of culture the media was refreshed by removal of 80µl of supernatant/well and addition of 90µl of fresh AIM-V/2.5% AB serum with IL-2 (40 IU/ml).

2.6.3 Preparation of ELISPOT Plates

96-well ELISPOT plates (PVDF membrane, MAIPS4510; EMD Millipore, Etobicoke, ON) were prepared by pre-wetting with 70% ethanol followed by Dulbecco's PBS (DPBS, without Ca²⁺ and Mg²⁺; Gibco–Life Technologies, Burlington, ON). ELISPOT plates were coated with 50µl/well of rabbit anti-human IgM antibody (Fc_{5µ} fragment; Jackson ImmunoResearch) at 10 µg/ml (500 ng/well) in DPBS (without Ca²⁺ and Mg²⁺) or with 50 µl/well of rabbit anti-human IgG antibody (Fc_γ fragment; Jackson ImmunoResearch) at 10 µg/ml (500 ng/well) in DPBS (without Ca²⁺ and Mg²⁺) and left overnight at 4°C. Wells were washed with DPBS and blocked with commercial blocking buffer (SuperBlock Blocking Buffer – Blotting; Pierce–Thermo Scientific, Rockford, IL) for 1.5 hours at RT. Wells were washed 2x with DPBS and incubated for 1 hour at 37°C with AIM-V media (no serum). Media was then removed and fresh media with IL-2 added [80µl of AIM-V (without serum) + IL-2 (40IU/ml)].

2.6.4 Cell Culture in ELISPOT Plates

Cultured cells were harvested and transferred to v-bottom 96-well plates (Costar, Corning–Life Sciences). Cells were washed with AIM-V media (no serum) and counted on the MACSQuant flow cytometer. Cells were re-seeded at 1x10³-5x10⁴ cells/well in appropriate wells to the ELISPOT plates (100µl total volume per well) in AIM-V (without serum) + IL-2 (40IU/ml) and cultured overnight at 37°C.

2.6.5 Detection of Secreted Antibody

Following overnight culture, ELISPOT plates were washed 2x with DPBS and 6x with wash buffer (0.05% Tween-20 and 1/10 SuperBlock Blocking Buffer (Pierce–Thermo Scientific) in DPBS). Biotinylated antigen was then added to selected wells: 100ng/well of A₃PAA-biotin, B₃PAA-biotin, or α -gal-PAA-biotin (Glycotect, Gaithersburg, MD) in 50 μ l incubation buffer (1/10 SuperBlock Blocking Buffer in DPBS). Following an overnight incubation at 4°C, plates were washed 6x with wash buffer. Streptavidin-horseradish peroxidase (SaV-HRP; 5ng/well; Southern Biotech, Birmingham, AL) was added to wells previously incubated with biotinylated antigen. For detection of total IgM ASC, HRP-conjugated goat anti-human IgM antibody (μ -chain specific; 25ng/well; Southern Biotech) was added to the appropriate wells (Figure 2-3). Following 1-hour incubation at RT, plates were washed 6x with wash buffer and 2x with DPBS before incubation for 10 min at RT with AEC substrate (Sigma-Aldrich). Plates were then rinsed with distilled water (dH₂O) and dried.

2.6.6 Image Acquisition and Analysis of Spots

Plates were scanned using a CTL ImmunoSpot Analyzer using ImmunoCapture software (version 6.3) (Cellular Technology Ltd., Shaker Heights, OH). The number of spots per well (each spot representing an antibody-secreting B cell) was quantified using ImmunoSpot software (version 5.0.3) (Cellular Technology Ltd.). Data were analyzed as the number of ASC normalized to ~100,000 viable input cells/ELISPOT well. Results are expressed as the number of IgM, anti-A, anti-B or anti- α -gal ASC, as well as the total number of IgM or IgG ASC.

2.7 Protocol Optimization: Phospho-specific Flow Cytometry

2.7.1 Stimulations & Treatments Used in Phospho-specific Flow Cytometry (PPF) Assay

Cells in the PPF assay were stimulated with combinations of the following: 1 μ g/ml, 2.5 μ g/ml, 5 μ g/ml, 10 μ g/ml, 15 μ g/ml, or 20 μ g/ml of soluble affiniPure or AF488-labelled

F(ab')₂ fragment goat anti-human IgM (Fc_{5μ} fragment specific; Jackson ImmunoResearch), 10μg/ml anti-IgM cross-linker (affinipure F(ab')₂ fragment donkey-anti goat IgG; Jackson ImmunoResearch), 10μg/ml of anti-Human IgM derived from a HB57 hybridoma cell line (specific for human mu heavy chain; ATCC, Manassas, VA), or 10μg/ml anti-Human IgM derived from a HB138 hybridoma cell line (specific for Fab portion of human IgM; ATCC). In addition, biotinylated F(ab')₂ fragment goat anti-human IgM [Fc_{5μ} fragment specific; Jackson ImmunoResearch) was bound to SaV microspheres and presented to Ramos cells.

Other stimulators in the PPF assay included 2μg/ml of CpG ODN2006 (Invivogen), synthesized CD22L bound to a beta lacto globulin (BLG) carrier protein (Sigma-Aldrich) at 1μg/ml, 2.5μg/ml, 5μg/ml and 20μg/ml. The CD22L-BLG conjugates were synthesized as part of an ongoing collaboration of the Glyconanotechnology in Transplantation (GNT) Group. CD22L conjugates were synthesized by the labs of Dr. Todd Lowary (CD22L synthesis) (154) and Dr. Chris Cairo (conjugation of CD22L to BLG). Both Dr. Lowary and Dr. Cairo are researchers in the Department of Chemistry at the University of Alberta and the Alberta Glycomics Centre.

In addition to adding stimulators, Ramos cells were also incubated with 20μl (1:2 dilution) of FITC-labeled anti-human CD22 (BD Biosciences) to examine whether this antibody would affect the signaling kinetics.

2.7.2 PPF Assay

Ramos cells and FACS-sorted CD27⁺IgM⁺ and CD27⁻IgM⁺ B cells were used in the PPF assays. Ramos cells were collected from 37°C cell culture and the CD27⁺IgM⁺ and CD27⁻IgM⁺ B cells were isolated from thawed splenocyte samples on day 1 as per *section 2.4.2.5*. The isolated cells were incubated overnight at 37°C in R-10 media (1.0x10⁶ cells/ml). Cells were washed 1x in R-10 media, counted using the MACSQuant flow cytometer, resuspended to 0.5x10⁶ cells in 500μl R-10 media and placed in a 2ml eppendorf tubes (Fisher Scientific, Ottawa, ON). The cells were then placed at 37°C for 30 minutes to rest. Following, the appropriate stimulator was added (see *section 2.7.1*) to the cells at time points including: 0.5min, 1min, 2min, 4min, 6min, 8min, 10min, 12min, 15min, 16min, 20min, 32min, 45min and 60min. To stop the reaction (at time point 0 seconds) 50μl of 16%

paraformaldehyde (Electron Microscopy Sciences, Hatfield, PA) was added to each sample. All samples were vortexed and incubated for 10 minutes at RT. 1 ml of 1xPBS (pH 7.4) was then added to each sample followed by centrifugation at 830xg for 5 minutes. PBS was discarded and 1 ml cold (< minus 20°C) >99% methanol (EMD Millipore) was added to the samples to permeate the cells, which were then vortexed and placed on ice for 10 minute incubation. Following incubation, 1 ml of PBS was added to the cells in methanol. Samples were vortexed, centrifuged at 830xg for 5 minutes, and their liquid discarded. 1.5ml FSB was then added followed by vortexing and centrifuging at 830xg for 5 minutes. Finally, cells were resuspended in FSB. All samples were stained (as per *section 2.3.1*) in 100µl FSB with relevant Phospho-specific antibodies and the corresponding isotypes. All samples were incubated with flow cytometric antibodies for 30 minutes at 4°C in the dark. Following incubation the cells were washed 2x in FSB, resuspended in 100µl and immediately run on the MACSQuant flow cytometer.

2.7.3 Quantification of Intracellular Signals PLCγ2 (pY759) and CD22 (pY822) After PPF Assay

To evaluate the level of phosphorylation of PLCγ2(pY759), located downstream the B cell receptor, and CD22(pY822), located on the intracellular tail of CD22, Phospho-specific fluorescent antibodies were used: anti-PLCγ2(pY759)-Alexa Fluor (AF)488 or AF647 (clone: K86-689.37; BD Biosciences) and anti-CD22(pY822)-PE (clone:12a/CD22; BD Biosciences) (Figure 2-4). Data acquired were subsequently analyzed using FlowJo software.

2.8 Neuraminidase Treatment of Cells

2.8.1 Neuraminidase (from *Arthrobacter ureafaciens*) Treatment of Ramos Cells

Ramos cells were collected from 37°C cell culture, washed 1x in serum-free RPMI media (Invitrogen) and counted on the MACSQuant flow cytometer. After the count, the cells were washed 1x in 4-(2-Hydroxyethyl) piperazine-1-ethanesulfonic acid (HEPES) Buffered Saline (HeBs Buffer) [(HEPES (Sigma-Aldrich) + sodium chloride (NaCl) (Sigma-

Aldrich)] and resuspended to $1-5 \times 10^6$ cells in 1ml HeBs buffer. Neuraminidase (sialidase) from *Arthrobacter ureafaciens* (Roche, Mississauga, ON) was added to cells at 20mU/ml, 50mU/ml, or 100mU/ml to remove CD22L from the cell surface. The cells were vortexed and incubated with neuraminidase in a 37°C water bath for 30 minutes. Following incubation cells were washed 1x in HeBs + 1% bovine serum albumin (VWR International) and 1x in FSB. After last wash, cells were stained as per *section 2.8.2* and analyzed on the on the MACSQuant flow cytometer.

In addition, PPF assays were performed as per *section 2.7.2*. affiniPure F(ab')₂ Fragment Goat Anti-Human IgM (10µg/ml; Fc_{5µ} fragment specific; Jackson ImmunoResearch) was used as the stimulator. Following the PPF assays, the quantification of the intracellular signals PLCγ2 (pY759) and CD22 (pY822) was performed as per *section 2.7.3*.

2.8.2 Analysis of Neuraminidase Treatment

In order to quantify the expression of CD22L on the cell surface before and after neuraminidase treatment, cells were stained with 1µl undiluted Sambucus Nigra (SNA)-FITC lectin (Vector Labs, Burlington, ON) as per *section 2.3.1*. SNA binds preferentially to sialic acids attached to galactose in α-2,6 linkage and to a lesser degree, the α-2,3 linkage. Data acquired were subsequently analyzed using FlowJo software.

2.9 Synthesizing Anti-IgM Coated Microspheres

2.9.1 Attaching Anti-IgM to Streptavidin Microspheres

SaV coated microspheres (Polysciences, Warrington, PA) were used as a scaffold for the presentation of bound anti-IgM (biotinylated F(ab')₂ fragment goat anti-human IgM [Fc_{5µ} fragment specific; Jackson ImmunoResearch]) to Ramos cells. Using the biotin-binding capacity of the microspheres, the optimal concentration of anti-IgM was calculated and further titrated to reach maximum binding. SaV microspheres were washed 3x in 1ml 1xPBS. For all washes the microspheres were centrifuged at 10,000 rpm in the micro-centrifuge for 10min at RT. After washing the microsphere aliquots (1 aliquot = 50×10^6 microspheres) were

resuspended to 0.5mg/ml in wash buffer. Various volumes of biotinylated anti-IgM (12µl, 6µl, 3µl, 1.5µl, and 0.75µl; stock concentration: 1.7mg/ml) were added to each aliquot of microspheres. The microspheres and anti-IgM were incubated together at RT for 1 hour with gentle mixing every 20 minutes. After incubation the microspheres were washed 2x in PBS. The final wash was done in FSB in preparation for staining and detection of anti-IgM. In the case of preparing the microspheres for the PPF assay for stimulation of Ramos cells, the final wash was performed in R-10 media.

2.9.2 Detection of Anti-IgM on Microspheres

In order to quantify the bound anti-IgM on the surface of the SaV microspheres after incubation, microspheres were washed 2x (as per *section 2.9.1*). The microspheres were then added with 100µl FSB and stained with 1µl of fluorescent AF647 F(ab')₂ fragment donkey anti-goat IgG [H+L] (Jackson ImmunoResearch). The microspheres were incubated for 30 minutes at 4°C in the dark. After incubation the microspheres were washed 1x in FSB and run on the MACSQuant Flow Cytometer. Data acquired were subsequently analyzed using FlowJo software.

2.10 Statistical Analyses

2.10.1 CD22 Expression on B cell Subsets of PBMCs

Statistical analysis was performed with Graph Pad 5.0 using the Kruskal-Wallis Test followed by a post-hoc test using the Dunn's Multiple Comparison Test. Statistical significance was expressed as $p < 0.05$ (*).

2.10.2 CD22 Expression on B cell Subsets of splenocytes

Statistical analysis was performed with Graph Pad 5.0 using the One-way ANOVA followed by a post-hoc test using the Bonferroni. Statistical significance was expressed as $p < 0.05$ (*) and $p < 0.0001$ (***)).

2.10.3 CD22 Expression and age correlation on B cell Subsets of splenocytes and PBMCs

Statistical analysis was performed with Graph Pad 5.0 using the Spearman Correlation (r_s). Statistical significance was expressed as $p < 0.0001$ (***) and $r_s = -0.599$.

2.10.4 Differences in CD22 Expression of CD27⁺IgM⁺ B cell Subsets

Statistical analysis was performed with Graph Pad 5.0 using the Mann Whitney U Test (two-tailed). Statistical significance was expressed as $p < 0.05$ (*).

2.11 Tables & Figures

Table 2-1. Listing of staining antibodies used in this project

Antibody	Clone	Fluorochrome	Company
CD19	SJ25C1	eFluor 450	Affymetrix eBioscience
CD19	HIB19	eFluor 780	Affymetrix eBioscience
CD22	S-HCL-1	FITC	BD Pharmingen
CD22	S-HCL-1	APC	BD Pharmingen
CD22 (pY822)	12a/CD22	PE	BD Pharmingen
CD27	O323	APC-Cy7	Biologend
CD27	O323	PerCP-eFluor 710	Affymetrix eBioscience
CD27	M-T271	PE	Miltenyi Biotec Inc.
CD27	M-T271	APC	Miltenyi Biotec Inc.
CD38	HIT2	PE-Cy7	BD Pharmingen
IgD	IA6-2	APC-H7	BD Pharmingen
IgM	G20-127	PE	BD Pharmingen
IgM	PJ2-22H3	APC	Miltenyi Biotec Inc.
PLCy2 (pY759)	K86.689.37	Alexa Fluor 647	BD Pharmingen
PLCy2 (pY759)	K86.689.37	Alexa Fluor 488	BD Pharmingen

Table 2-2. B cell subsets based on expression of the cell surface markers CD19, IgM, CD27, IgD and CD38

Phenotype	B cell Subset
CD27 ⁻ IgM ⁻ IgD ⁻	non-conventional memory B cells
CD27 ⁻ IgM ⁻ IgD ⁺	naïve B cells
CD27 ⁻ IgM ⁺ IgD ⁺	naïve B cells
*CD27 ⁻ IgM ⁺ IgD ⁺ CD38 ^{high}	recent bone marrow emigrants
CD27 ⁺ IgM ⁻	class-switched memory B cells
CD27 ⁺ IgM ⁺	memory B cells

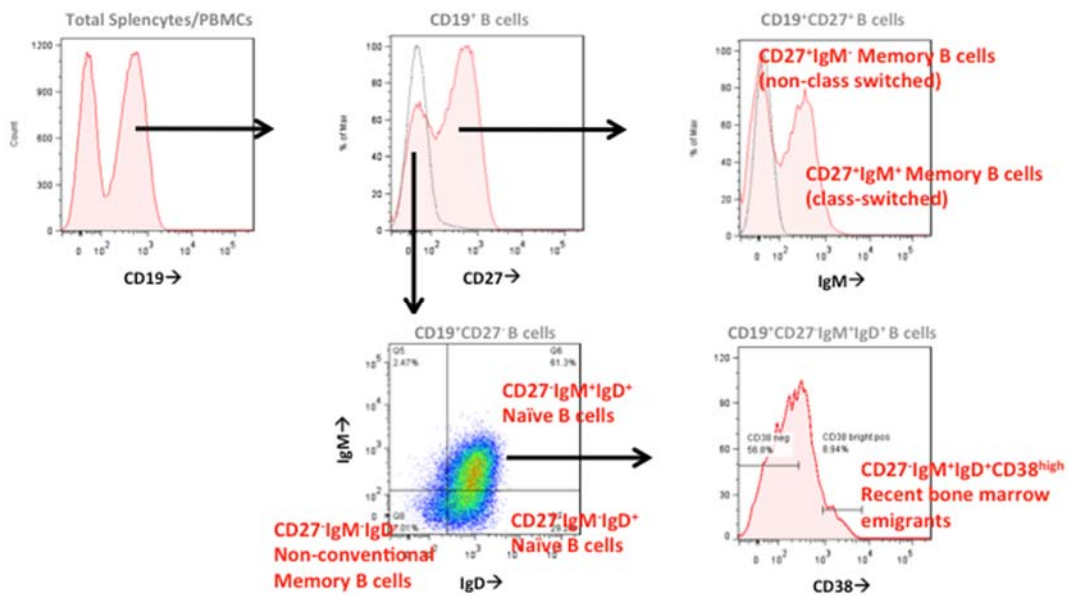


Figure 2-1. Gating strategy for characterizing B cell subsets in splenocyte and PBMC samples. First a doublet-discrimination was performed (not shown) followed by gating on total lymphocytes based on forward-scatter and side-scatter (not shown). B cells were defined as CD19 positive cells. CD19⁺ cells were further analyzed for the expression of CD27, IgM, IgD and CD38. The following B cell subsets have been delineated: CD27⁺IgM⁺ (non-class switched memory B cells), CD27⁺IgM⁻ (class-switched memory B cells), CD27⁻IgM⁺IgD⁺ (naïve B cells), CD27⁻IgM⁻IgD⁺ (naïve B cells), CD27⁻IgM⁺IgD⁻ (precursor B cells) and CD27⁻IgM⁺IgD⁺CD38^{high}.

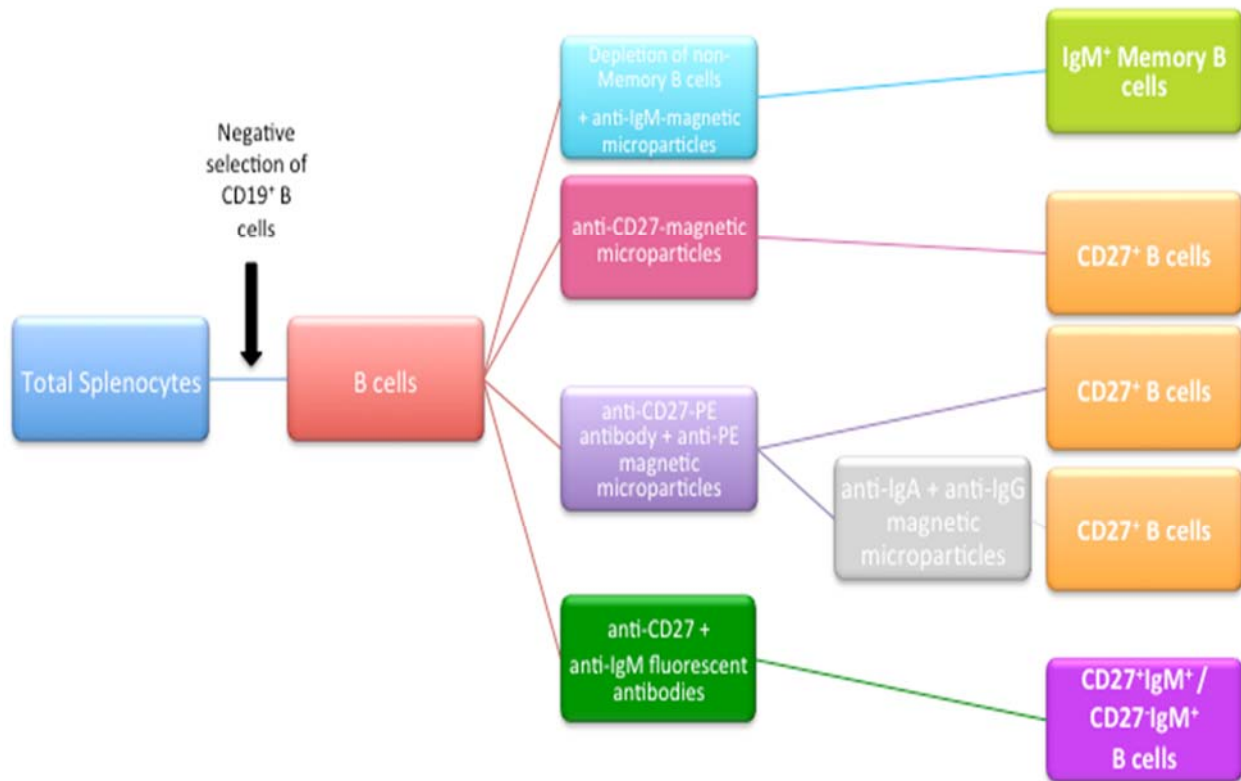


Figure 2-2. Optimization of B cell isolation of CD27⁺IgM⁺ B cells from total splenocytes. CD19⁺ B cells were first isolated by negative selection from total splenocytes. The first protocol involved IgM⁺ Memory B cell isolation from the B cells. In addition we also tried to isolate CD27⁺ B cells via 2 different protocols: the first involved use of anti-CD27 magnetic microparticles and magnetic activated cell sorting (MACS). The second protocol used anti-CD27-PE antibody followed by anti-PE magnetic microparticles and MACS. The addition of anti-IgA and anti-IgG magnetic microparticles was also added to this protocol to further deplete the IgA and IgG expressing B cells. Lastly, we went on to perform fluorescent activated cell sorting (FACS) using anti-CD27 and anti-IgM antibodies to directly detect and isolate the CD27⁺IgM⁺ B cells and CD27⁻IgM⁺ B cells.

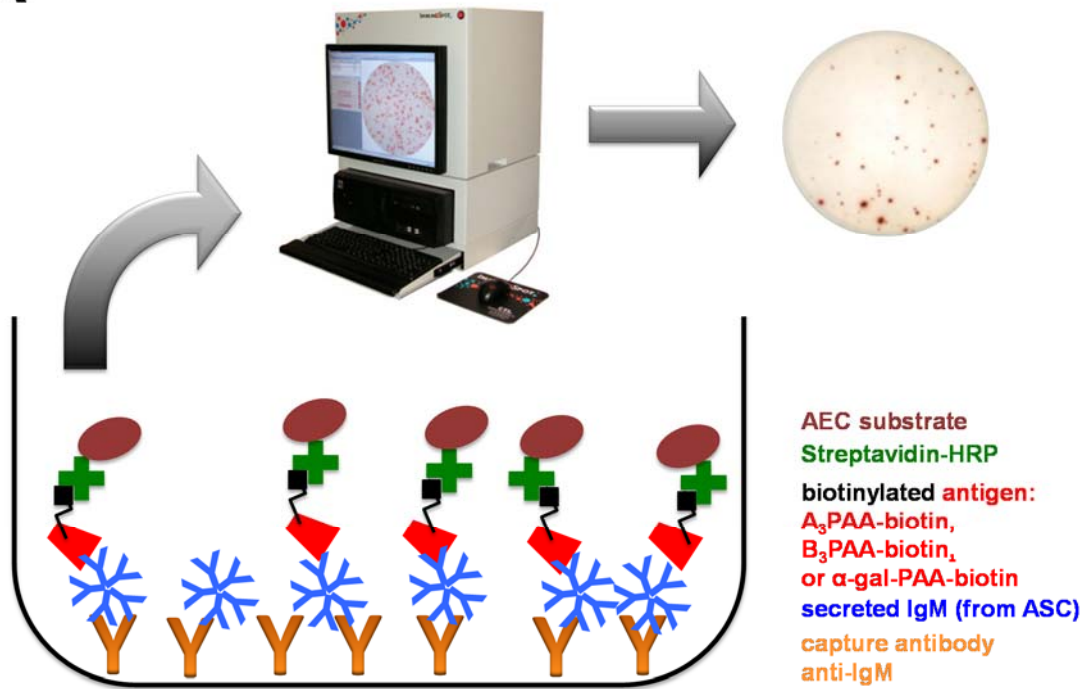
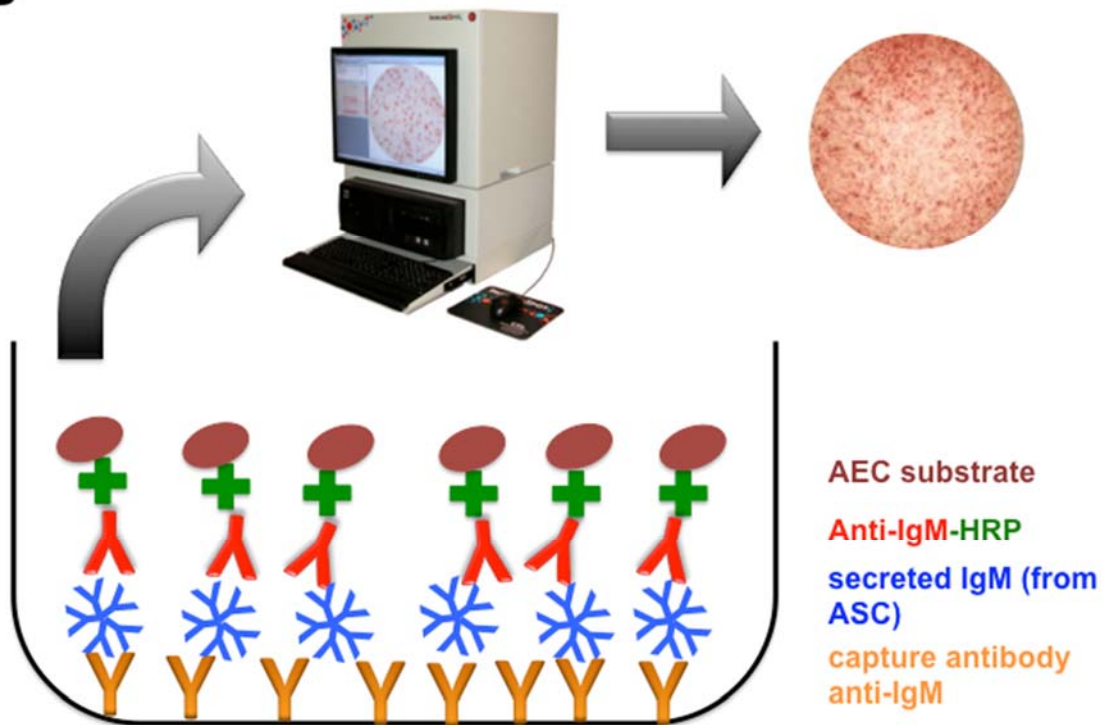
A**Antigen-specific IgM ELISPOT****B****Total IgM ELISPOT**

Figure 2-3. Outline of the B cell ELISPOT assay. (A) Antigen-specific IgM ELISPOT assay. Plates are coated with capture antibody (orange). B cells are deposited on the plate overnight. The secreted IgM antibody from the ASC (blue) is detected using 1 of 3 biotinylated antigens shown here (black-red). Antigens are detected using streptavidin-HRP (green) and AEC substrate (brown). Lastly, the spots are quantified using the CTL ImmunoSpot Analyzer and a picture is taken of each well. (B) Total IgM ELISPOT assay. Plates are coated with capture antibody (orange). B cells are deposited on the plate overnight. Total secreted IgM antibody from the ASC (blue) is detected using an anti-IgM-HRP antibody (red-green) and AEC substrate (brown). Lastly, the spots are quantified using the CTL ImmunoSpot Analyzer and a picture is taken of each well. (Image adapted from: <http://www.immunospot.com/>)

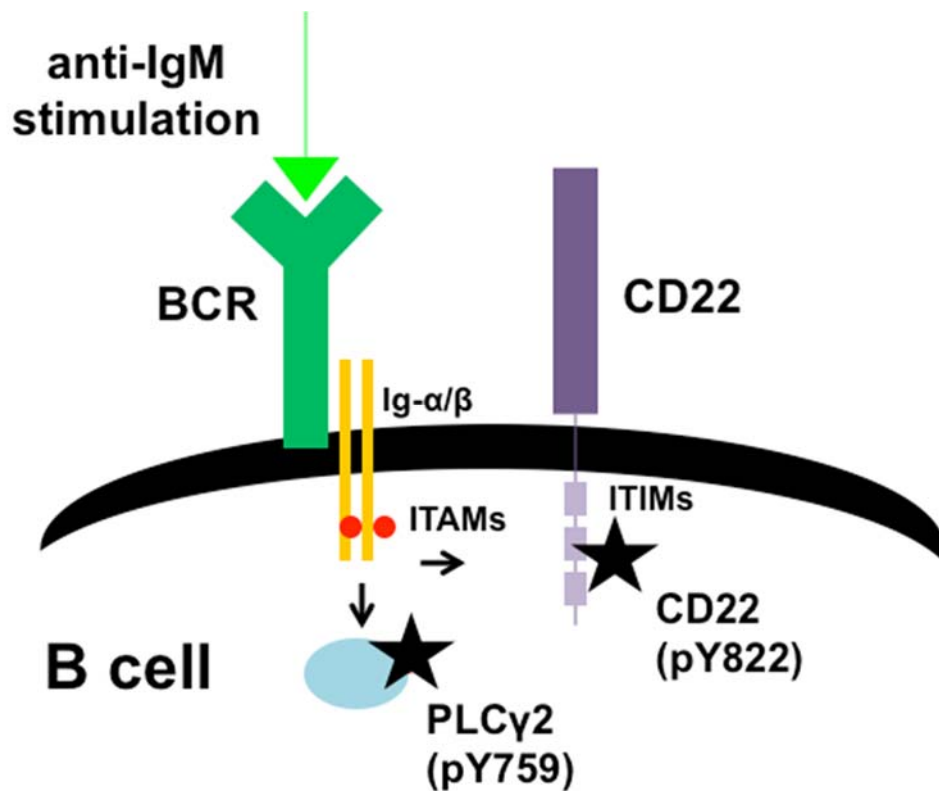


Figure 2-4. Phosphorylated intracellular signaling proteins PLC γ 2 (pY759) and CD22 (pY822) upon anti-IgM stimulation in the PPF assay. BCR signaling is initiated by the binding of BCR antigen and subsequent phosphorylation of immunoreceptor tyrosine-based activation motif (ITAM) tyrosine residues; located on the cytoplasmic tails of Ig α and Ig β . This ultimately leads to the phosphorylation of PLC γ 2 (pY759) and CD22 (pY822). Phosphorylated proteins pY759 and pY822, are represented by black stars.

CHAPTER THREE: RESULTS - ANALYSIS OF PRIMARY B CELLS: CD22 EXPRESSION, B CELL ISOLATIONS AND ELISPOT ANALYSIS

3.1 Introduction

To set the stage for eventual study of the potential role of CD22 in donor-specific B cell tolerance in infants following ABOi HTx, we initially investigated the expression of CD22 on various B cell subsets in peripheral blood and spleen across the lifespan of normal healthy humans. Subsequently, we optimized a protocol for the isolation of CD22⁺ CD27⁺IgM⁺ B cells from total splenocytes of infants (as defined in our experiments as individuals < 2 years in age) and older individuals due to the observed increase in CD22 expression in this particular B cell subset in infant samples. Lastly, a B cell ELISPOT assay was performed using the CD27⁺IgM⁺ and CD27⁻IgM⁺ splenic B cell subsets in attempt to determine the source of A/B antibody-secreting B cells.

3.2 Frequencies of various B cell subsets from infancy to elderly

First, we characterized various B cell subsets as relative frequencies of CD19⁺ B cells in the peripheral blood (n=49; age at time of sample: 3.5 months to 91 years) and spleen (n=40; age at time of sample: 4 days to 74 years) from the age of infancy to elderly. We sought to examine B cells at various stages in development; based on previous studies, the expression of CD27, IgM, IgD and CD38 was used to define the following B cell subsets: non-class-switched CD27⁺IgM⁺ memory B cells, class-switched CD27⁺IgM⁻ memory B cells, (73) CD27⁻IgM⁻IgD⁻, (155) CD27⁻IgM⁻IgD⁺ and CD27⁻IgM⁺IgD⁺ naïve B cells. (150) The CD27⁻IgM⁺IgD⁺ naïve B cells were further analyzed to examine the CD27⁻IgM⁺IgD⁺CD38^{high} (RBE). (151) B cell frequency data is presented as median and interquartile range (IQR) in Table 3-1 and Table 3-2.

Our peripheral blood frequencies were consistent with a study by van Gent *et al.*, (73) which also characterized B cell frequencies from peripheral blood in humans. In addition to peripheral blood B cell subsets, we examined B cell frequencies of subsets derived from the spleen. For the purposes of this project we will focus on the infant population. The frequency of the naïve B cell population (CD27⁻IgM⁺IgD⁺) contributed the largest B cell subset in

peripheral blood before the age of 2 years (median: 64.8%; IQR: 61.1-66.6). Likewise, naïve B cells made up the largest B cell subset in the spleen during infancy (median: 56.5%; IQR: 49.7-59.3). Splenic RBE (CD27⁻IgM⁺IgD⁺ CD38^{high}), a subset of naïve B cells, constituted three times the frequency (29.5%) compared to peripheral blood RBE (9.8%), consistent with findings that newly formed B cells emigrate from the bone marrow and home to the spleen for further maturation. (156) The CD27⁻IgM⁺IgD⁺ naïve B cell frequency decreased with age in B cells derived from both sources. In contrast, the frequency of the CD27⁻IgM⁻IgD⁺ naïve B cells remained relatively consistent across age. Similar to our findings in the CD27⁺IgM⁺ B cells, van Gent *et al.* reported the peripheral blood CD27⁺IgM⁺IgD⁺ B cells to constitute the highest memory cell population at birth, reaching a peak at 1-2 years. The frequency of the splenic CD27⁺IgM⁺ memory B cell subset was higher than that of class-switched CD27⁺IgM⁻ memory B cells before the age of 2 years.

3.3 CD22 Expression on B cell subsets throughout the lifetime

3.3.1 Differential expression of CD22 on spleen and peripheral blood B cell subsets

In mice, CD22 is present on the B cell surface beginning at the pre-B cell stage and is lost upon differentiation into plasma cells, (108, 109) and thus we were interested in examining the differential expression of CD22 on the various B cell subsets in humans (performed by analyzing the median fluorescent intensity (MFI) of CD22 by flow cytometry) (Figure 3-1). The expression of CD22 was analyzed on B cell subsets in both peripheral blood and spleen. In peripheral blood, CD27⁻IgM⁻IgD⁺ B cells had higher expression of CD22 compared to all other subsets, albeit not significant (Figure 3-2). In the spleen, CD27⁺IgM⁺ memory B cells had significantly higher expression of CD22 when compared to all other B cell subsets ($p < 0.05$; Figure 3-3). In contrast, CD22 expression was significantly the lowest on the CD27⁻IgM⁻IgD⁻ B cells ($p < 0.05$). We were interested if the increased expression of CD22 on the CD27⁺IgM⁺ memory B cells could be correlated with age.

3.3.2 Levels of CD22 expression correlate with age in the CD27⁺IgM⁺ B cells

Next, we analyzed the MFI of CD22 on all B cell subsets across different ages. Interestingly, a significant correlation with age was observed for the splenic CD27⁺IgM⁺ B cell subset ($p < 0.0001$; $r = 0.599$). Infant samples had the highest expression of CD22 and expression decreased with age (Figure 3-4 (A)). In contrast to splenic B cells, this correlation was not found for peripheral blood CD27⁺IgM⁺ B cells (Figure 3-4 (B)). The splenocyte data is also shown comparing the splenic CD27⁺IgM⁺ B cells of the infant group ($n = 8$) to the older individuals group ($n = 32$) (Figure 3-5).

3.4 Protocol optimization: B cell isolation of CD27⁺IgM⁺ B cells

3.4.1 Negative selection of CD19⁺ B cells was performed prior to B cell isolation

Due to our findings that CD22 expression was highest on the CD27⁺IgM⁺ infant B cells derived from the spleen, we were interested in isolating these cells to further determine if the A/B antigen-specific B cells (ASC) were derived from this population. The A/B ASC are the B cells responsible for secreting antibodies specific for the A/B blood-group antigens.

We tested several protocols to isolate the CD27⁺IgM⁺ B cell population from human splenocytes (Figure 2-2). In all protocols, we first isolated CD19⁺ B cells by negative selection. Magnetic isolation of CD19⁺ B cells without the use of columns (*section 2.4.1.1*) had similar purities to CD19⁺ isolation using automated Magnetic Activated Cell Sorting (MACS) (*section 2.4.1.2*) (Figure 3-6). Both methods resulted in CD19⁺ B cell purities that were greater than 95% and thus were used interchangeably in isolating CD19⁺ B cells from total splenocytes.

3.4.2 Various protocols used to isolate the CD27⁺IgM⁺ B cell population from total splenocytes

3.4.2.1 A commercially available IgM⁺ memory B cell isolation kit was ineffective in isolating CD27⁺IgM⁺ B cells

The first attempt to isolate IgM⁺ memory B cells involved a commercially available IgM⁺ memory B cell isolation kit from Miltenyi Biotec. The company's data sheet stated that this kit could effectively isolate CD27⁺IgM⁺ B cells using a two-step protocol (*section 2.4.2.1*). It included the negative selection of memory B cells followed by a positive selection for IgM⁺ memory B cells using MACS. The expression of CD27 and IgM on B cells was examined using flow cytometry. Following negative selection of memory B cells, the sample contained 61% CD27⁻ B cells. (Figure 3-7(B)) According to the data sheet, this step should have completely depleted the CD27⁻ B cell population. After positive selection of IgM⁺ B cells, the purity of the "CD27⁺IgM⁺ B cell fraction" was only 3% of the total population (Figure 3-7(C)); thus we proceeded with other protocols to try to improve the purity.

3.4.2.2 PE conjugated anti-CD27 antibody and anti-PE antibody microbeads by MACS was a successful method for isolating CD27⁺ B cells

To isolate memory B cells based on CD27 expression, we first used a different commercial kit from Miltenyi Biotec. It included labeling B cells with anti-CD27 antibody magnetic microbeads followed by MACS to positively select for the CD27⁺ B cells (*section 2.4.2.2*). Following the isolation (positive selection of CD27⁺ B cells) we were unable to detect CD27 expression on the B cells (Figure 3-8 (C)). The magnetic microbeads used in the isolation step may have blocked the binding sites for the detection antibodies used to check the purity of the isolated CD27⁺ B cells. Two different antibody clones were tested in order to detect CD27 (clones M-T271 and O323) and the same results were found with both.

Because of the poor isolation results obtained using commercially available kits, we next used a different approach to isolate CD27⁺ B cells: B cells were labeled with PE conjugated anti-CD27 antibody and subsequently incubated with anti-PE antibody magnetic microbeads. MACS was used to positively select for CD27⁺ B cells (*section 2.4.2.3*). The

purity of the isolated CD27⁺ B cells using this method was higher (86%) (Figure 3-9 (C)) than that using the commercial kits.

3.4.2.3 Enrichment of IgM⁺ B cells followed by PE-conjugated anti-CD27 antibody and anti-PE antibody microbeads and MACS isolation did not result in an enriched CD27⁺IgM⁺ B cell population

We wanted to further isolate the IgM⁺ B cells from the CD27⁺ B cell population. Because the protocol to isolate CD27⁺ memory B cells was based on positive selection, we decided to deplete IgA- and IgG-expressing B cells to enrich for IgM⁺ B cells. We depleted IgA- and IgG-expressing B cells together with non-CD19⁺-expressing B cells. We then isolated the CD27⁺ B cells using a PE-conjugated anti-CD27 antibody and anti-PE antibody magnetic microbeads. MACS was used to positively select for CD27⁺ B cells (*section 2.4.2.4*). Following the isolation, the purity of the desired CD27⁺IgM⁺ B cell population was 20%, with 57% of IgM⁺ B cells remaining in our sample (Figure 3-10 (B)).

3.4.2.4 Isolation by FACS resulted in high purities of CD27⁺IgM⁺ and CD27⁻IgM⁺ B cells

Because only low purities of CD27⁺IgM⁺ B cells were obtained using MACS, we moved on to a protocol using Fluorescent-Activated Cell Sorting (FACS). Isolated CD19⁺ B cells were stained with fluorescent anti-CD27 and anti-IgM antibodies and B cells were subsequently isolated by FACS (*section 2.4.2.5*). High purities of both CD27⁺IgM⁺ (93%) and CD27⁻IgM⁺ (96%) B cell populations were obtained following FACS (Figure 3-11 (B)).

The highly pure populations of CD27⁺IgM⁺ and CD27⁻IgM⁺ B cells after FACS were then used in further functional assays, namely ELISPOT assays and the Phospho-specific flow cytometry assays (*Chapter Four*).

3.5 B cell ELISPOT Assay

The highest levels of CD22 were found to be expressed on the CD27⁺IgM⁺ B cell splenocyte subset from infants, an age at which ABOi HTx can be safely performed. Due to donor-specific B cell tolerance in infants following ABOi HTx, we were interested in

investigating whether the increased expression of CD22 on these cells, played a role in B cell tolerance. First, it was necessary to establish whether this subset contained the A/B-specific ASC (plasma cells). Plasma cells are terminally differentiated cells that develop from plasmablasts. They secrete antibodies at high rates and no longer respond to antigen. (60-62) As previously mentioned, the A/B-specific ASC secrete antibodies directed at the A/B blood-group antigens.

Our results above demonstrate that the CD27⁺IgM⁺ and CD27⁻IgM⁺ B cells could be isolated with high purities. Therefore, we wanted to test the isolated cell populations for the presence of A/B-specific ASC using a B cell ELISPOT assay. Very few ASC are expected to be present in peripheral blood or spleen. (60, 157) However, culture of splenic or peripheral blood B cells in the presence of cytokines and mitogens has been shown to result in their differentiation into ASC (plasmablasts, plasma cells; (153, 158)). Using the ELISPOT assay we assessed the frequency of A/B-specific ASC, as well as proliferation and phenotype of splenic CD27⁺IgM⁺ and CD27⁻IgM⁺ B cells following culture with cytokines (IL-2, IL-10 and IL-15) and CpG mitogen.

3.5.1 Stimulation with CpG, IL-2, IL-10 and IL-15 results in B cell proliferation and changes in surface expression of CD22 in adult CD27⁺IgM⁺ and CD27⁻IgM⁺ B cells

We assessed the proliferation of isolated cells in our ELISPOT assay to ensure that the selected culture conditions were sufficient in stimulating our cells. We also examined the surface expression of CD22 and CD27 to analyze the changes that occurred in the 7-day culture. Adult splenic B cells were stained with proliferation dye and FACS-sorted (*section 3.4.2.4*) to yield CD27⁺IgM⁺ and CD27⁻IgM⁺ B cell subsets. After a 7-day cell culture period with CpG, IL-2, IL-10 and IL-15, we analyzed the proliferation of these B cell subsets by flow cytometry and examined their CD22 and CD27 expression after culture. Unstimulated cells and cells cultured with only cytokines were used as controls. As shown in Figure 3-12 (A and B), stimulation with CpG, IL-2, IL-10 and IL-15 resulted in proliferation of both the CD27⁺IgM⁺ and CD27⁻IgM⁺ B cells. Additionally, CD22 expression increased (more substantially in the CD27⁻IgM⁺ B cells) within the early divisions, followed by a decrease in CD22 expression on subsequent divisions (both subsets) suggesting that these cells may no longer be susceptible to CD22 inhibition after 7-day culture (Figure 3-13 (A and B)). This

data is important in future experiments because changes in the expression levels of CD22 on B cells, either an increased or decreased expression, can be combined with additional data such as the amount of A/B antibody production of the ASC.

Within the CD27⁺IgM⁺ B cell subset, a small portion (11%) of proliferating B cells expressed CD27 on their surface after stimulation and 7-day culture (Figure 3-14 (B)). It is important to note that the surface expression of CD27 changes as we are using this surface marker to distinguish between our 2 subsets, CD27⁺IgM⁺ and CD27⁻IgM⁺ B cells, and compare results.

3.5.2 A/B antibody-secreting B cells are primarily derived from the CD27⁺IgM⁺ B cells of infant and adult spleen

Prior to ELISPOT analysis, CD19⁺ B cells were isolated from total splenocytes, followed by MACS (with PE-conjugated anti-CD27 antibody and anti-PE antibody microbeads) or FACS protocols to yield isolated CD27⁺IgM⁺ and CD27⁻IgM⁺ B cell subsets (*section 2.4*). Following 6-7 days of culture with CpG, IL-2, IL-10 and IL-15, cells were counted and cultured overnight on ELISPOT plates. The number of spots representing ASC, derived from cells of the CD27⁺IgM⁺ and CD27⁻IgM⁺ populations, was quantified. Spots represent total IgM ASC and IgM ASC specific to A-antigen, B-antigen and α -gal-antigen. α -gal-specific ASC were assessed as a control since all individuals should contain α -gal specific memory B cells. (159) Results are presented for 3 experiments with a total of 9 separate samples from individuals ranging in age from 0.5 years to 66 years and comprising various blood types (Table 3-3). A general trend was observed in the samples when comparing the CD27⁺IgM⁺ and CD27⁻IgM⁺ B cell populations: the ASCs specific for A/B and α -gal were predominantly derived from the CD27⁺IgM⁺ B cell subset. In addition, there was a greater number of IgM ASC from the CD27⁺IgM⁺ subset compared with the CD27⁻IgM⁺ subset. (Figures 3-15 to 3-17). Despite protocol optimization, issues emerged with background binding on the ELISPOT plate, primarily with blood type A samples. The possibility that these could be auto-antibodies should be considered, but it is more likely due to technical issues. Nevertheless, this issue needs more attention when moving forward with these experiments.

3.6 Summary

Examination of CD22 expression on human B cell subsets across the lifespan demonstrated that infant CD27⁺IgM⁺ splenic B cells had the highest expression of CD22 when compared to all other splenic B cell subsets. An increased expression of CD22 on these infant B cells raised further questions as to whether the increased expression was involved in donor-specific B cell tolerance seen in infants following ABOi HTx.

We next developed a protocol to isolate CD27⁺IgM⁺ B cells in attempts to study these cells more closely in functional assays. Initial attempts to isolate the cells by MACS, using commercial isolation kits or PE-conjugated anti-CD27-antibodies and anti-PE antibody magnetic microbeads with or without anti-IgA and anti-IgG antibodies, failed to yield a pure population of CD27⁺IgM⁺ B cells. We ultimately determined that an effective protocol for isolating this B cell population was direct labeling of CD27 and IgM using fluorescent antibodies followed by FACS; this protocol yielded high purities (greater than 90%) of CD27⁺IgM⁺ and CD27⁻IgM⁺ B cells, allowing us to further study these individual subsets in functional assays, such as the ELISPOT.

Lastly, after 7-day culture with CpG, IL-2, IL-10 and IL-15, ELISPOT analysis revealed that A/B specific IgM ASCs were predominantly derived from CD27⁺IgM⁺ B cells. This was an important finding as there is little knowledge in the literature about the ABO ASC and their specific origin. Additionally, this new knowledge about the increased expression of the co-inhibitory CD22 molecule on these infant B cells, shown here to contain the A/B-specific ASC, may suggest that CD22 plays a role in B cell tolerance induction in the setting of infant ABOi transplantation.

3.7 Tables & Figures

Table 3-1. Frequency of peripheral blood B cell subsets in different age groups

Phenotype	Age (years) Samples (n)				
	< 2 (n=8)	2-<12 (n=8)	12-<19 (n=7)	19-<50 (n=16)	50-<95 (n=10)
CD27 ⁻ IgM ⁻ IgD ⁻	2.9 (2.4-5.4)	10.6 (7.3-12.6)	8.3 (7.1-12.5)	9.1 (7.1-11.7)	8.7 (4.7-11.7)
CD27 ⁻ IgM ⁻ IgD ⁺	22.1 (16.8-22.5)	26.3 (21.6-28.1)	31.6 (29.2-34.4)	26.0 (20.9-31.4)	32.3 (23.8-35.7)
CD27 ⁻ IgM ⁺ IgD ⁺	64.8 (61.1-66.6)	41.4 (35.2-51.0)	37.0 (32.1-40.2)	32.4 (26.7-38.7)	29.6 (24.9-31.7)
*CD27 ⁻ IgM ⁺ IgD ⁺ CD38 ⁺⁺	9.8 (6.7-15.2)	7.9 (5.7-11.1)	3.3 (2.1-5.2)	1.7 (1.2-2.8)	1.3 (0.9-2.2)
CD27 ⁺ IgM ⁻	1.6 (1.5-3.2)	10.6 (8.7-12.2)	11.5 (9.7-12.9)	15.0 (11.8-18.7)	13.8 (10.6-17.5)
CD27 ⁺ IgM ⁺	7.1 (2.8-7.6)	6.9 (6.2-9.2)	8.6 (4.6-8.9)	8.1 (6.2-14.4)	11.5 (4.8-20.3)

Frequency of various peripheral blood B cell subsets (as a percentage of all CD19⁺ B cells) is shown for distinct age groups listed as medians (upper line) and as the corresponding interquartile range (25th and 75th percentiles) (lower line). *CD27⁻IgM⁺IgD⁺CD38⁺⁺ B cells are expressed as a percentage of all CD27⁻IgM⁺IgD⁺ B cells.

Table 3-2. Frequency of splenic B cell subsets in different age groups

Phenotype	Age (years)				
	< 2 (n=8)	2-<12 (n=4)	12-<19 (n=8)	19-<50 (n=10)	50-<95 (n=10)
CD27 ⁺ IgM ⁺ IgD ⁻	8.8 (7.6-11.2)	23.7 (15.4-31.0)	24.0 (22.5-32.5)	32.7 (25.3-37.5)	23.8 (18.3-35.9)
CD27 ⁺ IgM ⁺ IgD ⁺	22.3 (17.6-27.9)	25.4 (21.1-32.7)	28.6 (25.6-32.5)	21.6 (16.8-27.8)	18.4 (9.5-21.5)
CD27 ⁺ IgM ⁺ IgD ⁺	56.5 (49.7-59.3)	21.6 (19.1-28.2)	18.0 (14.9-20.9)	13.3 (8.5-16.0)	13.6 (7.2-17.4)
*CD27 ⁺ IgM ⁺ IgD ⁺ CD38 ⁺⁺	29.5 (26.2-35.6)	8.3 (1.9-17.6)	2.1 (0.8-5.1)	0.6 (0.3-0.8)	1.5 (0.7-2.5)
CD27 ⁺ IgM ⁻	1.9 (1.4-3.9)	6.5 (3.6-10.6)	9.3 (7.1-13.6)	14.2 (7.7-17.3)	16.6 (8.0-32.0)
CD27 ⁺ IgM ⁺	4.4 (2.2-7.8)	7.5 (5.4-10.0)	6.6 (3.6-9.0)	7.6 (2.2-12.6)	10.2 (5.6-13.3)

Frequency of various splenic B cell subsets (as a percentage of all CD19⁺ B cells) is shown for distinct age groups listed as medians (upper line) and as the corresponding interquartile range (25th and 75th percentiles) (lower line). *CD27⁺IgM⁺IgD⁺CD38⁺⁺ B cells are expressed as a percentage of all CD27⁺IgM⁺IgD⁺B cells.

Table 3-3. Outline of ELISPOT experiments

Isolation Procedure ¹	Blood		IgM ASC per 100,000 input cells							
	Type	Age	CD27-IgM ⁺				CD27 ⁺ IgM ⁺			
			A	B	α -gal	Total IgM	A	B	α -gal	Total IgM
MACS	O	18.1	9	3	1	369	35	11	33	926
MACS	A	66.4	1	11	19	768	4	56	64	1622
MACS	B	2.3	3	0	1	2056	36	0	23	5290
MACS	A	18.2	0	0	14	2040	15	71	116	3877
FACS	A	20.8	0	1	1	1505	3	25	10	3238
FACS	O	18.1	0	0	65	5248	157	23	89	11148
FACS	A	25.3	3	0	3	3270	8	12	24	7258
FACS	A1	0.5	2	30	6	3024	6	78	44	4330
FACS	AB	25.7	2	2	2	1543	10	5	12	1909

Total IgM antibody-secreting cells (ASC), IgM ASC specific for A, B antigens and α -gal antigen following culture of isolated CD27⁻IgM⁺ and CD27⁺IgM⁺ B cells. ¹MACS: magnetic-activated cell sorting, FACS: fluorescent-activated cell sorting.

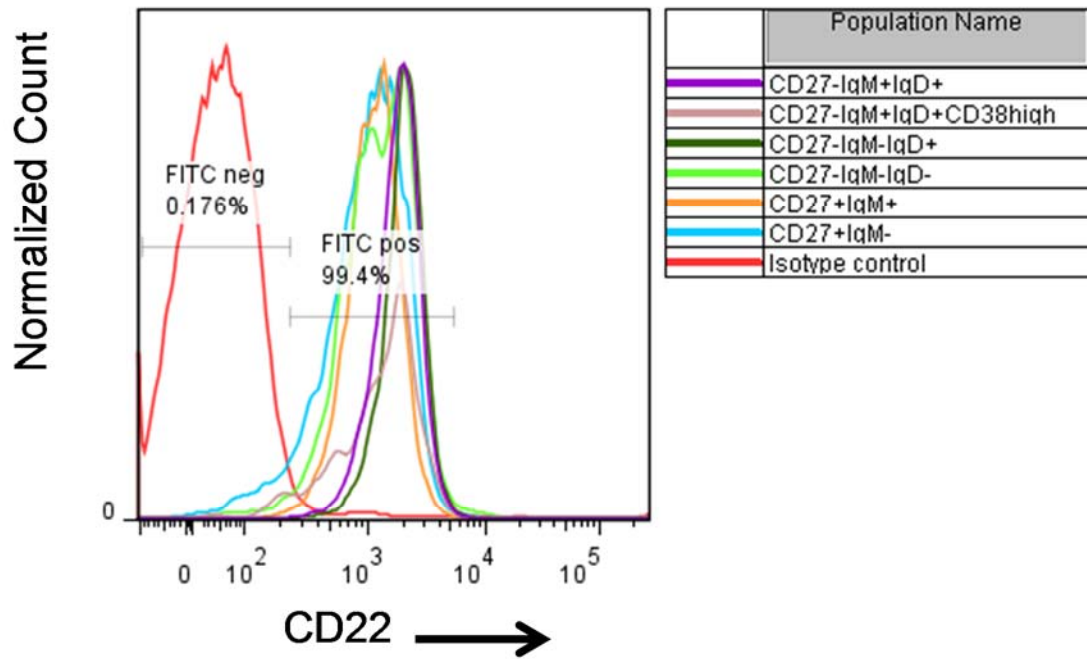
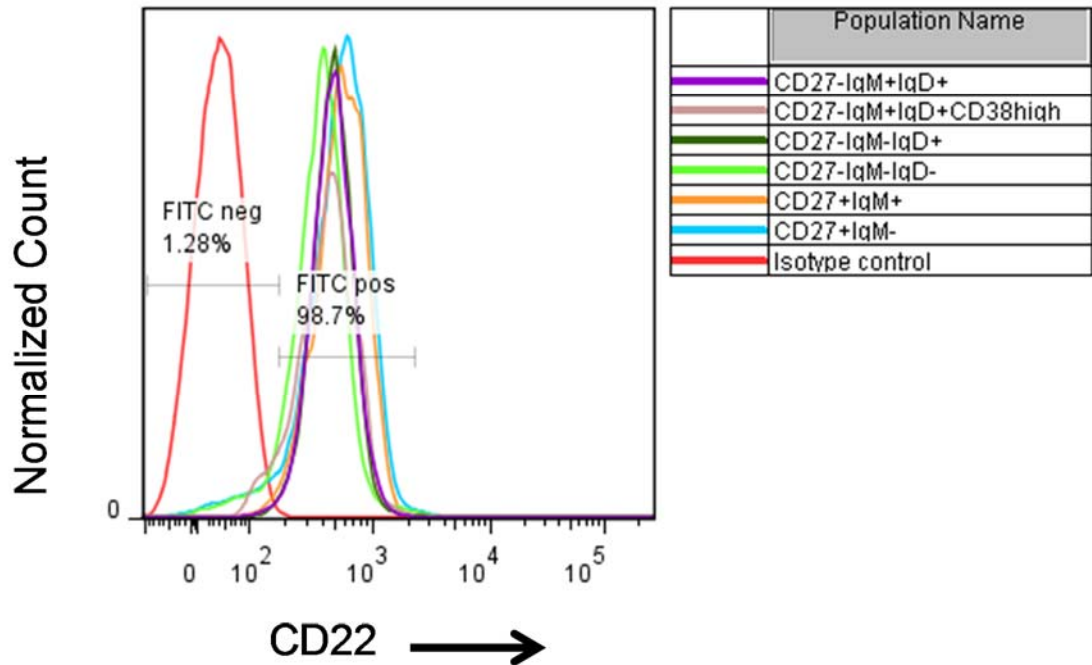
A**B**

Figure 3-1. CD19⁺ B cells within this study expressed the surface molecule CD22. B cells were stained with fluorescent antibodies against CD22, CD27, IgM, IgD and CD38. The level of CD22 expression was investigated on the indicated (A) PBMC and (B) splenic B cell subsets by flow cytometry. CD22 expression is represented by a right shift in the histograms (gating was performed as depicted in Figure 2-1). Shown are 2 randomly selected samples.

PBMCs

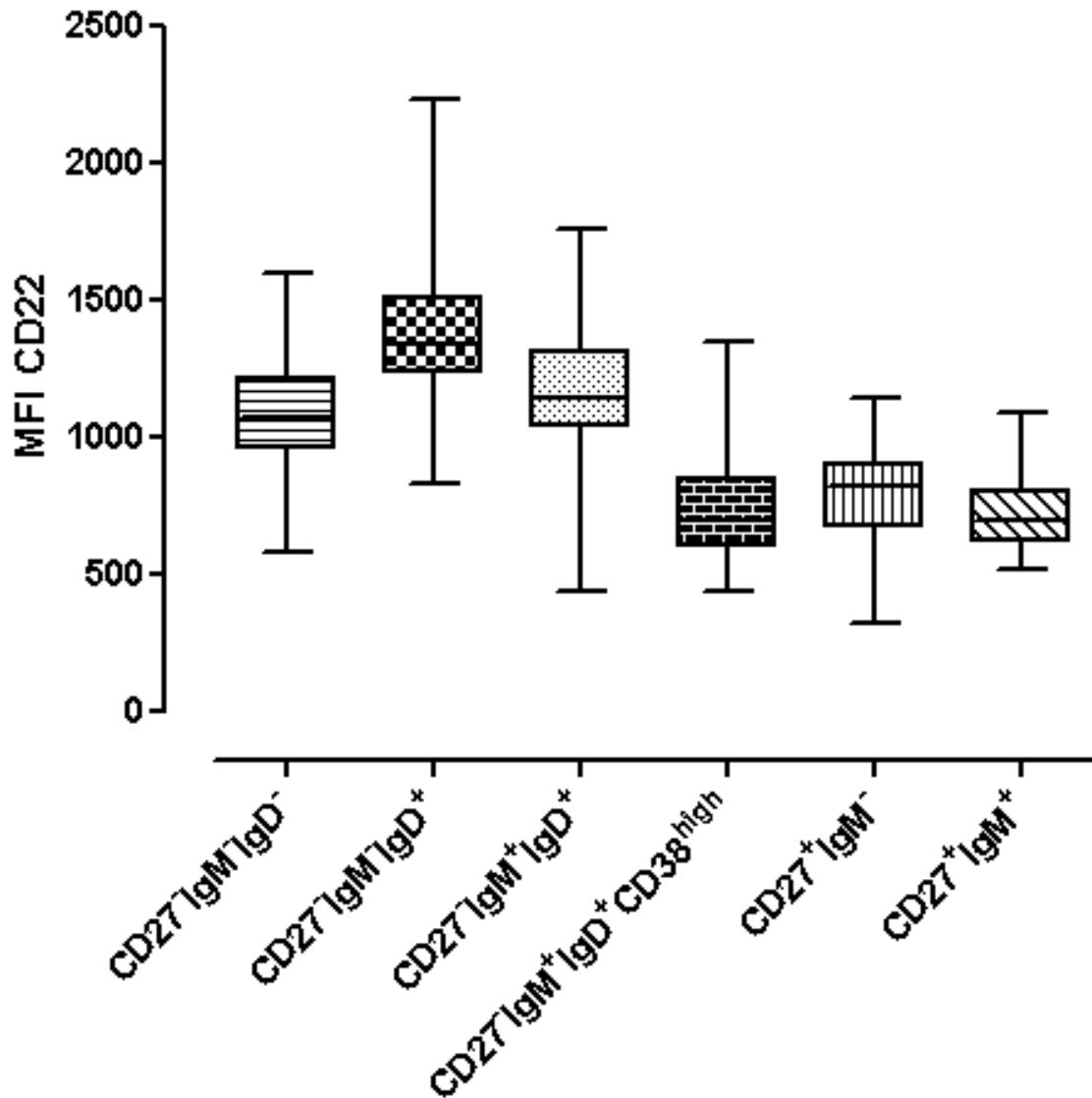


Figure 3-2. CD22 expressed amongst the peripheral B cell subsets. B cells from peripheral blood (n=49; age: 3.5 months – 91 years) were stained with fluorescent antibodies against CD22, CD27, IgM, IgD and CD38. The level of CD22 expression was analyzed on the indicated B cell subsets by flow cytometry (gating was performed as depicted in Figure 2-1). Due to the non-normal distribution of the data, the Kruskal-Wallis statistical test was used. Upon post-hoc testing with the Dunn's Multiple Comparison test, no significant differences were found amongst B cell subsets. CD22 expression is represented as median fluorescence intensity (MFI).

Splenocytes

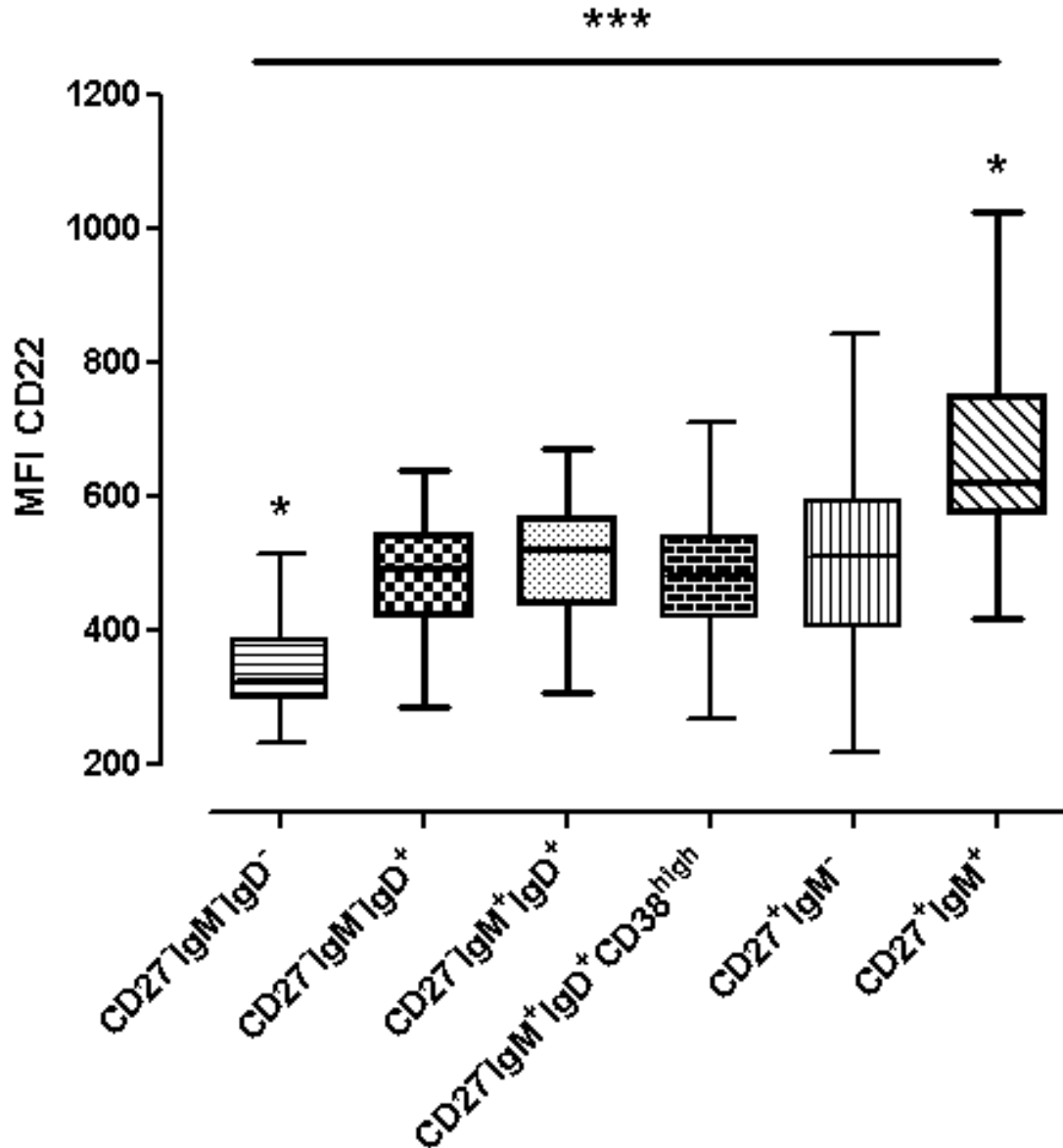


Figure 3-3. CD22 expression was highest on splenic CD27⁺IgM⁺ B cells and lowest on splenic CD27⁻IgM⁻IgD⁻ B cells. B cells from the spleen (n=40; ages: 4 days – 74 years) were stained with fluorescent antibodies against CD22, CD27, IgM, IgD and CD38. The level of CD22 expression level was analyzed on the indicated B cell subsets by flow cytometry (gating was performed as depicted in Figure 2-1). CD22 expression was significantly different amongst the splenic B cell subsets (***p<0.0001; One-way ANOVA). Upon further post-hoc testing using the Bonferroni test, CD22 expression was significantly higher on the CD27⁺IgM⁺ B cell subset (*p<0.05) and significantly lower on the CD27⁻IgM⁻IgD⁻ B cell subset (*p<0.05) when compared to all other B cell subsets. CD22 expression is represented as median fluorescence intensity (MFI).

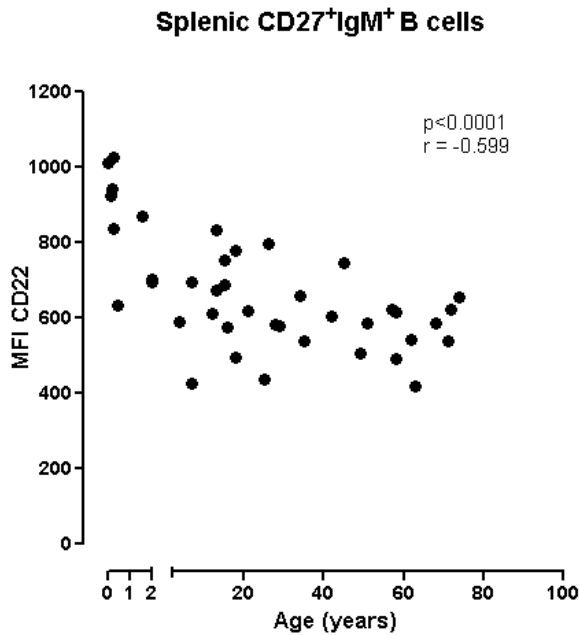
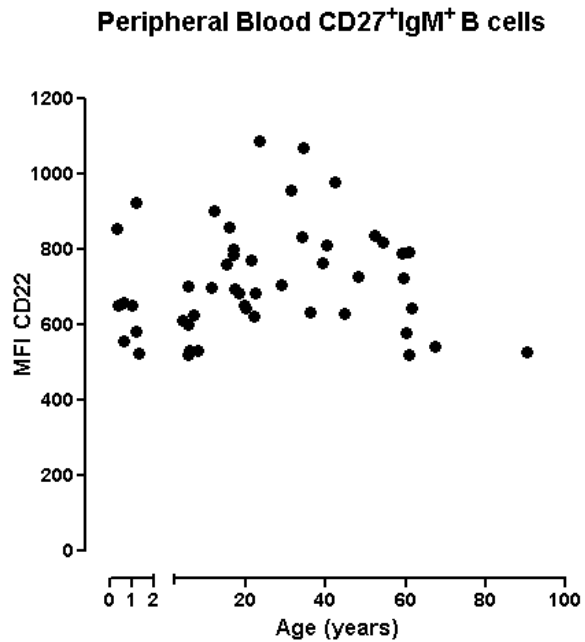
A**B**

Figure 3-4. CD22 expression of splenic CD27⁺IgM⁺ B cells, but not of peripheral blood CD27⁺IgM⁺ B cells, was correlated with age. CD22 expression level was analyzed on CD27⁺IgM⁺ B cells from the spleen and peripheral blood by flow cytometry (gating was performed as depicted in Figure 2-1). (A) A significant negative correlation between CD22 expression and age was observed in splenic CD27⁺IgM⁺ B cells ($p < 0.0001$; $r_s = -0.599$; Spearman correlation). CD22 expression was highest in CD27⁺IgM⁺ infant B cells and expression decreased with age. (B) No significant correlation was observed for CD27⁺IgM⁺ peripheral blood B cells. CD22 expression is represented as median fluorescence intensity (MFI).

Splenic CD27⁺IgM⁺ B cells

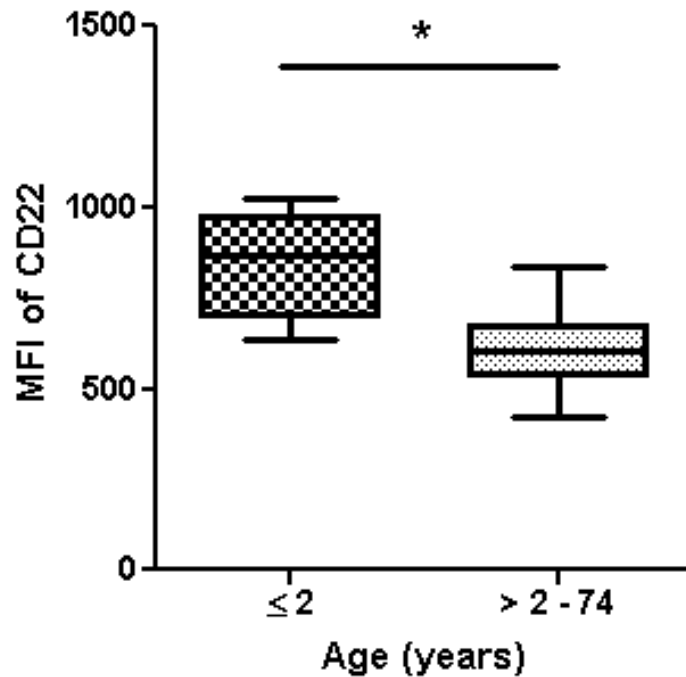


Figure 3-5. CD22 expression on infant CD27⁺IgM⁺ splenic B cells was significantly higher than on CD27⁺IgM⁺ B cells of older individuals. CD22 expression level was analyzed on CD27⁺IgM⁺ B cells from the spleen by flow cytometry (gating was performed as depicted in Figure 2-1). Using a 2-tailed Mann Whitney U Test, a significant difference in the expression of CD22 was observed between CD27⁺IgM⁺ infant (≤ 2 years) B cells (n=8) and older individuals (>2 years) (n=32) (*p<0.05). CD22 expression is represented by median fluorescence intensity (MFI).

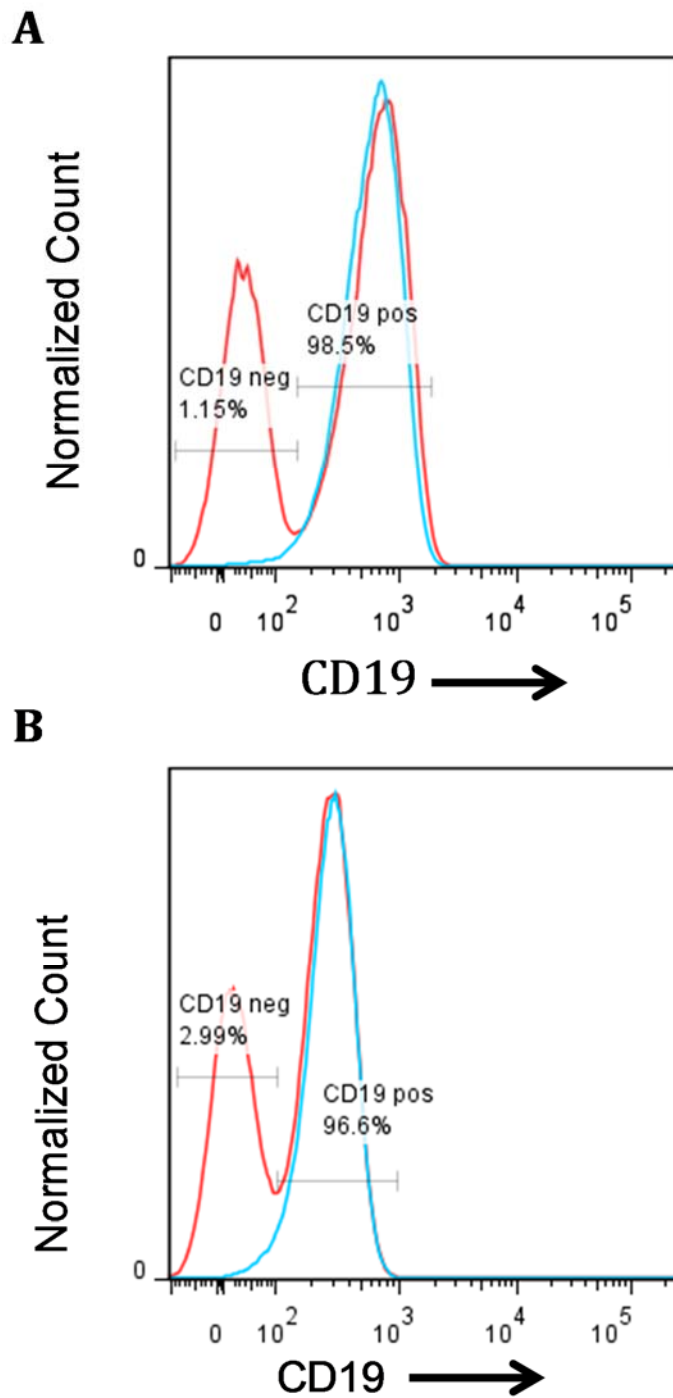


Figure 3-6. CD19⁺ B cell isolation purities were similar between magnetic sort and automated MACS. CD19⁺ B cells were isolated from total splenocytes by means of (A) magnetic isolation of CD19⁺ B cells without the use of columns or (B) isolation using automated MACS. The level of CD19 expression within total splenocytes was analyzed by flow cytometry before (red line) and after B cell isolation (blue line), and is represented by a right shift in the histograms.

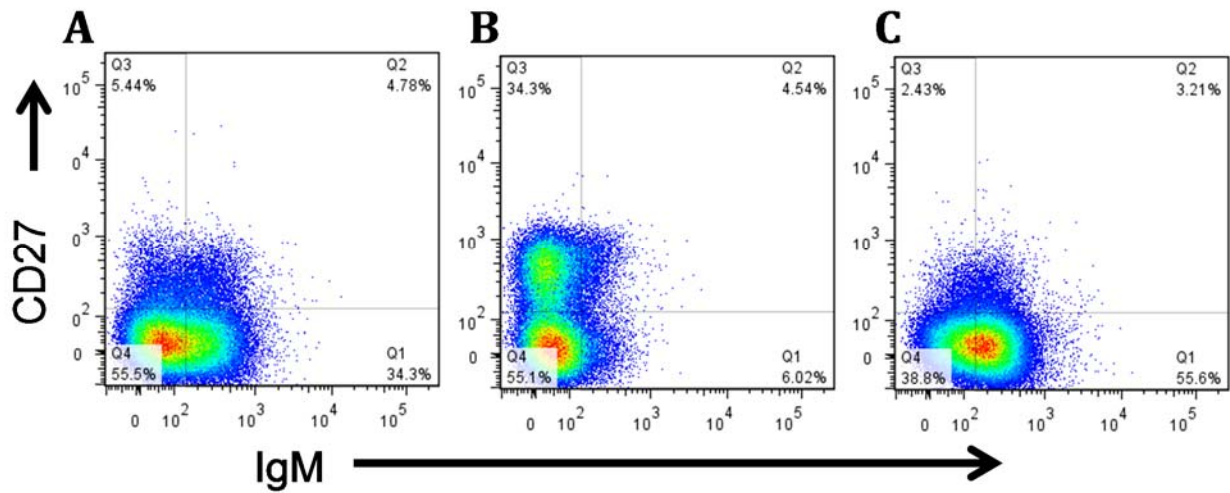


Figure 3-7. IgM⁺ Memory B cell isolation using an isolation kit was ineffective at sorting the IgM⁺ Memory B cells. IgM⁺ Memory B cells were isolated from total splenocytes (adult) using an IgM⁺ Memory B cell isolation kit. The expression of CD27 and IgM was analyzed on (A) the total splenocyte fraction prior to isolation, (B) the “Memory B cell fraction” after negative selection of Memory B cells, and lastly (C) the “IgM⁺ Memory B cell fraction” following positive selection for IgM. Data are representative of 3 experiments.

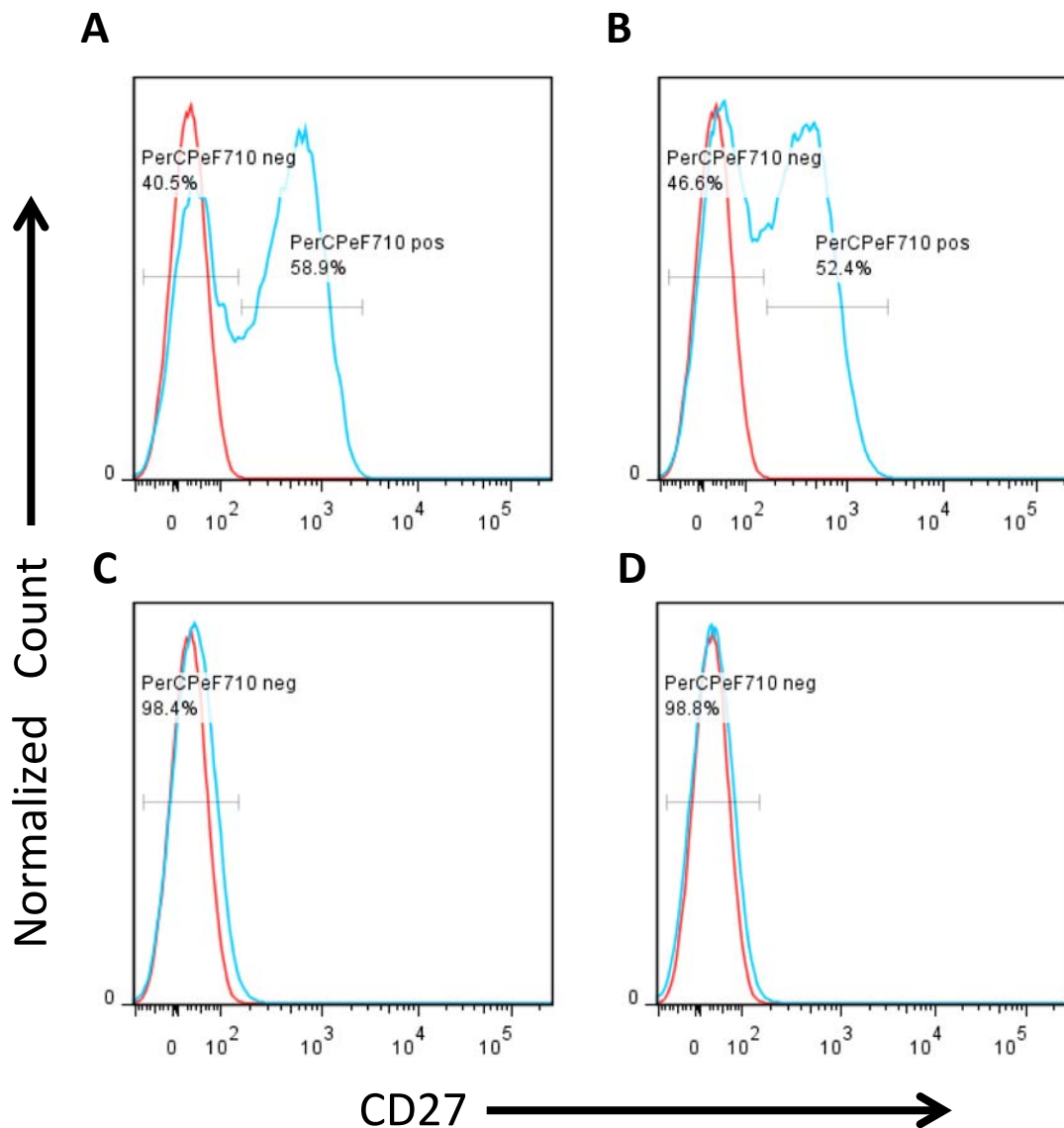


Figure 3-8. CD27⁺ Memory B cell isolation using an isolation kit was ineffective at sorting the CD27⁺ B cells. CD19⁺ B cells were negatively selected from total splenocytes (adult) and labeled with anti-CD27 magnetic microbeads followed by MACS. Using flow cytometry methods we analyzed CD27 expression, represented by a right shift in the histograms, (A) within the total splenocyte population prior to isolations, (B) following negative selection of the CD19⁺ B cells and (C) following positive selection with CD27-PE magnetic microbeads: the CD27⁺ B cell population. (D) The non-CD27⁺ B cell population shown following positive selection using CD27-PE magnetic microbeads. Red lines represent isotype controls and blue lines represent experimental samples. Data are representative of 3 experiments.

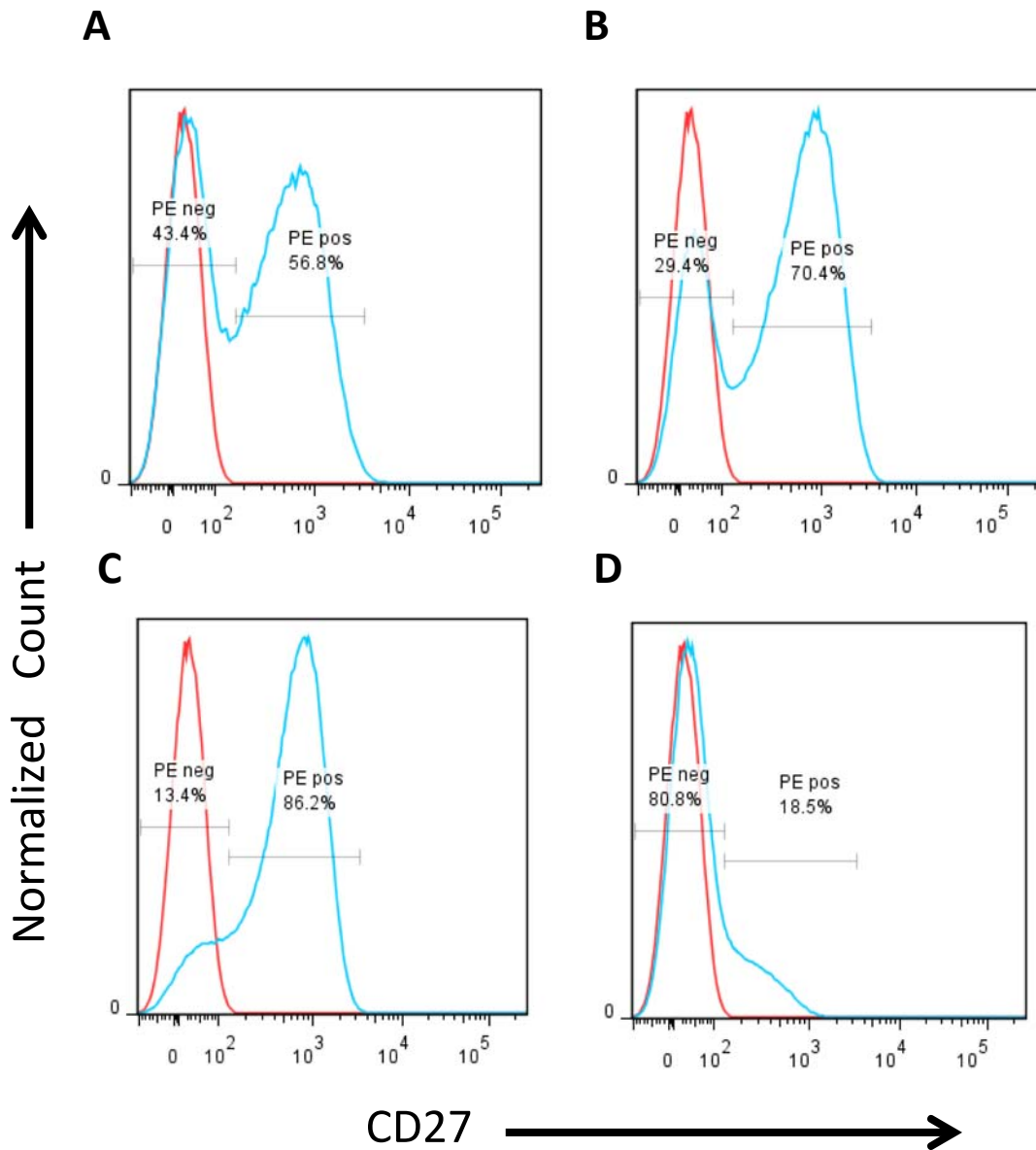


Figure 3-9. CD27⁺ Memory B cell isolation, with CD27-PE antibody + anti-PE magnetic microbeads and MACS, was effective at sorting the CD27⁺ B cells. CD19⁺ B cells were negatively isolated from total splenocytes (adult) and labeled using CD27-PE antibody + anti-PE magnetic microbeads followed by MACS. Using flow cytometry methods we analyzed the level of CD27 expression, represented by a right shift in the histograms, (A) within the total splenocyte population, (B) following negative selection of CD19⁺ B cells and (C) following positive selection with CD27-PE antibody and anti-PE magnetic microbeads. (D) The non-CD27⁺ B cell population is shown following positive selection using CD27-PE antibody and anti-PE magnetic microbeads. Red lines represent isotype controls and blue lines represent experimental samples. Data are representative of 3 experiments.

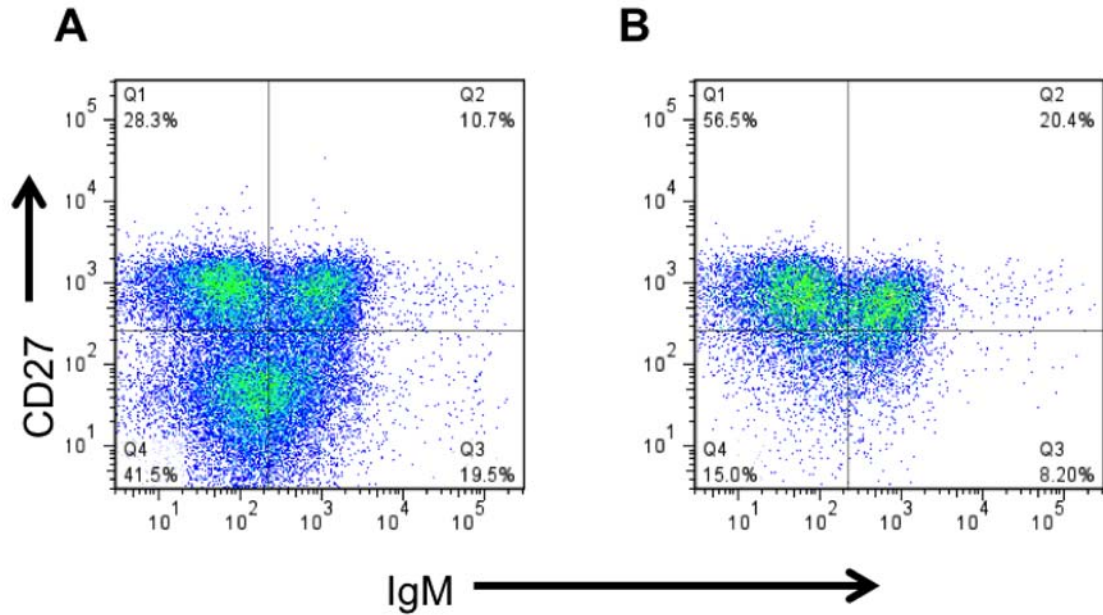


Figure 3-10. CD27⁺IgM⁺ B cell isolation, using anti-CD27-PE, anti-PE magnetic microbeads and anti-IgA/anti-IgG antibodies and MACS, was ineffective at sorting the CD27⁺IgM⁺ B cells. CD19⁺ B cells were negatively selected from total splenocytes (adult). In addition to the negative selection step, we added anti-IgA and anti-IgG antibodies to this protocol to also deplete IgA- and IgG-expressing B cells. We then labeled with CD27-PE antibody + anti-PE magnetic microbeads followed by MACS. Using flow cytometry methods, we analyzed the co-expression of CD27 and IgM (A) within the total splenocyte population and (B) following positive selection of CD27⁺ B cells with CD27-PE antibody, anti-PE magnetic microbeads and anti-IgA and anti-IgG antibodies. Data are representative of 5 experiments.

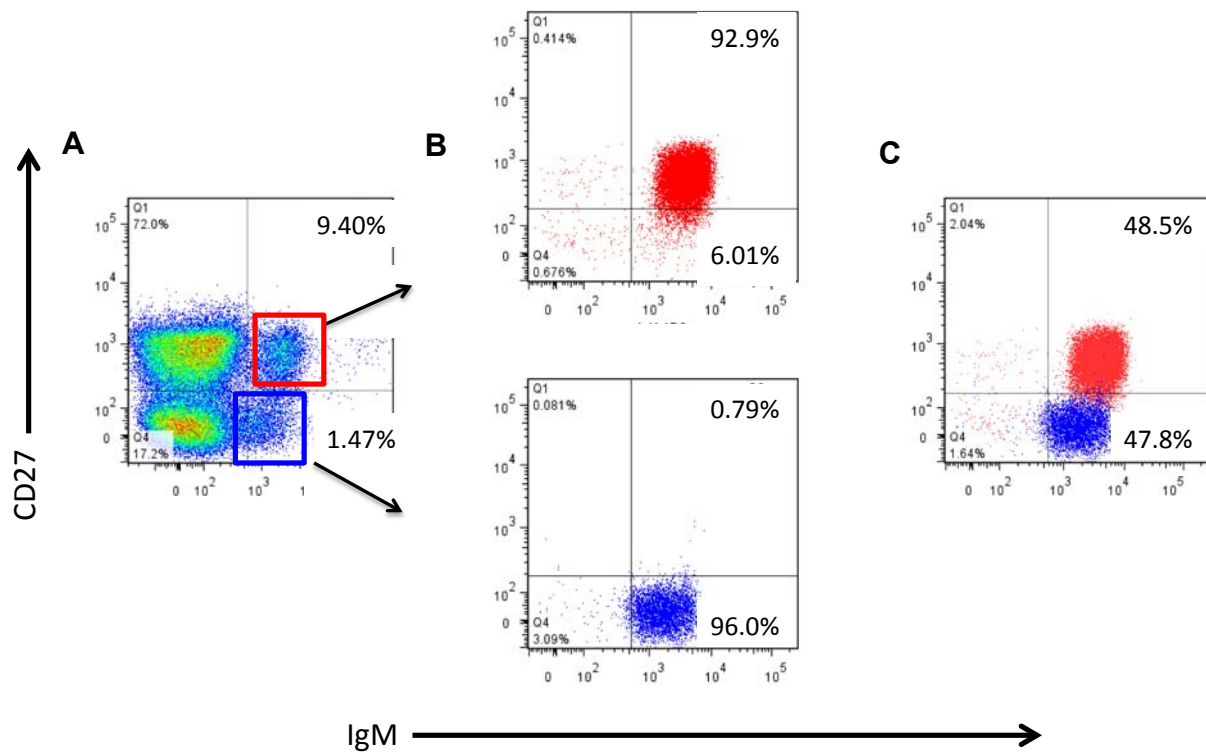


Figure 3-11. FACS resulted in high purities of CD27⁺IgM⁺ and CD27⁻IgM⁺ B cells. CD19⁺ B cells were negatively selected from total splenocytes (adult) and labeled with fluorescent anti-CD27 and anti-IgM antibodies. Labelled B cells were then sorted by FACS. Using flow cytometry methods we analyzed the expression of CD27 and IgM within (A) the total splenocyte population and (B) the CD27⁺IgM⁺ and CD27⁻IgM⁺ B cell populations following FACS. (C) An overlay of the CD27⁺IgM⁺ and CD27⁻IgM⁺ B cell populations. Data are representative of 12 experiments.

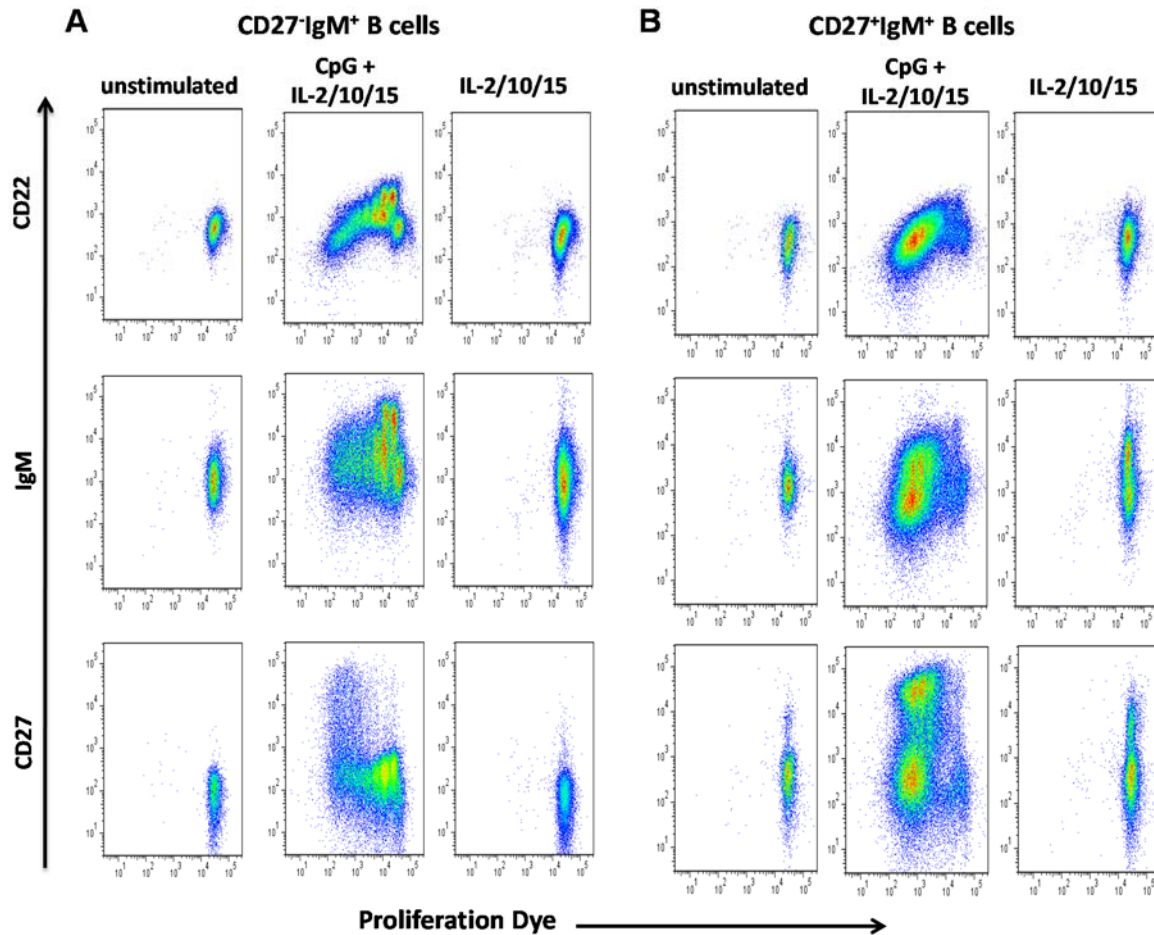


Figure 3-12. CpG, IL-2, IL-10 and IL-15 stimulation resulted in proliferation of CD27⁺IgM⁺ and CD27⁻IgM⁺ B cells (adult). (A) Splenic CD27⁻IgM⁺ and (B) CD27⁺IgM⁺ B cells were isolated by FACS (CD27⁺IgM⁺ purity: 91.5%; CD27⁻IgM⁺ purity: 89.7%), as per section 3.4.2.3. Following isolation, the cells were cultured for 7 days with CpG, IL-2, IL-10 and IL-15 stimulation (middle columns) and compared to unstimulated (left columns) and cytokine-only stimulation controls (right columns). Proliferation and surface expression of CD22, IgM and CD27 were measured by flow cytometry. Proliferating cells are represented by successive halving of the expression of VioBlue proliferation dye. Data are representative of 3 experiments.

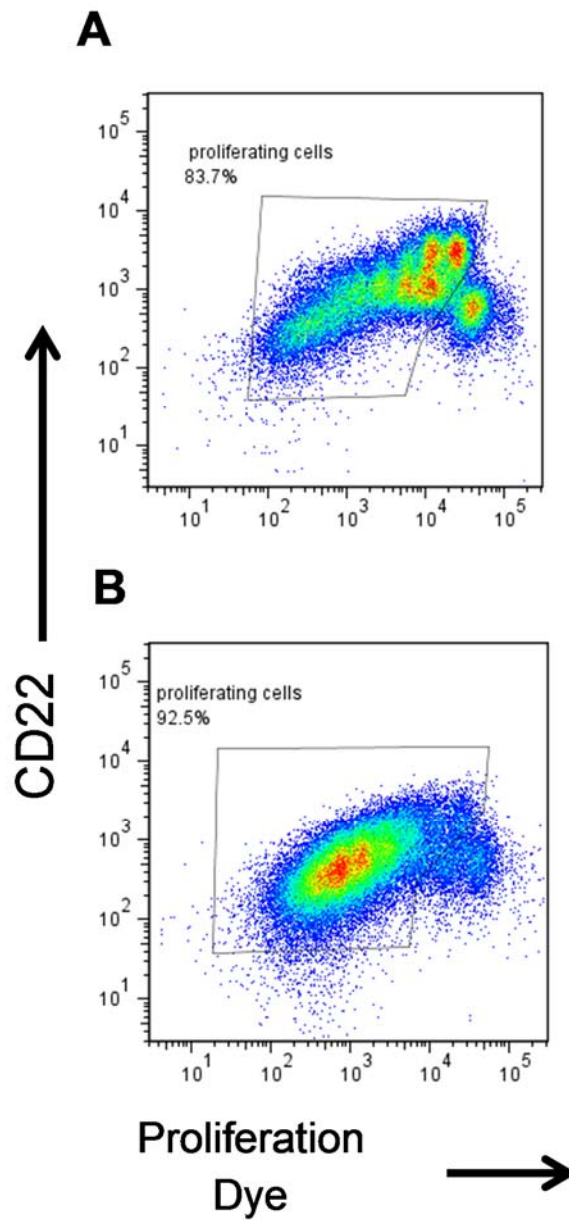


Figure 3-13. CD22 expression decreases on proliferating B cells (adult). Splenic CD27⁺IgM⁺ and CD27⁻IgM⁺ B cells were isolated by FACS (CD27⁺IgM⁺ purity: 91.5%; CD27⁻IgM⁺ purity: 89.7%), as per section 3.4.2.3. Following isolation, the cells were cultured for 7 days with CpG, IL-2, IL-10 and IL-15 stimulation. Proliferation and surface expression of CD22 was measured by flow cytometry. CD22 expression on proliferating (A) CD27⁻IgM⁺ and (B) CD27⁺IgM⁺ B cells. Proliferation represented by successive halving of the expression of VioBlue proliferation dye. Data from Figure 3-12.

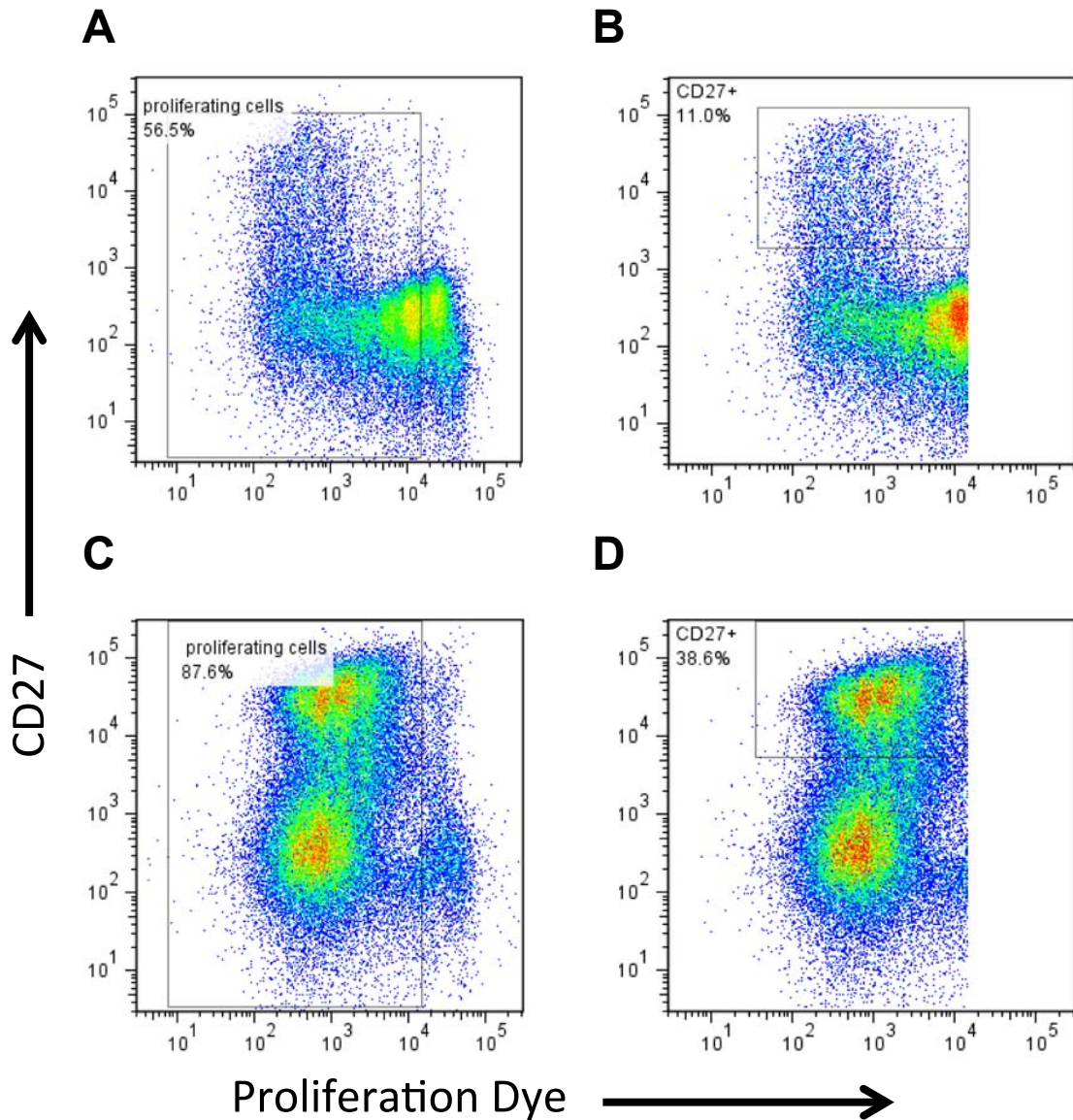


Figure 3-14. A percentage of proliferating CD27⁻ B cells became CD27⁺ after culture with CpG, IL-2, IL-10 and IL-15. Splenic CD27⁺IgM⁺ and CD27-IgM⁺ B cells were isolated by FACS (CD27⁺IgM⁺ purity: 91.5%; CD27-IgM⁺ purity: 89.7%), as per section 3.4.2.3. Following isolation, the cells were cultured for 7 days with CpG, IL-2, IL-10 and IL-15 stimulation. Proliferation and surface expression of CD27 was measured by flow cytometry. Proliferating (A) CD27-IgM⁺ and (C) CD27⁺IgM⁺ B cells are represented by successive halving of the expression of VioBlue proliferation dye. CD27 expression was analyzed within the proliferating cells of the (B) CD27-IgM⁺ and (D) CD27⁺IgM⁺ B cells. Data are representative of 3 experiments. Data from Figure 3-12.

Blood Type O, 18 years

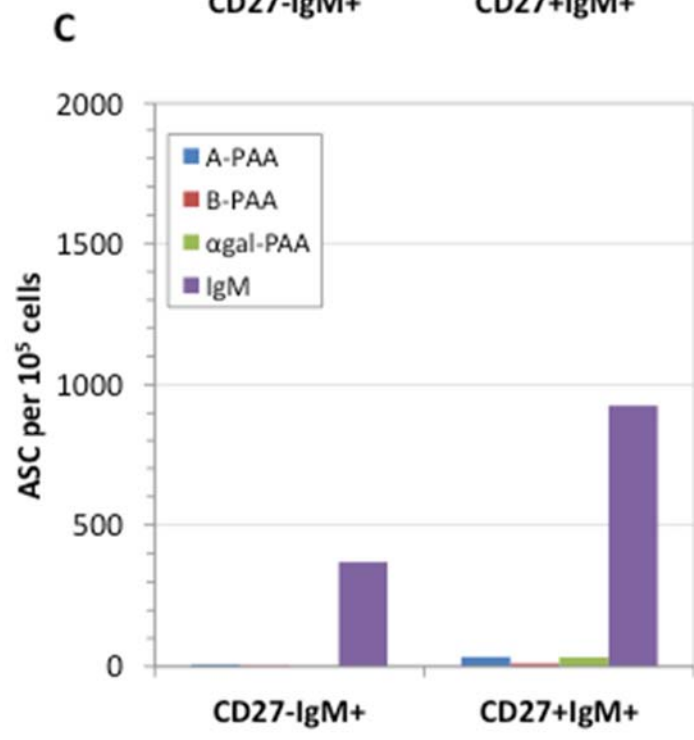
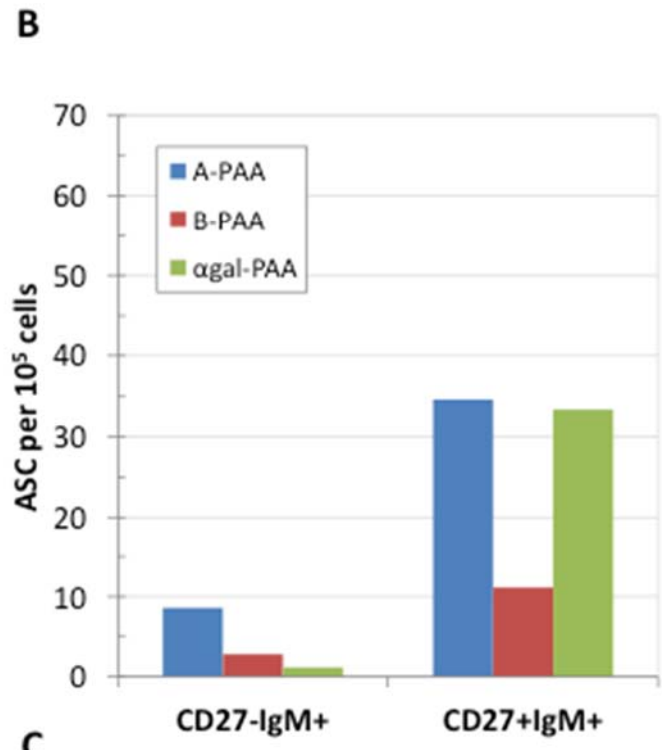
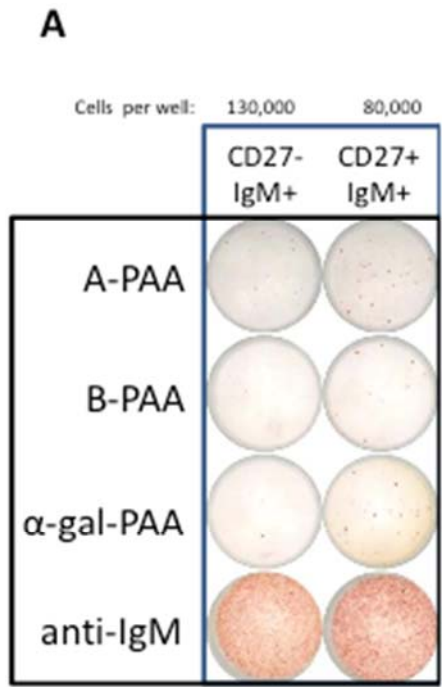


Figure 3-15. ELISPOT of CD27⁻IgM⁺ and CD27⁺IgM⁺ B cells isolated from splenocytes from a blood type O individual (18 years of age) by MACS. (Section 3.4.2.3.) The MACS purities were: CD27⁻IgM⁺: 45.7% (CD27⁻ cells in this population were 83%) and CD27⁺IgM⁺: 12.4% (CD27⁺ cells in this population were 85%). Following 7 days of culture with CpG, IL-2, IL-10 and IL-15, cells were counted and cultured overnight on ELISPOT plates. (A) Antibody-secreting cell (ASC) spots derived from cells isolated from the CD27⁻IgM⁺ (130,000 viable cells per well) and CD27⁺IgM⁺ (80,000 viable cells per well) populations. Spots represent total IgM ASC and IgM ASC specific to A-antigen (A-PAA), B-antigen (B-PAA) and α -gal-antigen (α -gal-PAA). (B) Number of IgM ASC specific to A-, B- and α -gal and (C) number of total IgM A/B ASC derived from CD27⁻IgM⁺ and CD27⁺IgM⁺ B cells are shown again for comparison.

Blood Type A, 66 years

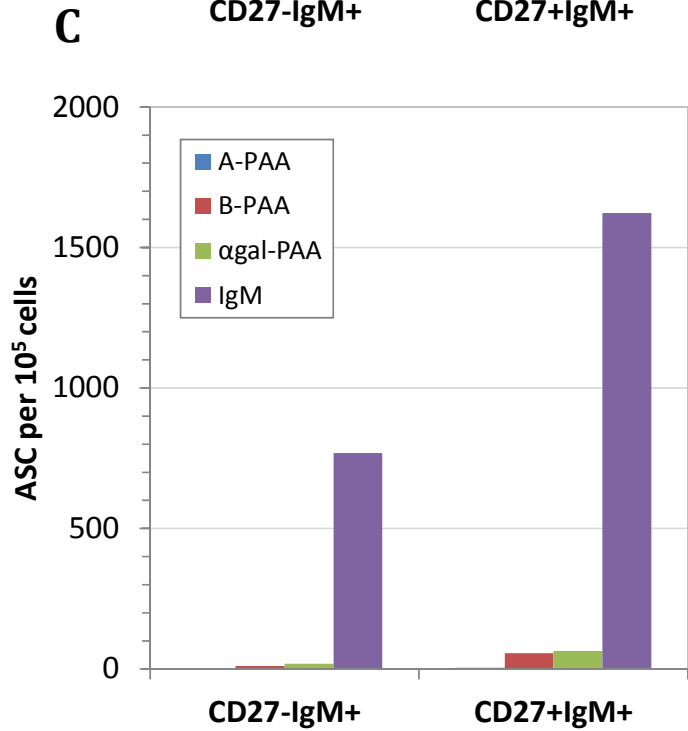
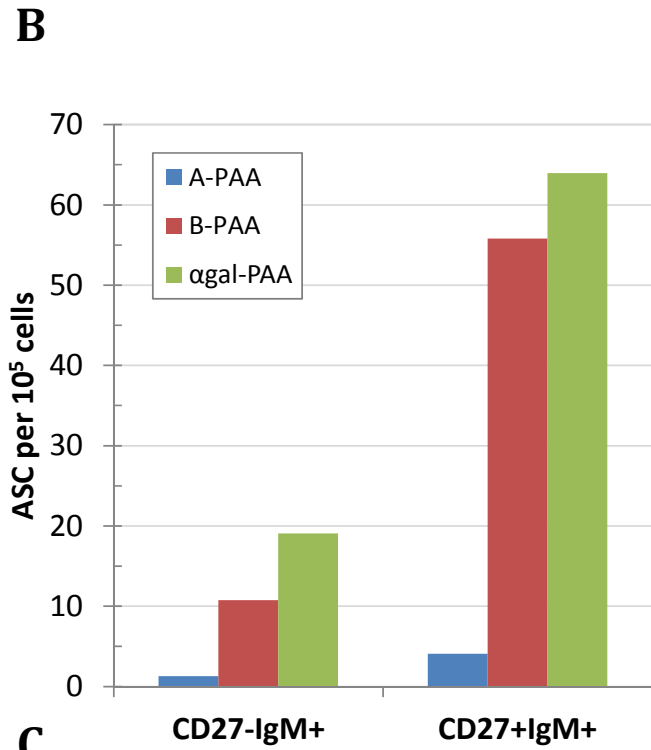
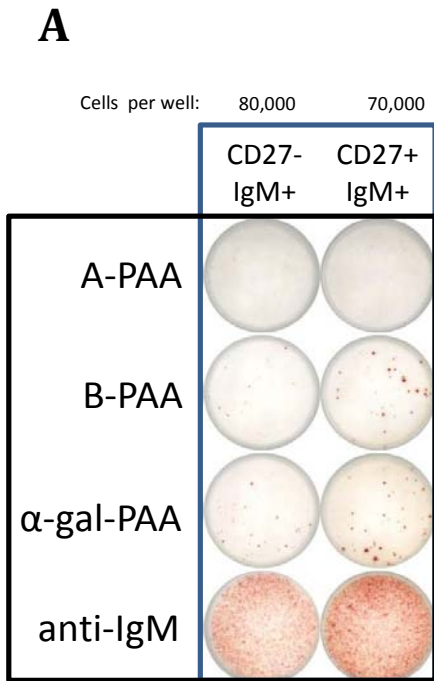


Figure 3-16. B cell ELISPOT of CD27⁻IgM⁺ and CD27⁺IgM⁺ B cells isolated from splenocytes from a blood type A individual (66 years of age) by MACS. (Section 3.4.2.3.) The MACS purities were: CD27⁻IgM⁺: 32.1% (CD27⁻ cells in this population were 78%) and CD27⁺IgM⁺: 26.4% (CD27⁺ cells in this population were 93%). Following 7 days of culture with CpG and cytokines, cells were counted and cultured overnight on ELISPOT plates. (A) ASC spots derived from cells isolated from the CD27⁻IgM⁺ (80,000 viable cells per well) and CD27⁺IgM⁺ (70,000 viable cells per well) populations. Spots represent total IgM ASC and IgM ASC specific to A-antigen (A-PAA), B-antigen (B-PAA) and α -gal-antigen (α -gal-PAA). (B) Number of IgM ASC specific to A-, B- and α -gal and (C) number of total IgM A/B ASC derived from CD27⁻IgM⁺ and CD27⁺IgM⁺ B cells are shown again for comparison.

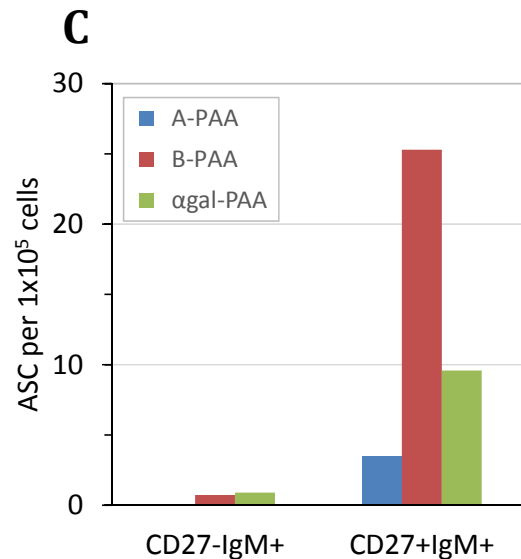
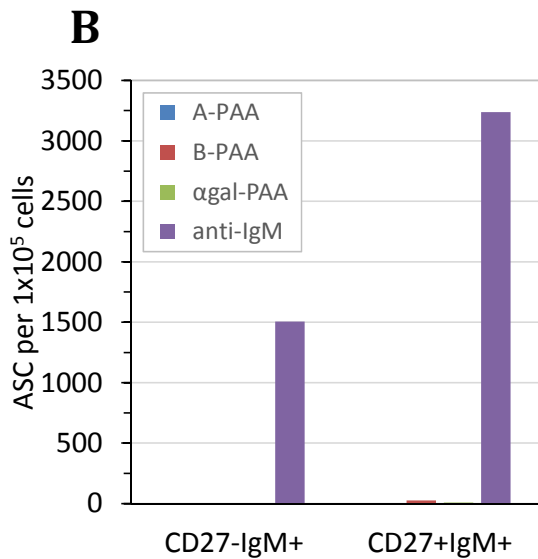
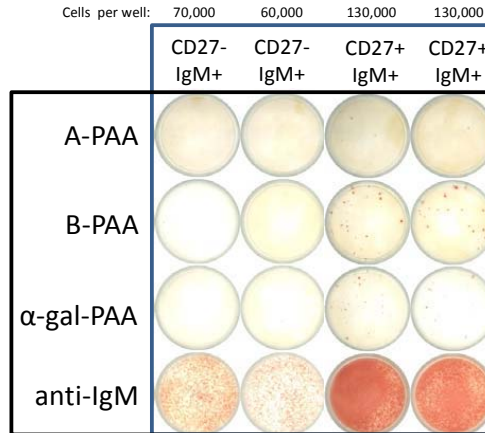
A**Blood Type A, 21 years**

Figure 3-17. B cell ELISPOT of CD27-IgM⁺ and CD27⁺IgM⁺ B cells isolated from splenocytes from a blood type A individual (21 years of age) by FACS. (Section 3.4.2.4) The FACS purities were: CD27-IgM⁺: 97.2% and CD27⁺IgM⁺: 85.5%. Following 7 days of culture with CpG and cytokines, cells were counted and cultured overnight on ELISPOT plates. (A) ASC spots derived from cells isolated from the CD27-IgM⁺ (70,000 or 60,000 viable cells per well) and CD27⁺IgM⁺ (130,000 viable cells per well) populations. Spots represent total IgM ASC and IgM ASC specific to A-antigen (A-PAA), B-antigen (B-PAA) and α -gal-antigen (α -gal-PAA). (B) Number of total IgM ASC and (C) number of IgM ASC specific to A-, B- and α -gal derived from CD27-IgM⁺ and CD27⁺IgM⁺ B cells.

CHAPTER FOUR: RESULTS - PHOSPHO-SPECIFIC FLOW CYTOMETRY (PPF) ASSAYS TO STUDY INFANT B CELL SIGNALING

4.1 Introduction

As previous results from Chapter three demonstrated an increased expression of CD22 on the CD27⁺IgM⁺ B cells of infants, coupled with the previously defined role of CD22 as an co-inhibitory molecule of the B cell, (2) we sought to determine if the increased expression on infant B cells had an effect on B cell signaling. To begin our investigation, we first optimized a PPF assay, designed to study immune cell signaling, (160) in Ramos cells upon BCR and/or CD22 stimulation.

This chapter describes various stimulations used in the PPF assay and subsequent examination of the signaling kinetics downstream the BCR (pY759) and CD22 (pY822). Optimization of the PPF assay in Ramos cells will allow us to move this technique into primary B cells and closely examine signaling patterns of infants and older individuals.

4.2 Results: Protocol optimization of PPF assays

4.2.1 Ramos cells express CD19, CD22, CD27 and IgM cell surface markers

We used a Ramos cell line to optimize the PPF assay and examine B cell signaling. We chose this particular cell line as it had been shown to bind both anti-IgM and α 2,6-linked sialic acids, (161) also known as CD22L. We investigated cell surface expression of CD19, CD22, CD27 and IgM and confirmed that Ramos cells were positive for these markers. (162-164) (Figure 4-1. Expression of CD22 and IgM on Ramos cells is crucial because our experimental design would later involve engagement of both the BCR (with anti-IgM) and CD22 (with CD22L) to study the direct effect of CD22 signaling on B cell signaling.

4.2.2 BCR stimulation with anti-IgM Ab initiates distinct signaling kinetics in Ramos cells

First, Ramos cells were stimulated using various concentrations of F(ab')₂ fragment goat-anti human IgM antibody (Ab). Phosphorylation of the intracellular epitope pY759 (PLC γ 2) was analyzed to determine B cell activation at several time points after BCR

stimulation. (129) With increasing concentrations of anti-IgM antibodies from 1µg/ml to 10µg/ml, a respective increase in the MFI of phosphorylated PLCγ2 was observed (Figure 4-2). Concentrations higher than 10µg/ml did not further increase the MFI, suggesting optimal B cell activation at this concentration. Therefore, we used 10µg/ml anti-IgM Ab stimulation in future PPF assays, consistent with previous studies.(165, 166)

Kinetics of PLCγ2 (pY759) phosphorylation showed a rapid increase in phosphorylated pY759 within the first four minutes after stimulation. The phosphorylation peaked at 12 minutes followed by a gradual decrease (Figure 4-3). We also examined the phosphorylation of pY822, a tyrosine residue located within the ITIM of CD22. As we were not directly stimulating through CD22 at this point, we did not expect to see the same level of phosphorylation as in the pY759. However, we did expect to see some phosphorylation as previous studies have shown that crosslinking of the BCR results in the rapid phosphorylation of CD22. (4, 167) Indeed, a rapid increase in MFI in the first four minutes was observed for pY822 phosphorylation after BCR stimulation. Similar to pY759, the MFI of pY822 also peaked at 12 minutes (Figure 4-4).

We tested anti-IgM Ab stimulation in combination with anti-IgM cross-linker (F(ab')₂ fragment donkey-anti goat IgG; 10µg/ml) to test whether further cross-linking the BCR would enhance the phosphorylation of pY759 and pY822. Kinetics of pY759 phosphorylation was not affected by the addition of anti-IgM cross-linker but differences were observed for the level of pY759 phosphorylation: the MFI of pY759 was lower in the combined stimulation compared to anti-IgM Ab stimulation alone. Kinetics and the MFI of pY822 were similar between anti-IgM Ab alone and the combined stimulation (Figure 4-5A). In additional experiments we tested anti-IgM Ab derived from two separate commercial hybridoma cells lines (clones: HB57 and HB138). Although stimulation of Ramos cells with this anti-IgM Ab resulted in an increased MFI of pY759, the MFI was much lower than the MFI observed after stimulation with the F(ab')₂ fragment (Figure 4-5 (B) and (C)). Thus according to the conditions tested, stimulation of Ramos cells with 10µg/ml affinity-purified F(ab')₂ fragment goat-anti human IgM resulted in maximal phosphorylation of pY759 as well as phosphorylation of pY822. As we move forward with the PPF assay in our primary cells we can begin with stimulation of the BCR using 10µg/ml affinity-purified F(ab')₂ fragment goat-anti human IgM.

4.2.3 Ramos cells can be stimulated with anti-IgM Ab bound to SaV-coated microspheres

In order for CD22 to bind CD22L and subsequently inhibit the activation of the B cell, CD22L must be in close proximity to the B cell antigen. (129) In an experimental setting, a platform is required onto which both anti-IgM and CD22L can be added. We explored the use of streptavidin (SaV)-coated microspheres for this purpose. We bound biotinylated F(ab')₂ fragment goat-anti human IgM Ab onto SaV microspheres. The maximum binding capacity of anti-IgM Ab to 50x10⁶ microspheres was a volume of 3μl (stock concentration: 1.7μg/μl) (Figure 4-6). Ramos cells were stimulated with anti-IgM Ab coated microspheres (ratio: 1 Ramos cell: 100 microspheres) for five minutes. Stimulation with anti-IgM Ab bound to microspheres resulted in an increase in pY759 phosphorylation compared to the unstimulated control; however, the level of phosphorylation was lower compared to stimulation with the soluble anti-IgM Ab control (Figure 4-7). Further studies are underway to increase the efficiency of this assay, including the titration of Ramos cell to microsphere ratio and the addition of biotinylated CD22L onto the microspheres along with the anti-IgM Ab.

4.2.4 The TLR9 pathway did not affect the signaling kinetics of PLCγ2 (pY759) and CD22 (pY822)

To investigate whether the observed signaling kinetics of PLCγ2 and CD22 were specifically due to BCR engagement and subsequent activation we tested CpG DNA, an additional stimulator of B cells, as a negative control. CpG DNA stimulates B cells through TLR9 (168) and activates a different signaling cascade that does not involve PLCγ2. As expected, the MFIs for both pY759 and pY822 remained unchanged, indicating that phosphorylation of these proteins in our system is specifically not due to activation through the TLR signaling cascade (Figure 4-8).

4.2.5 Approaches to study the effect of CD22 binding on downstream signaling

Next we used a couple of approaches to determine the effects of CD22 binding on downstream signaling and B cell inhibition. These experiments included: neuraminidase

treatment of Ramos cells to cleave the CD22-CD22L *cis* bindings on the cell surface, in order to free up CD22 so it could engage the BCR and inhibit the BCR signal (129) and the incubation our Ramos cells with high avidity ligands to promote CD22-CD22L binding in *trans* to assess whether this interaction could inhibit the BCR signal. (129)

We assessed CD22L expression on Ramos cells with and without neuraminidase treatment. Ramos cells had high expression of CD22L, which decreased after treatment with neuraminidase (Figure 4-9). The signaling kinetics of pY759 in neuraminidase treated Ramos cells was comparable to that of untreated Ramos cells (Figure 4-10 (A)). This suggests that releasing CD22 from its *cis* bindings by treatment with neuraminidase was not enough to inhibit the B cell signal. In contrast, phosphorylation of pY822 of treated cells tended to be lower at all time points when compared to untreated controls, albeit not significantly (Figure 4-10 (B)). These findings may suggest that the disrupted CD22-CD22L *cis* bindings following neuraminidase treatment resulted in a lowered pY822 signal.

As CD22 was said to be involved in B cell tolerance *in vivo* upon exposure of a high affinity ligands presented in *trans*, (2) we sought to engage CD22 in a similar way. To do so, we used CD22L conjugates generated through an ongoing GNT collaboration. CD22L was bound onto a BLG protein carrier in high or low binding densities. Ramos cells were stimulated for 12 minutes with CD22L-BLG conjugates at various concentrations and were compared to non-CD22L-BLG stimulated controls. The cells were also stimulated with anti-IgM Ab in order to determine if addition of the conjugates could inhibit the BCR signal. Addition of CD22L-BLG conjugates had no effect on the pY759 phosphorylation of Ramos cells at any of the concentrations tested Figure 4-11 (A). If they were to effectively inhibit the B cells, we would expect a decreased phosphorylation of pY759. (48) Similarly, there was no effect of the CD22L-BLG conjugates on the pY822 phosphorylation. In this case we might expect an increase in phosphorylation of pY822 should CD22 engage its ligand (Figure 4-11 (B)). These results may indicate that the CD22L did not bind the CD22 on the Ramos cells or that the BCR and CD22 need to be cross-linked. Further studies are necessary to determine whether presenting CD22L in this manner can effectively bind the CD22 on Ramos cells and result in alterations of the signaling kinetics: an increased pY822 and decreased pY759.

4.3 Summary

We successfully set up a PPF protocol in Ramos cells to analyze signaling responses of the BCR (PLC γ 2, pY759) and CD22 (pY822) upon stimulation with anti-IgM Ab. We are currently further optimizing this protocol for use in primary B cells of infants and adults (*Appendix A*) to define B cell signaling kinetics in these populations. Additional PPF studies involving CD22 engagement, including the effective use of CD22L conjugates on BLG proteins or SaV microspheres in conjunction with anti-IgM, are also underway. With this information we hope to begin to understand B cell signaling differences between infants and older individuals to further elucidate B cell tolerance mechanisms following infant ABOi HTx.

4.4 Figures

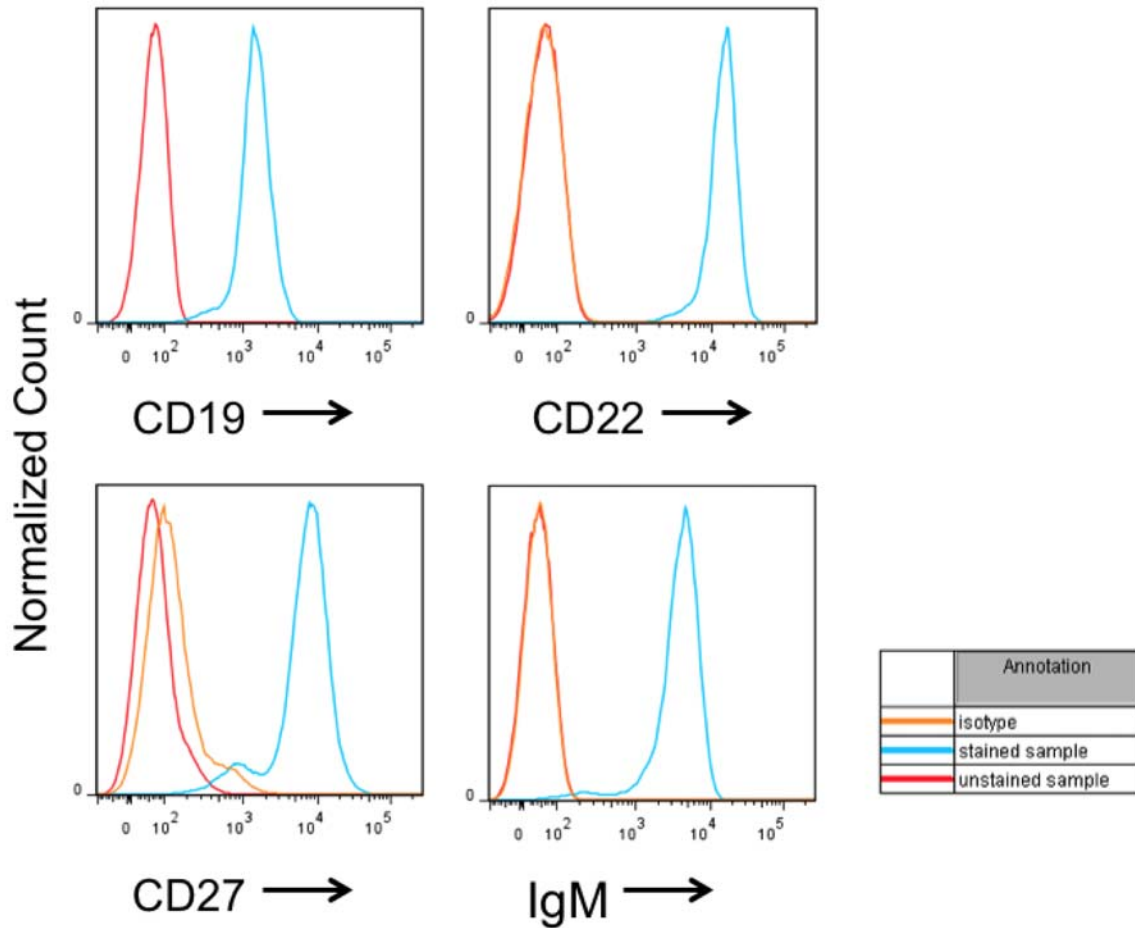


Figure 4-1. Ramos cells expressed surface markers CD19, CD22, CD27 and IgM. Cells were stained with antibodies directed against CD19, CD22, CD27 and IgM. Using multi-colour flow cytometry we evaluated the expression levels of CD22, CD27 and IgM within the CD19⁺ B cells. The orange line represents isotype controls and the red line represents unstained Ramos cells. Data are representative of 4 experiments.

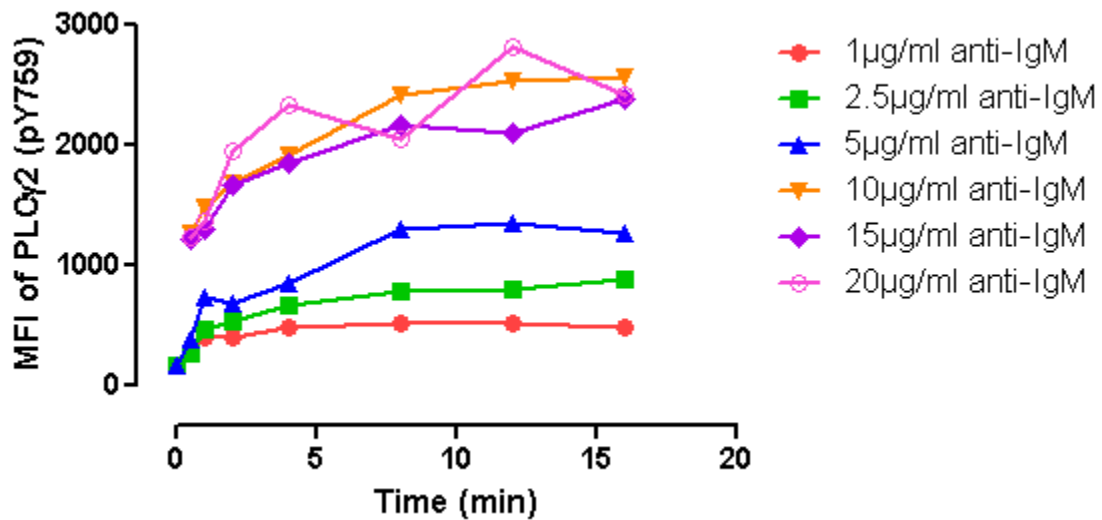


Figure 4-2. 10μg/ml anti-IgM Ab was optimal stimulation of Ramos cells in the Phospho-specific flow (PPF) assay. Ramos cells were stimulated with various concentrations of anti-IgM Ab: 1, 2.5, 5, 10, 15 and 20μg/ml for the duration of 0.5, 1, 2, 4, 8, 12 and 16 minutes. Following stimulation, the cells were fixed, permeabilized and stained with anti-PLCγ (pY759) Ab to analyze the level of pY759 phosphorylation, represented as the median fluorescent intensity (MFI) of PLCγ2 (pY759). Data from a single experiment are shown.

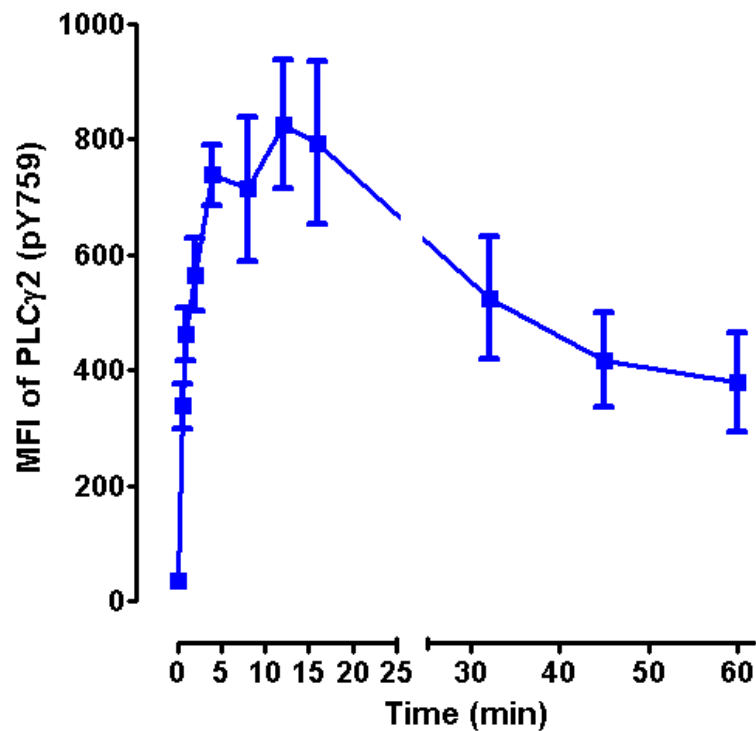


Figure 4-3. PLC γ 2 (pY759) signaling kinetics of Ramos cells upon anti-IgM Ab stimulation. Phosphorylation of the intracellular epitope pY759 (PLC γ 2) was determined by flow cytometry at the indicated time points following stimulation with anti-IgM Ab. The level of pY759 phosphorylation is represented as the MFI of PLC γ 2 (pY759) minus the MFI of the isotype control. Median and standard error are shown. Data represent eight experiments.

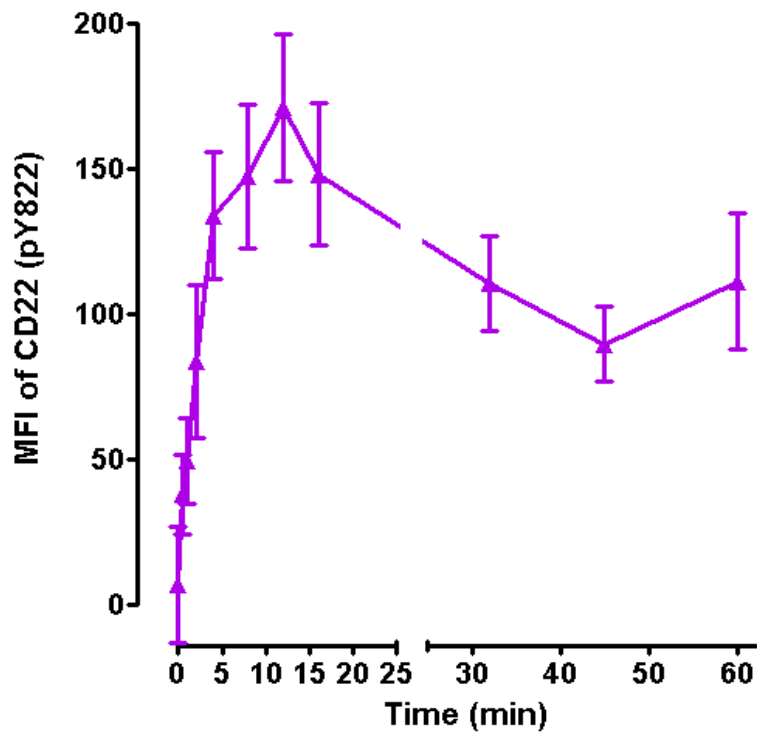


Figure 4-4. CD22 (pY822) signaling kinetics of Ramos cells upon anti-IgM Ab stimulation. Phosphorylation of the intracellular epitope pY822 (CD22) was determined by flow cytometry at the indicated time points following stimulation with anti-IgM Ab. The level of pY822 phosphorylation is represented as the MFI of CD22 (pY822) minus the MFI of the isotype control. Median and standard error are shown. Data represent eight experiments.

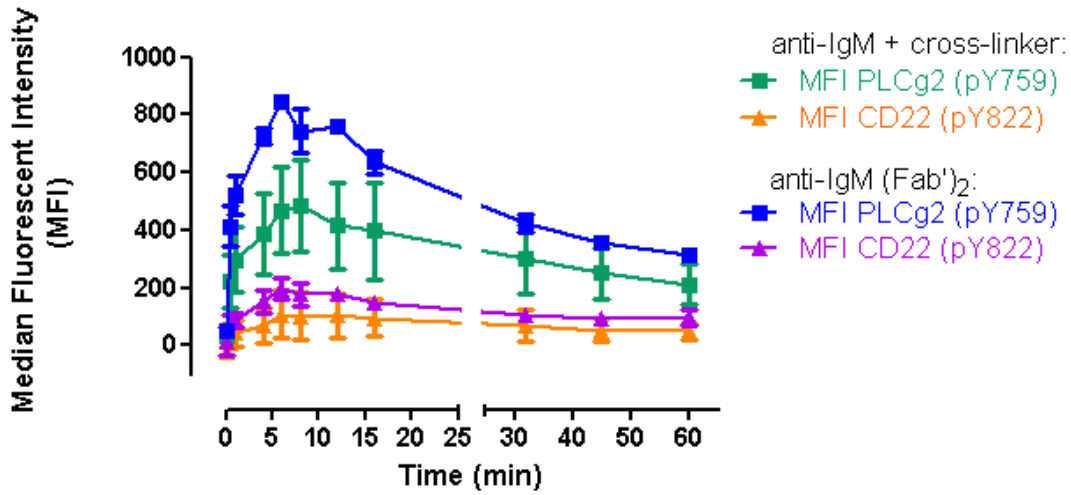
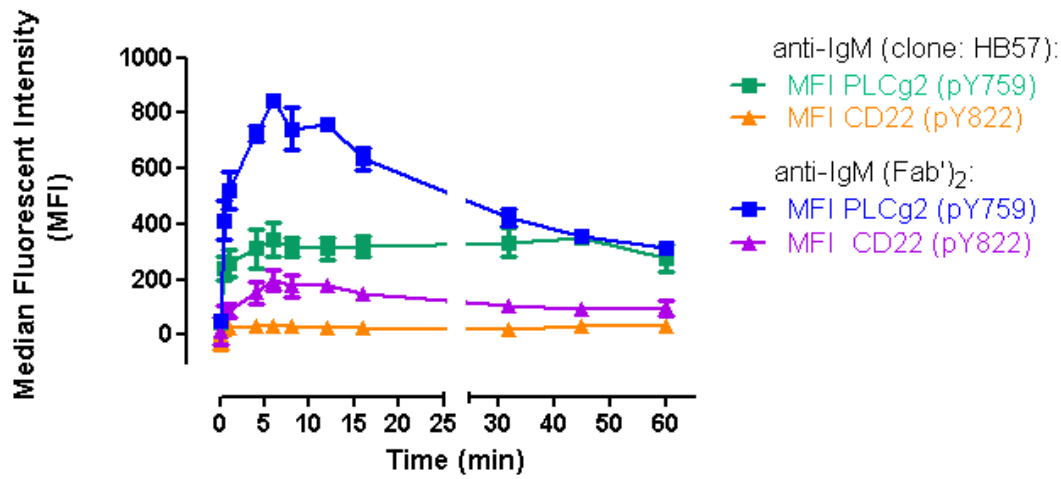
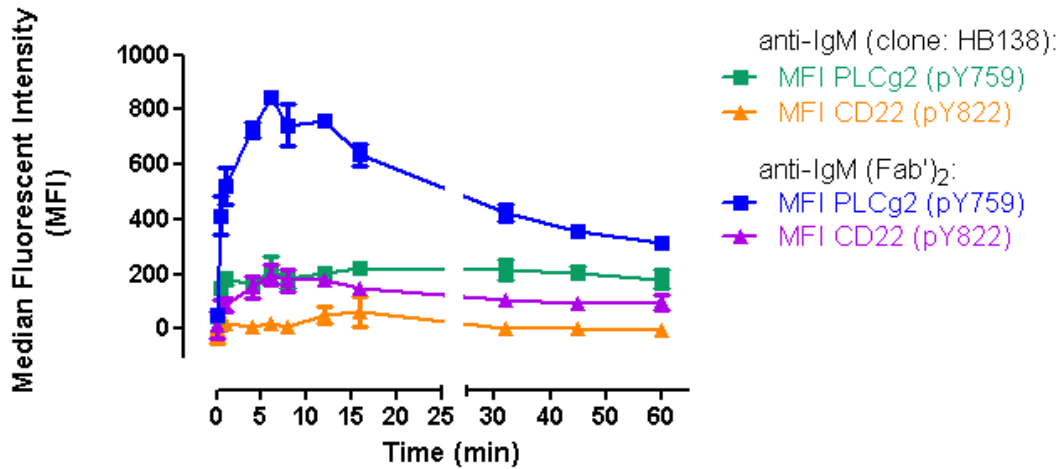
A**B****C**

Figure 4-5. Anti-IgM Ab (Fab')₂ stimulation alone was optimal in inducing PLC γ 2 (pY759) and CD22 (pY822) signaling kinetics in PPF assay of Ramos cells. Ramos cells were stimulated with (A) a combination of anti-IgM antibodies (affinipure F(ab')₂ fragment goat-anti human IgM) and anti-IgM cross-linker (affinipure F(ab')₂ fragment donkey-anti goat IgG), (B) anti-IgM Ab (clone HB57; derived from a hybridoma cell line) or (C) anti-IgM (clone HB138; derived from a hybridoma cell line) for the duration of the indicated time points. Signaling kinetics of PLC γ 2 and CD22 are presented as the MFI of pY759 and pY822, respectively (minus the MFI of the isotype controls). Anti-IgM Ab (affinipure F(ab')₂ fragment goat-anti human IgM) stimulation alone was used as a control. Median and standard error are shown. Data represent three experiments.

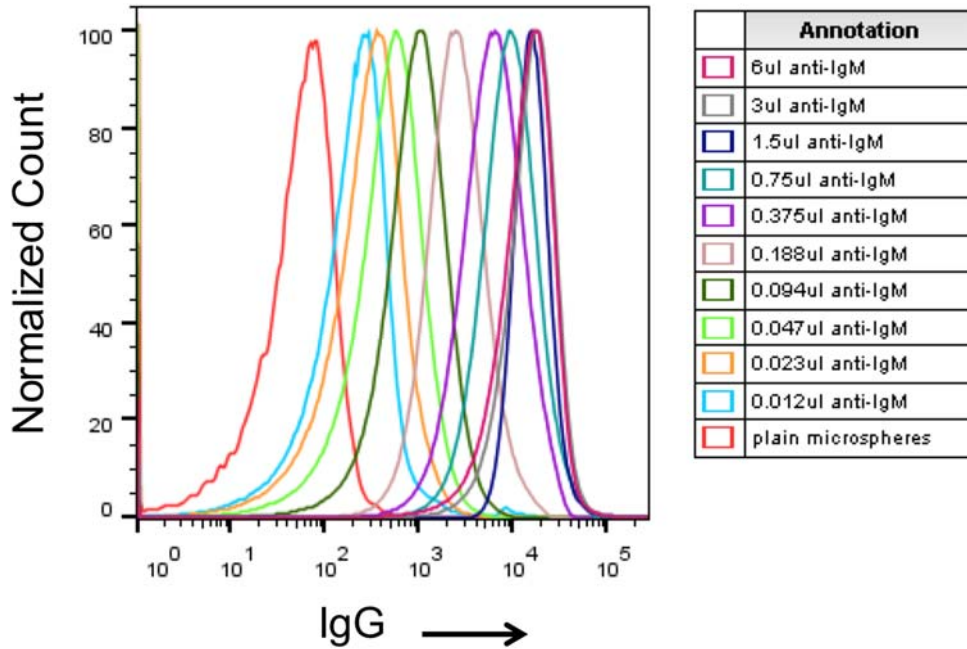


Figure 4-6. Bound biotinylated anti-IgM Ab could be detected on SaV microspheres. Various volumes of biotinylated anti-IgM Ab (F(ab')₂ fragment goat-anti human IgM; stock concentration: 1.7µg/µl) were incubated with SaV microspheres (50x10⁶ microspheres per condition). Following incubation, the microspheres were washed and bound anti-IgM on the microspheres was detected using flow cytometry with a AF647-conjugated donkey anti-goat IgG Ab. Data are representative of 3 experiments.

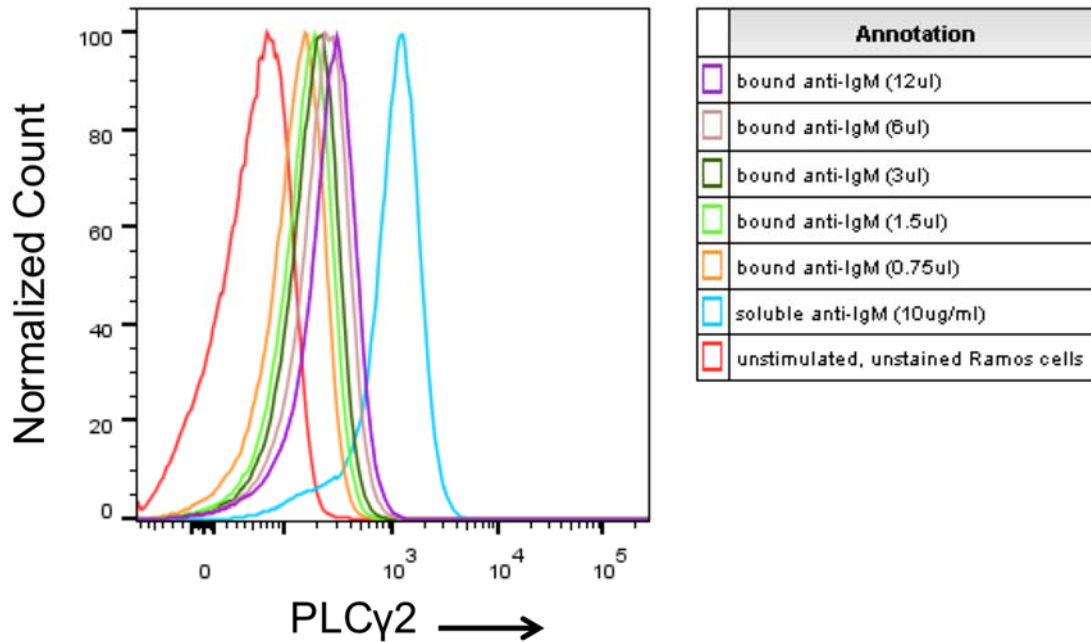


Figure 4-7. Stimulation with anti-IgM Ab bound to SaV microspheres led to the phosphorylation of PLC γ 2 (pY759). Ramos cells were stimulated for five minutes with SaV microspheres bound with various volumes of biotinylated anti-IgM Ab. Expression of PLC γ 2 was detected using flow cytometry with an AF647-conjugated anti-PLC γ 2 Ab. Soluble anti-IgM Ab (F(ab')₂ fragment goat-anti human IgM) stimulation was used as a control. Red line represents unstimulated, unstained Ramos cells. Data are representative of 3 experiments.

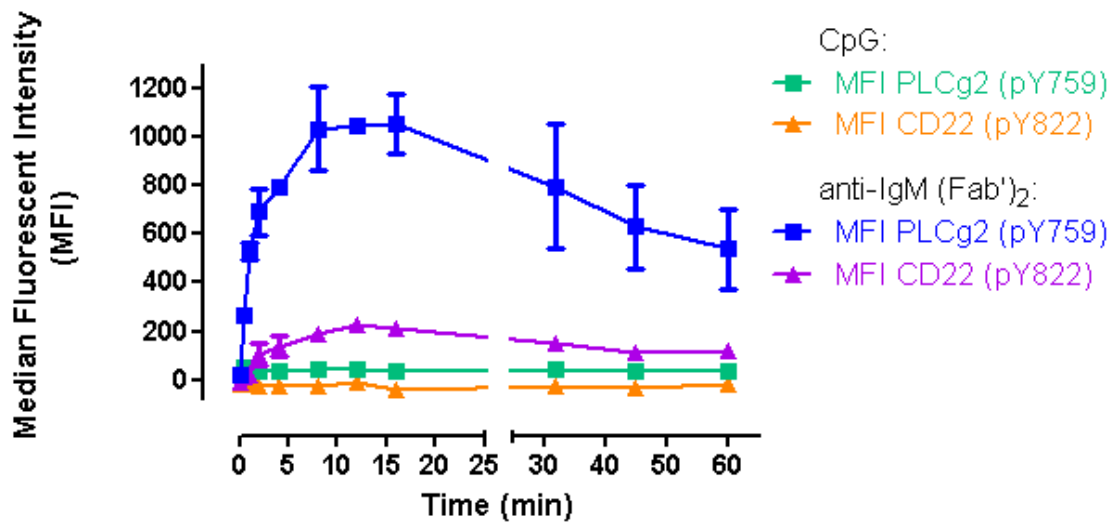


Figure 4-8. PLC γ 2 (pY759) and CD22 (pY822) signaling kinetics in Ramos cells not due to activation through the CpG-TLR signaling cascade. Ramos cells were stimulated with 2 μ g/ml of CpG for the duration of the indicated time points. Signaling kinetics of Ramos cells are presented as the MFIs of pY759 and pY822 minus the MFI of the respective isotype controls. Anti-IgM Ab (affinipure F(ab')₂ fragment goat-anti human IgM) stimulation was used as a control. Median and standard error are shown. Data represent two experiments.

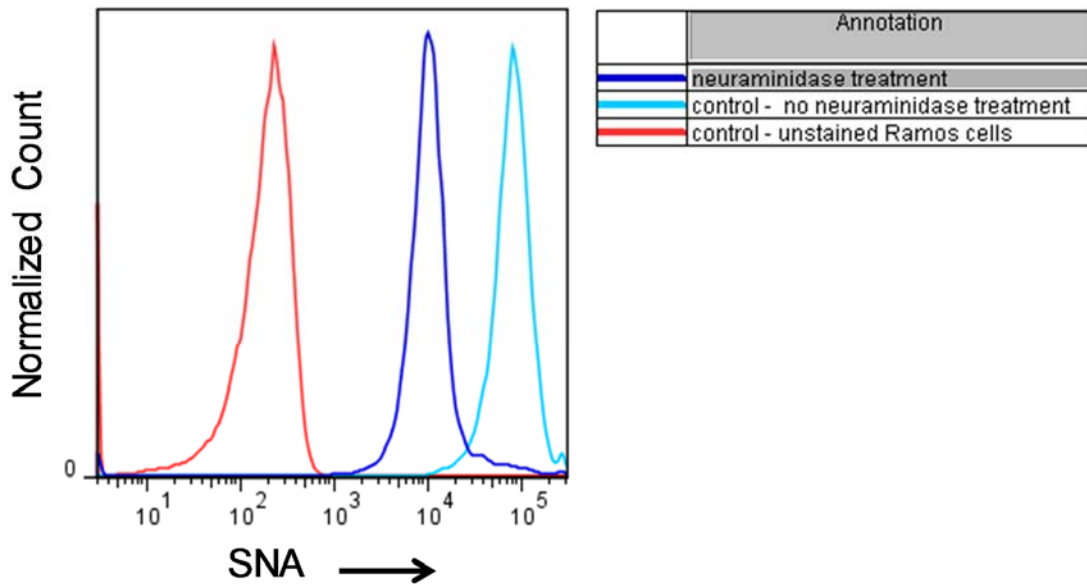


Figure 4-9. Neuraminidase treatment resulted in cleaving the CD22L on the surface of Ramos cells. Ramos cells were treated with neuraminidase (dark blue) followed by a staining with FITC-conjugated SNA lectin to determine the expression of CD22L on the Ramos cell surface. Ramos cells without neuraminidase treatment were used as a control (light blue line). Red line represents unstimulated, unstained Ramos cells. Data are representative of four experiments.

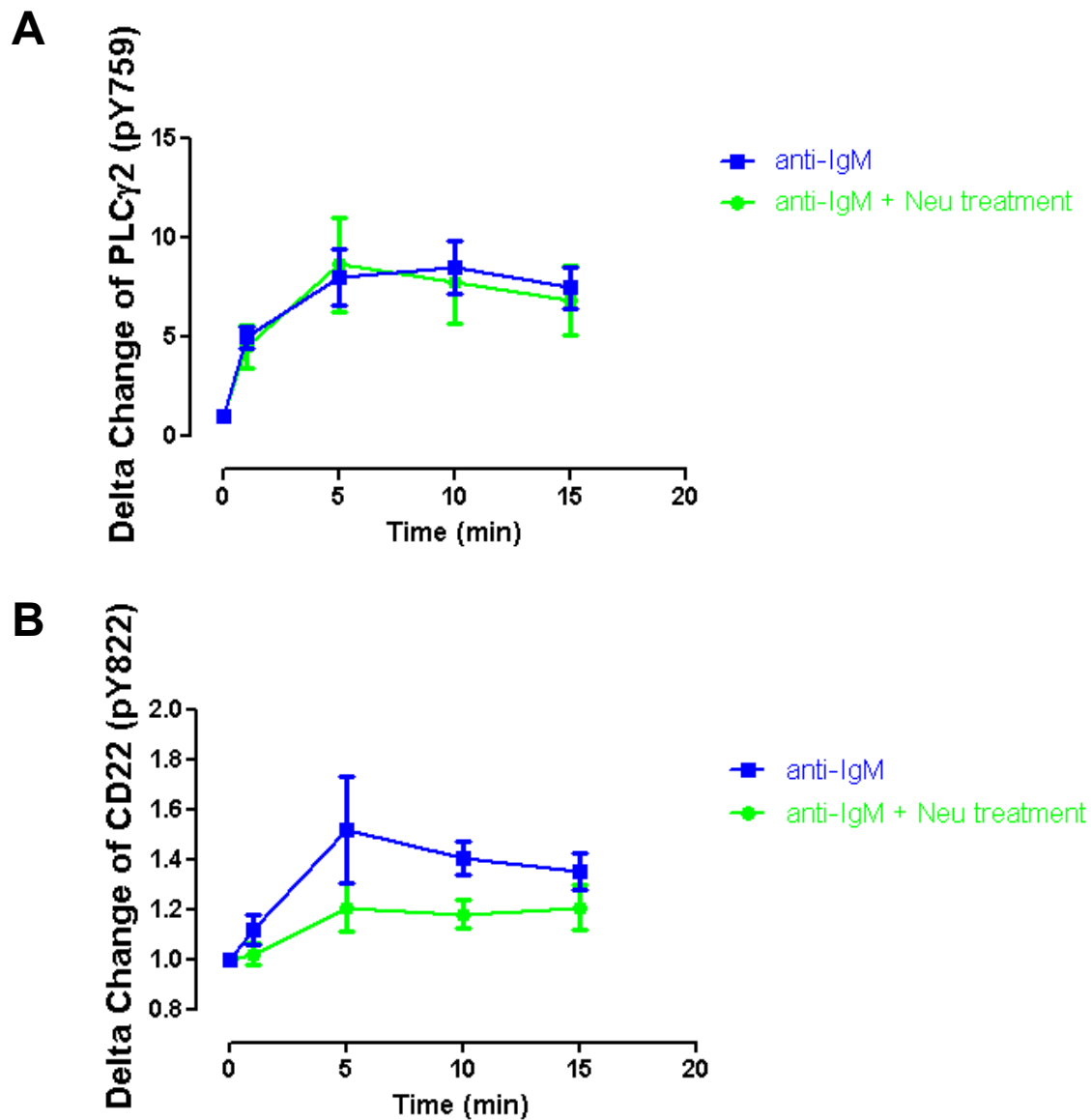


Figure 4-10. Neuraminidase treatment did not affect PLC γ 2 (pY759) and CD22 (pY822) signaling kinetics in Ramos cells. Following neuraminidase treatment, Ramos cells were stimulated with anti-IgM Ab (affinipure F(ab')₂ fragment goat-anti human IgM) for 1, 5, 10 and 15 minutes. Signaling kinetics of Ramos cells are presented as the Delta change of the MFI, defined as the MFI of time point (x) divided by MFI of time-point 0 (unstimulated), for (A) pY759 and (B) pY822. No significant difference was found in the pY822 signaling (2way ANOVA). Ramos cells without neuraminidase treatment were used as a control. Median and standard error are shown. Data represent four experiments.

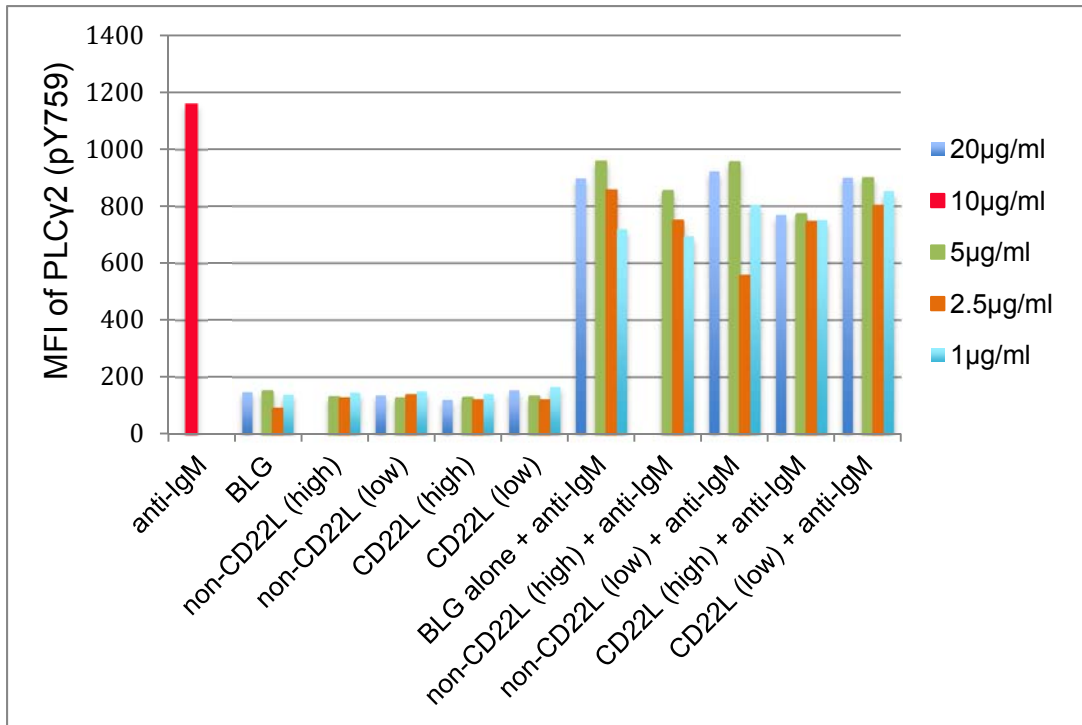
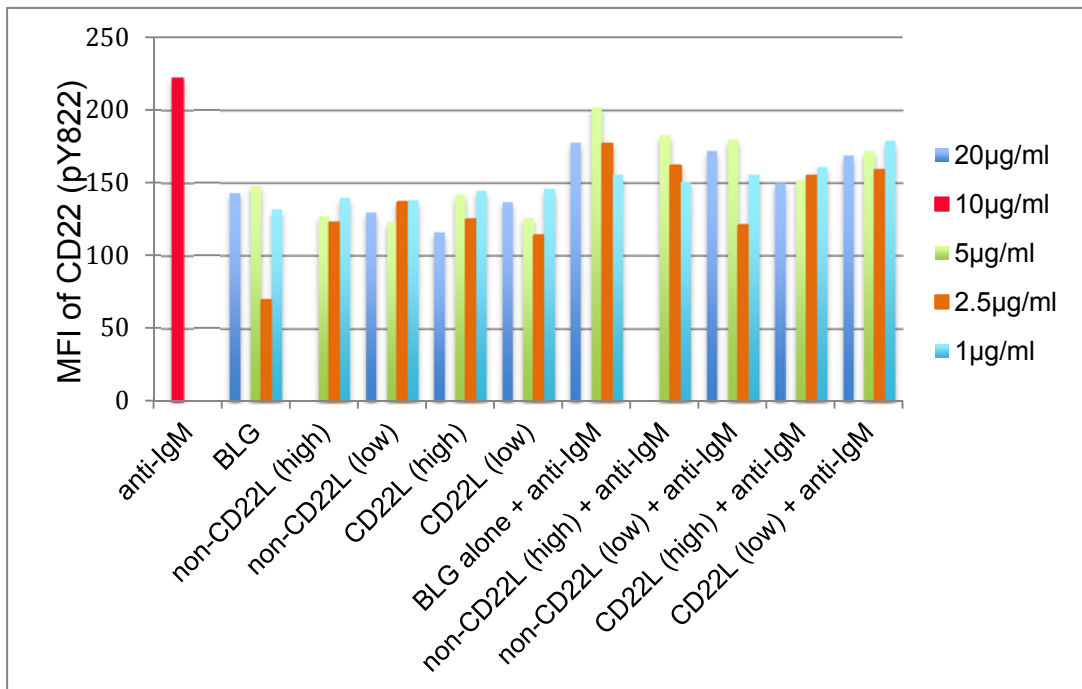
A**B**

Figure 4-11. Stimulation with CD22L-BLG conjugates did not affect PLC γ 2 (pY759) and CD22 (pY822) phosphorylation in Ramos cells. Ramos cells were stimulated for 12 minutes with 1 μ g/ml, 2.5 μ g/ml, 5 μ g/ml and 20 μ g/ml CD22L-BLG conjugates and compared to non-CD22L-BLG conjugate controls. The CD22L and non-CD22L were bound to the BLG protein carriers at high and low densities. In addition, Ramos cells were stimulated for 12 minutes with anti-IgM Ab (affinipure F(ab')₂ fragment goat-anti human IgM) together with CD22L-BLG conjugates at the same concentrations as above. Signaling of BCR and CD22 is represented as the MFI of (A) pY759 and (B) pY822, respectively. Soluble anti-IgM stimulation and BLG were used as controls. Data from a single experiment are shown.

CHAPTER FIVE: DISCUSSION

5.1 Analysis of primary B cells: CD22 expression, B cell isolations and ELISPOT analysis

CD22 has been previously identified as a co-inhibitory molecule of B cells. (101, 136, 169-171) Duong *et al.* (2) demonstrated that CD22 is involved in *in vivo* B cell tolerance to TI-2 antigens in mice. Based on these findings, together with knowledge that carbohydrate antigens, such as ABO antigens, are TI-2 antigens, (97) we were interested in determining whether CD22 plays a role in the development of donor-specific B cell tolerance to donor A/B antigens in infants following ABOi HTx.

We examined various naïve and memory B cells subsets in the peripheral blood and spleen including: recent bone marrow emigrants (CD27⁻IgM⁺IgD⁺CD38^{high}), naïve B cells (including both CD27⁻IgM⁻IgD⁺ and CD27⁻IgM⁺IgD⁺ populations), CD27⁻IgM⁻IgD⁻ B cells, memory B cells (CD27⁺IgM⁺) and class-switched memory B cells (CD27⁺IgM⁻). It is worth noting that the CD27⁻IgM⁻IgD⁻ B cells were defined solely based on three surface markers and thus we cannot determine if they are class-switched memory cells expressing IgG or IgA (172) or naïve B cells. These populations can be differentiated by expression of the ATP-binding cassette B1 transporter on naïve B cells but not memory cells. (173)

Our results demonstrated that one particular B cell subset, CD27⁺IgM⁺ B cells from the spleen, had significantly higher expression of CD22 in infants (defined in our study as individuals < 2 years in age) compared to older individuals. The increased expression of CD22 on infant CD27⁺IgM⁺ B cells may suggest that these cells have greater propensity to CD22-mediated inhibition.

From our studies, there was no one infant B cell subset from the peripheral blood with significantly increased expression of CD22 when compared to all other subsets. Viemann *et al.* (174) also looked at the surface expression of CD22 on human B cells. They compared cord blood samples to adult blood samples and found no differences in CD22 expression. Based on differential expression of CD22 that we observed between splenic and peripheral blood CD27⁺IgM⁺ B cells, this may suggest functional differences in these B cells. We have not yet tested the functionality of the CD27⁺IgM⁺ B cells from peripheral blood versus

spleen. Due to low frequencies of CD27⁺IgM⁺ B cells in peripheral blood we were unable to obtain enough PBMC to isolate this subset using FACS. It is important to note that the differences observed in CD22 expression in PBMC vs. splenocytes may be related to the B cells themselves. They are derived from different clinical sources and, as previously mentioned, there are unavoidable differences in the manner the samples are handled before processing. For example, spleen samples may not be processed for up to 24 hours, which may affect the expression of B cell surface markers, including CD22.

Some technical aspects need to be considered when interpreting our data derived from peripheral blood and spleen. Firstly, the primary cells used in these experiments were from frozen PBMC and splenocyte samples. Since freezing and thawing processes may affect cell frequency and viability, samples with a post-thaw viability less than 85% were not used. Although standardized processing protocols are in place, minor deviations in sample processing may also affect the quality of the cells. In addition, the time between sample collection and processing is different for spleen tissue and peripheral blood. Generally, for spleen samples the timeframe from collection of the tissue in the operating room to time of tissue processing could be up to 24 hours. Additionally, as the spleen samples are obtained from organ donors, there may be variability in the quality of the tissue. Peripheral blood samples, in contrast, are usually collected and processed within 6 hours. Secondly, there were a limited number of infant spleen samples available for use in these experiments. An advantage of our study was that we were able to assess B cell phenotype from spleen and peripheral blood of numerous individuals from different age groups. Nonetheless, a potential drawback of the study is that we still had relatively small sample sizes for certain age groups (for statistical purposes).

To work towards understanding whether the higher expression of CD22 on CD27⁺IgM⁺ B cells in infants is likely to play a role in B cell tolerance after ABOi HTx, we were interested in investigating whether this population contained A/B-specific ASC. To assess this question, it was necessary to first isolate the CD27⁺IgM⁺ B cells. Initial attempts at isolating these B cells with commercial isolation kits and MACS were unsuccessful. A possible reason for this may have been because the kits were designed for isolation of B cells from peripheral blood (we adjusted parameters in the kits to maximize isolation from spleen). We moved on to use PE-conjugated anti-CD27 antibody and anti-PE microbeads followed by

MACS, which resulted in a high purity of CD27⁺ B cells. Since this protocol was based on positive selection, additional isolation of IgM⁺ B cells had to be done by negative selection. Anti-IgA and anti-IgG biotinylated antibodies were added to the existing negative B cell isolation step, however, this did not deplete all IgM⁻ B cells and a substantial proportion of these cells remained following isolation. As we did not further examine the IgM⁻ population from this sort, it is unclear whether the depletion of IgA⁺ and/or IgG⁺ cells was insufficient or whether these cells were IgA⁻IgG⁻IgM⁻. Ultimately, a technique using FACS effectively isolated the CD27⁺IgM⁺ B cells from both infant and adult samples with high purities. The CD27⁻IgM⁺ B cell subset was used as a comparison control in the ELISPOT assays. With highly pure populations of CD27⁺IgM⁺ and CD27⁻IgM⁺ B cells after FACS we were able to assess whether the CD27⁺IgM⁺ B cells contained A/B ASC.

Work in our laboratory has demonstrated that, although rare in number, anti-A/B antibody-secreting B cells can be detected and quantified in human peripheral blood using a B cell ELISPOT assay. ((1), Motyka, unpublished data) This assay was used to determine whether the A/B-specific ASC could be derived from CD27⁺IgM⁺ memory B cells from spleen. The ELISPOT assay is a highly sensitive technique used for detection, measurement and functional analysis of immune cells. (175, 176) Our B cell ELISPOT protocol is based on the work of Dr. Martin Zand (152) with modifications optimized in our lab to include the specific detection of IgM antibody-secreting B cells. The number of antigen-specific B cells was detected using the Immunospot analyzer/software and compared to the total number of antibody-secreting B cells. The production of α -gal specific antibodies was used as a positive control in our ELISPOT assays. Anti- α -gal is a natural antibody produced in humans, apes and Old World monkeys. It is directed against the carbohydrate antigen α -gal epitope with the structure Gal α 1-3Gal β 1-4GlcNAc-R that is expressed in non-primate mammals, New World monkeys and prosimians. (159)

It has been reported that CD27⁻ B cells do not express TLRs and require stimulation through the BCR in order to express TLR-9 and become responsive to CpG. (177) On the other hand, Huggins *et al.* (152) described that naive B cells could increase TLR-9 expression and proliferate in response to CpG stimulation without BCR signaling. After assessing the proliferation of CD27⁺IgM⁺ and CD27⁻IgM⁺ B cells after 7-day culture with CpG, IL-2, IL-10 and IL-15, our proliferation studies were consistent with what Huggins *et*

al. reported: proliferation of both subsets occurred, thus CD27⁻ B cells were responsive to CpG without prior BCR stimulation.

From the ELISPOT results we concluded that IgM A/B-specific ASCs were predominantly derived from the CD27⁺IgM⁺ memory B cell subset. However, there was production of anti-A/B antibodies from the CD27⁻IgM⁺ B cell subset as well. Therefore, it is also possible that ASC were derived from the CD27⁻IgM⁺ B cells. Future studies are needed to study this in detail. We assessed the surface expression of CD27 after 7-day culture. About 10% of the proliferating CD27⁻IgM⁺ B cells up regulate CD27. As this population contained up to 10% CD27⁺IgM⁺ memory B cells after 7-day culture, this could be an additional explanation for the anti-A/B antibody production from the CD27⁻IgM⁺ B cell subset.

Since B cells in the ELISPOT assay were stimulated for differentiation into ASC, the cell frequencies observed in the results may not represent the original frequency of functional A/B-specific B cells of the starting sample. Another caveat of the ELISPOT assay was the use of FACS-sorted cells. Issues with FACS could include cell activation, instrument performance, exposure of cells to multiple stainings, washes and the physical sorting itself.

Our results showing that infant splenic CD27⁺IgM⁺ B cells have increased expression of co-inhibitory CD22 and that the CD27⁺IgM⁺ B cells also contained the ASC, are consistent with our hypothesis that CD22 may be involved in B cell tolerance to donor A/B antigens following infant ABOi HTx. The increased CD22 expression on infant B cells may be involved in inhibiting B cell responses to A/B antigens present within the donor graft and may contribute to the induction of tolerance following infant ABOi HTx. We further investigated the functional effect of CD22 on B cell signaling.

5.2 PPF assays to study infant B cell signaling

Crucial to defining the role of CD22 in donor-specific B cell tolerance after ABOi infant HTx is investigating the ability of CD22 to inhibit signaling in infant B cells. The PPF assay enables examination of multiple intracellular signaling molecules of immune cells at a single-cell level. (160) We first optimized the PPF assay using a Ramos B cell line. Use of the cell line offered minimal variation between samples and an abundant supply of cells. Assessing intracellular signaling kinetics in Ramos cells involved stimulation with F(ab')₂

anti-human IgM Ab. We measured the phosphorylation of PLC γ 2 (at tyrosine Y759), an intracellular signaling protein located downstream from the BCR, a protein also involved in calcium mobilization and B cell activation. (178) We also examined the phosphorylation of CD22 (at tyrosine Y822), found within the ITIM on the intracellular tail of CD22. (127) In our studies we defined B cell activation as the increase in phosphorylation of Y759 (PLC γ 2). We were also interested in measuring the activation state of CD22 to determine whether engaging CD22 with its ligand would result in increased phosphorylation of Y822 (CD22). Based on previous studies of the co-inhibitory function of CD22, we predicted that upon engagement of CD22 with its ligand we would see increased phosphorylation of Y822 (CD22) and decreased phosphorylation of Y759 (PLC γ 2).

To assess the effects of CD22-CD22L *cis* binding on B cell signaling we used neuraminidase, an enzyme that cleaves sialic acids (CD22L) on cell surfaces, to disrupt the *cis* interactions of CD22-CD22L on the surface of the B cell. (179) As *cis* interactions are thought to sequester CD22 away from the BCR so that the B cell can be activated (129), we predicted that after neuraminidase treatment, CD22 could then interact with the BCR and inhibit the B cell signal. However, neuraminidase treatment had no effect on intracellular signaling of the Ramos cells; this finding may suggest that disrupting *cis* binding alone is not sufficient in altering signaling kinetics. Additional studies including engagement of CD22 with its ligand in combination with neuraminidase may provide additional insights on the impact of disrupting *cis* binding.

5.3 Future Directions

In this thesis, we have made important initial steps to characterize the potential role of CD22 in B cell tolerance to donor A/B antigens after ABOi HTx. Future experiments assessing the similarities and/or differences in B cell signaling between infant and adult CD27⁺IgM⁺ B cells, both before and after the engagement of CD22, are underway. Preliminary data showed that our optimized protocol for the PPF assay could be used successfully in primary cells. B cell signaling was observed in FACS-sorted CD27⁺IgM⁺ and CD27⁻IgM⁺ B cells from infant and adult splenic B cells upon stimulation with anti-IgM Ab (Appendix A). It will be difficult, however, to FACS-sort these subsets from PBMC due to

limited volumes of peripheral blood obtained from infants combined with low frequencies of A/B-specific B cells. A major advantage of the PPF assay is that multiple parameters can be used to identify specific B cell subsets and sorting is not required. However, not all antibodies for cell surface staining are compatible with the PPF assay protocol. Future experiments will include identifying antibodies that can withstand the treatment of the PPF protocol and optimization of surface staining in order to effectively gate on the CD27⁺IgM⁺ B cells during analysis. In addition, in combination with future PPF assays it is imperative that we also compare total PLC γ 2 of infants and older individuals as they may have different total expressions levels. To date, we have looked at the phosphorylation of one specific tyrosine residue of PLC γ 2, pY759, in Ramos cells and primary B cells. Examining total PLC γ 2 will allow us to compare infant and adult signaling more effectively.

In our first attempts to engage CD22 in *trans* we incubated CD22L (conjugated to a BLG protein carrier at high and low binding densities) with Ramos cells for 12 minutes. Anti-IgM Ab was added separately to the Ramos cells to ensure stimulation of the B cell and thus produce measurable pY759 signal. As mentioned above, we expected engagement of CD22 with CD22L to have a greater effect on inhibiting the B cell signal when compared to the non-CD22L controls. However, we saw no difference in the PLC γ 2 phosphorylation between the CD22L and the non-CD22L controls. An explanation may be that the CD22L and the anti-IgM stimulating Ab were not close enough in proximity to one another to inhibit the B cell effectively, as they were added to the cells separately. Co-polymers, expressing both CD22L and anti-IgM Ab present on the same surface, have been shown to inhibit the B cell signal successfully. (129) Furthermore, the higher the level of CD22 substitution, the more effective the inhibition of the B cell signal. Thus, it may be a requirement that CD22L and anti-IgM Ab be in close proximity to each other, perhaps presented on the same surface. Future plans include adding biotinylated CD22L onto SaV microspheres alongside our biotinylated-anti-IgM at various concentrations and examining both PLC γ 2 and CD22 signaling with the PPF assay (Appendix B). We have shown that it is possible to add biotinylated anti-IgM to SaV microspheres and stimulate the Ramos cells in a PPF assay. Since infant samples have a higher level of CD22 expression than older individuals on their CD27⁺IgM⁺ B cells, we would expect these cells to be more susceptible to inhibition when compared to other B cell subsets (described herein) and to samples of older individuals.

In order to prove my hypothesis that CD22 present on host B cells binds to CD22L present on donor heart tissue (or cells derived from donor heart) and, together with specific BCR binding to graft A/B antigens, inhibits B cell activation leading to donor-specific B cell tolerance in the infant ABOi HTx setting, it is important to define the presence of CD22L on the vascular endothelium of the heart. If the endothelium of the heart does express CD22L, tolerance of the B cells could be occurring at the site of the graft (or at sites of graft-derived cells). A study by Kitagawa *et al.* (125) demonstrated that the enzyme responsible for synthesizing the NeuAca α 2,6Gal linkage of the CD22 ligand, is detectable in both fetal and adult human heart tissue. However, Nitschke *et al.* (180) did not detect CD22L expression on mouse vasculature structures of the spleen, lymph, heart and liver. Further investigation is necessary for direct examination of the expression of CD22L on vascular endothelium of human cardiac tissue. Nitschke *et al.* (180) did show CD22L to be expressed in the bone marrow sinusoidal endothelium and has been implicated in CD22-dependent homing of B cells. If CD22L is not expressed on vascular endothelium of cardiac tissue, an alternative explanation may be that B cell tolerance occurs within the bone marrow, or in other non-graft sites with high CD22L expression. If this were the case, the donor A/B antigens would also have to be present in the bone marrow or other non-graft sites, alongside the CD22L.

There is great interest in exploiting the natural mechanisms of CD22-CD22L binding as an alternative therapeutic approach to diseases such as cancers. Chen *et al.* (181) developed liposomal nanoparticles decorated with CD22 ligands to selectively target cancerous B cells. Liposomal doxorubicin displaying high-affinity ligands for CD22 targeted and delivered chemotherapeutic treatment to CD22-expressing B cells. These liposomes induced complete remissions in mice with various human B cell lymphomas. A similar study examining human and murine B cells demonstrated that it was possible to kill CD22-expressing B cells by subjecting them to sialoside probes conjugated to the toxin saporin. This resulted in toxin uptake by the cells and further toxin-mediated killing of the B cell lymphoma lines. (114) Together these results illustrate that it is possible to manipulate the natural mechanisms of CD22 and its ligands for clinical therapy purposes. Similar CD22-directed therapeutic strategies could be investigated in the transplant setting. As part of an ongoing GNT collaboration, we have developed nanoparticles that are decorated with A/B blood group antigens. It may be possible to decorate these nanoparticles with synthetic

CD22L in addition to A/B antigens and test their ability to induce tolerance of A/B-antigen specific B cells.

5.4 Significance

Our lab group has previously demonstrated that infant transplant recipients of ABOi heart transplants develop tolerance to graft ABO antigens, however tolerance mechanisms remain unclear. Understanding the signaling mechanisms in B cells will provide insight into the inhibitory pathways involved in B cell tolerance after ABOi infant HTx. This may generate helpful new knowledge that may allow new insights. Together this could lead to consideration of new approaches which may enable us to the expand ABOi transplantation to include the much larger population of older patients awaiting transplantation, thus leading toward an ultimate goal of decreased waiting list mortality.

Results presented in this thesis that support the hypothesis that CD22 may contribute to B cell tolerance to donor A/B antigens following ABOi infant HTx include increased expression of CD22 on infant CD27⁺IgM⁺ B cells which were shown to contain the A/B-specific ASC. Ultimately, in order to link the results of this study into the realm of ABO-related responses, additional studies are necessary to investigate further the function of A/B ASC of infants and adults upon engagement of CD22.

CHAPTER SIX: REFERENCES

1. Fan X, Ang A, Pollock-Barziv SM, Dipchand AI, Ruiz P, Wilson G, et al. Donor-specific B-cell tolerance after ABO-incompatible infant heart transplantation. *Nature medicine*. 2004;10(11):1227-33.
2. Duong BH, Tian H, Ota T, Completo G, Han S, Vela JL, et al. Decoration of T-independent antigen with ligands for CD22 and Siglec-G can suppress immunity and induce B cell tolerance in vivo. *The Journal of experimental medicine*. 2010;207(1):173-87.
3. Lanoue A, Batista FD, Stewart M, Neuberger MS. Interaction of CD22 with alpha2,6-linked sialoglycoconjugates: innate recognition of self to dampen B cell autoreactivity? *European journal of immunology*. 2002;32(2):348-55.
4. Jellusova J, Nitschke L. Regulation of B cell functions by the sialic acid-binding receptors siglec-G and CD22. *Frontiers in immunology*. 2011;2:96.
5. Dipchand AI, Kirk R, Edwards LB, Kucheryavaya AY, Benden C, Christie JD, et al. The Registry of the International Society for Heart and Lung Transplantation: Sixteenth Official Pediatric Heart Transplantation Report--2013; focus theme: age. *The Journal of heart and lung transplantation : the official publication of the International Society for Heart Transplantation*. 2013;32(10):979-88.
6. Mitchell SC, Korones SB, Berendes HW. Congenital heart disease in 56,109 births. Incidence and natural history. *Circulation*. 1971;43(3):323-32.
7. Hoffman JI, Kaplan S. The incidence of congenital heart disease. *J Am Coll Cardiol*. 2002;39(12):1890-900.
8. Maron BJ, Towbin JA, Thiene G, Antzelevitch C, Corrado D, Arnett D, et al. Contemporary definitions and classification of the cardiomyopathies: an American Heart Association Scientific Statement from the Council on Clinical Cardiology, Heart Failure and Transplantation Committee; Quality of Care and Outcomes Research and Functional Genomics and Translational Biology Interdisciplinary Working Groups; and Council on Epidemiology and Prevention. *Circulation*. 2006;113(14):1807-16.
9. Bailey LL, Nehlsen-Cannarella SL, Doroshow RW, Jacobson JG, Martin RD, Allard MW, et al. Cardiac allotransplantation in newborns as therapy for hypoplastic left heart syndrome. *N Engl J Med*. 1986;315(15):949-51.

10. West LJ. Antibodies and ABO-incompatibility in pediatric transplantation. *Pediatr Transplant*. 2011;15(8):778-83.
11. Rydberg L. ABO-incompatibility in solid organ transplantation. *Transfus Med*. 2001;11(4):325-42.
12. Cartron JP, Colin Y. Structural and functional diversity of blood group antigens. *Transfus Clin Biol*. 2001;8(3):163-99.
13. Mollicone R, Candelier JJ, Mennesson B, Couillin P, Venot AP, Oriol R. Five specificity patterns of (1----3)-alpha-L-fucosyltransferase activity defined by use of synthetic oligosaccharide acceptors. Differential expression of the enzymes during human embryonic development and in adult tissues. *Carbohydr Res*. 1992;228(1):265-76.
14. Oriol R, Mollicone R, Couillin P, Dalix AM, Candelier JJ. Genetic regulation of the expression of ABH and Lewis antigens in tissues. *APMIS Suppl*. 1992;27:28-38.
15. Yamamoto F, Clausen H, White T, Marken J, Hakomori S. Molecular genetic basis of the histo-blood group ABO system. *Nature*. 1990;345(6272):229-33.
16. Watkins WM. Biochemistry and Genetics of the ABO, Lewis, and P blood group systems. *Advances in human genetics*. 1980;10:1-136, 379-85.
17. Fong SW, Qaqundah BY, Taylor WF. Developmental patterns of ABO isoagglutinins in normal children correlated with the effects of age, sex, and maternal isoagglutinins. *Transfusion*. 1974;14(6):551-9.
18. Springer GF, Horton RE. Blood group isoantibody stimulation in man by feeding blood group-active bacteria. *The Journal of clinical investigation*. 1969;48(7):1280-91.
19. Wuttke NJ, Macardle PJ, Zola H. Blood group antibodies are made by CD5+ and by CD5- B cells. *Immunol Cell Biol*. 1997;75(5):478-83.
20. Starzl TE, Ishikawa M, Putnam CW, Porter KA, Picache R, Husberg BS, et al. Progress in and deterrents to orthotopic liver transplantation, with special reference to survival, resistance to hyperacute rejection, and biliary duct reconstruction. *Transplantation proceedings*. 1974;6(4 Suppl 1):129-39.
21. Stock PG, Sutherland DE, Fryd DS, Ascher NL, Payne W, Simmons RL, et al. ABO-compatible mismatching decreases 5-year actuarial graft survival after renal transplantation. *Transplantation proceedings*. 1987;19(6):4522-4.

22. Paul LC, Baldwin WM, 3rd. Humoral rejection mechanisms and ABO incompatibility in renal transplantation. *Transplantation proceedings*. 1987;19(6):4463-7.
23. Gugenheim J, Samuel D, Reynes M, Bismuth H. Liver transplantation across ABO blood group barriers. *Lancet*. 1990;336(8714):519-23.
24. Alexandre GP, Squifflet JP, De Bruyere M, Latinne D, Reding R, Gianello P, et al. Present experiences in a series of 26 ABO-incompatible living donor renal allografts. *Transplant Proc*. 1987;19(6):4538-42.
25. Zschiedrich S, Kramer-Zucker A, Janigen B, Seidl M, Emmerich F, Pisarski P, et al. An update on ABO-incompatible kidney transplantation. *Transplant international : official journal of the European Society for Organ Transplantation*. 2014.
26. Danovitch GM. Cultural barriers to kidney transplantation: a new frontier. *Transplantation*. 2007;84(4):462-3.
27. Hardacre H. Response of Buddhism and Shinto to the issue of brain death and organ transplant. *Cambridge quarterly of healthcare ethics : CQ : the international journal of healthcare ethics committees*. 1994;3(4):585-601.
28. Cooper DK. Clinical survey of heart transplantation between ABO blood group-incompatible recipients and donors. *J Heart Transplant*. 1990;9(4):376-81.
29. West LJ, Pollock-Barziv SM, Dipchand AI, Lee KJ, Cardella CJ, Benson LN, et al. ABO-incompatible heart transplantation in infants. *N Engl J Med*. 2001;344(11):793-800.
30. Urschel S, Larsen IM, Kirk R, Flett J, Burch M, Shaw N, et al. ABO-incompatible heart transplantation in early childhood: an international multicenter study of clinical experiences and limits. *J Heart Lung Transplant*. 2013;32(3):285-92.
31. Roche SL, Burch M, O'Sullivan J, Wallis J, Parry G, Kirk R, et al. Multicenter experience of ABO-incompatible pediatric cardiac transplantation. *Am J Transplant*. 2008;8(1):208-15.
32. Henderson HT, Canter CE, Mahle WT, Dipchand AI, LaPorte K, Schechtman KB, et al. ABO-incompatible heart transplantation: analysis of the Pediatric Heart Transplant Study (PHTS) database. *J Heart Lung Transplant*. 2012;31(2):173-9.
33. Owen RD. Immunogenetic Consequences of Vascular Anastomoses between Bovine Twins. *Science*. 1945;102(2651):400-1.

34. Burnet FM, Fenner F. The production of antibodies. 2d ed. Melbourne,: Macmillan; 1949. viii, 142 p. p.
35. Billingham RE, Brent L, Medawar PB. Actively acquired tolerance of foreign cells. *Nature*. 1953;172(4379):603-6.
36. Ramsdell F, Fowlkes BJ. Clonal deletion versus clonal anergy: the role of the thymus in inducing self tolerance. *Science*. 1990;248(4961):1342-8.
37. Zinkernagel RM, Hengartner H. Regulation of the immune response by antigen. *Science*. 2001;293(5528):251-3.
38. Anderson D, Billingham RE, Lampkin GH, Medawar PB. The use of skin grafting to distinguish between monozygotic and dizygotic twins in cattle. *Heredity*. 1951;5(3):379-97.
39. Lederberg J. Genes and antibodies. *Science*. 1959;129(3364):1649-53.
40. Billingham RE, Brent L, Medawar PB. The antigenic stimulus in transplantation immunity. *Nature*. 1956;178(4532):514-9.
41. Dorsch S, Roser B. Suppressor cells in transplantation tolerance. I. Analysis of the suppressor status of neonatally and adoptively tolerized rats. *Transplantation*. 1982;33(5):518-24.
42. Kappler JW, Roehm N, Marrack P. T cell tolerance by clonal elimination in the thymus. *Cell*. 1987;49(2):273-80.
43. Klinman NR. The "clonal selection hypothesis" and current concepts of B cell tolerance. *Immunity*. 1996;5(3):189-95.
44. McCarthy SA, Bach FH. The cellular mechanism of maintenance of neonatally induced tolerance to H-2 class I antigens. *Journal of immunology*. 1983;131(4):1676-82.
45. Ramsdell F, Lantz T, Fowlkes BJ. A nondeletional mechanism of thymic self tolerance. *Science*. 1989;246(4933):1038-41.
46. Streilein JW. Neonatal tolerance of H-2 alloantigens. Procuring graft acceptance the "old-fashioned" way. *Transplantation*. 1991;52(1):1-10.
47. West LJ. B-cell tolerance following ABO-incompatible infant heart transplantation. *Transplantation*. 2006;81(3):301-7.
48. Packard TA, Cambier JC. B lymphocyte antigen receptor signaling: initiation, amplification, and regulation. *F1000prime reports*. 2013;5:40.

49. Tonegawa S. [Molecular biology of immunologic recognition]. *Tanpakushitsu kakusan koso Protein, nucleic acid, enzyme*. 1987;32(3):239-50.
50. Brack C, Hirama M, Lenhard-Schuller R, Tonegawa S. A complete immunoglobulin gene is created by somatic recombination. *Cell*. 1978;15(1):1-14.
51. Pieper K, Grimbacher B, Eibel H. B-cell biology and development. *The Journal of allergy and clinical immunology*. 2013;131(4):959-71.
52. Benlagha K, Guglielmi P, Cooper MD, Lassoued K. Modifications of Igalpha and Igbeta expression as a function of B lineage differentiation. *The Journal of biological chemistry*. 1999;274(27):19389-96.
53. Ichii M, Oritani K, Kanakura Y. Early B lymphocyte development: Similarities and differences in human and mouse. *World journal of stem cells*. 2014;6(4):421-31.
54. Clatworthy MR. B cell responses to allograft--more common than we thought? *Am J Transplant*. 2013;13(7):1629-30.
55. MacLennan IC. Germinal centers. *Annual review of immunology*. 1994;12:117-39.
56. Kocks C, Rajewsky K. Stepwise intraclonal maturation of antibody affinity through somatic hypermutation. *Proceedings of the National Academy of Sciences of the United States of America*. 1988;85(21):8206-10.
57. Pasqualucci L, Migliazza A, Fracchiolla N, William C, Neri A, Baldini L, et al. BCL-6 mutations in normal germinal center B cells: evidence of somatic hypermutation acting outside Ig loci. *Proceedings of the National Academy of Sciences of the United States of America*. 1998;95(20):11816-21.
58. Li Z, Woo CJ, Iglesias-Ussel MD, Ronai D, Scharff MD. The generation of antibody diversity through somatic hypermutation and class switch recombination. *Genes Dev*. 2004;18(1):1-11.
59. Manis JP, Tian M, Alt FW. Mechanism and control of class-switch recombination. *Trends Immunol*. 2002;23(1):31-9.
60. Radbruch A, Muehlinghaus G, Luger EO, Inamine A, Smith KG, Dorner T, et al. Competence and competition: the challenge of becoming a long-lived plasma cell. *Nature reviews Immunology*. 2006;6(10):741-50.
61. Shapiro-Shelef M, Calame K. Regulation of plasma-cell development. *Nat Rev Immunol*. 2005;5(3):230-42.

62. Moser K, Tokoyoda K, Radbruch A, MacLennan I, Manzi RA. Stromal niches, plasma cell differentiation and survival. *Curr Opin Immunol*. 2006;18(3):265-70.
63. Liu YJ, Johnson GD, Gordon J, MacLennan IC. Germinal centres in T-cell-dependent antibody responses. *Immunol Today*. 1992;13(1):17-21.
64. Agematsu K, Hokibara S, Nagumo H, Komiyama A. CD27: a memory B-cell marker. *Immunology today*. 2000;21(5):204-6.
65. Agematsu K, Nagumo H, Oguchi Y, Nakazawa T, Fukushima K, Yasui K, et al. Generation of plasma cells from peripheral blood memory B cells: synergistic effect of interleukin-10 and CD27/CD70 interaction. *Blood*. 1998;91(1):173-80.
66. Cerutti A, Cols M, Puga I. Marginal zone B cells: virtues of innate-like antibody-producing lymphocytes. *Nat Rev Immunol*. 2013;13(2):118-32.
67. Weller S, Braun MC, Tan BK, Rosenwald A, Cordier C, Conley ME, et al. Human blood IgM "memory" B cells are circulating splenic marginal zone B cells harboring a prediversified immunoglobulin repertoire. *Blood*. 2004;104(12):3647-54.
68. Tangye SG. To B1 or not to B1: that really is still the question! *Blood*. 2013;121(26):5109-10.
69. Montecino-Rodriguez E, Dorshkind K. B-1 B cell development in the fetus and adult. *Immunity*. 2012;36(1):13-21.
70. Bhat NM, Mithal A, Bieber MM, Herzenberg LA, Teng NN. Human CD5+ B lymphocytes (B-1 cells) decrease in peripheral blood during pregnancy. *J Reprod Immunol*. 1995;28(1):53-60.
71. Donze HH, Lue C, Julian BA, Kutteh WH, Kantele A, Mestecky J. Human peritoneal B-1 cells and the influence of continuous ambulatory peritoneal dialysis on peritoneal and peripheral blood mononuclear cell (PBMC) composition and immunoglobulin levels. *Clin Exp Immunol*. 1997;109(2):356-61.
72. Griffin DO, Holodick NE, Rothstein TL. Human B1 cells in umbilical cord and adult peripheral blood express the novel phenotype CD20+ CD27+ CD43+ CD70. *The Journal of experimental medicine*. 2011;208(1):67-80.
73. van Gent R, van Tilburg CM, Nibbelke EE, Otto SA, Gaiser JF, Janssens-Korpela PL, et al. Refined characterization and reference values of the pediatric T- and B-cell compartments. *Clinical immunology*. 2009;133(1):95-107.

74. Parker DC. T cell-dependent B cell activation. Annual review of immunology. 1993;11:331-60.
75. Dintzis HM, Dintzis RZ, Vogelstein B. Molecular determinants of immunogenicity: the immunon model of immune response. Proceedings of the National Academy of Sciences of the United States of America. 1976;73(10):3671-5.
76. Lesinski GB, Westerink MA. Novel vaccine strategies to T-independent antigens. Journal of microbiological methods. 2001;47(2):135-49.
77. Campbell KS, Cambier JC. B lymphocyte antigen receptors (mIg) are non-covalently associated with a disulfide linked, inducibly phosphorylated glycoprotein complex. The EMBO journal. 1990;9(2):441-8.
78. Gold MR, Matsuuchi L, Kelly RB, DeFranco AL. Tyrosine phosphorylation of components of the B-cell antigen receptors following receptor crosslinking. Proceedings of the National Academy of Sciences of the United States of America. 1991;88(8):3436-40.
79. Hombach J, Tsubata T, Leclercq L, Stappert H, Reth M. Molecular components of the B-cell antigen receptor complex of the IgM class. Nature. 1990;343(6260):760-2.
80. Clatworthy MR. B-cell regulation and its application to transplantation. Transpl Int. 2014;27(2):117-28.
81. Weber M, Treanor B, Depoil D, Shinohara H, Harwood NE, Hikida M, et al. Phospholipase C-gamma2 and Vav cooperate within signaling microclusters to propagate B cell spreading in response to membrane-bound antigen. The Journal of experimental medicine. 2008;205(4):853-68.
82. Ransom JT, Harris LK, Cambier JC. Anti-Ig induces release of inositol 1,4,5-trisphosphate, which mediates mobilization of intracellular Ca⁺⁺ stores in B lymphocytes. Journal of immunology. 1986;137(2):708-14.
83. Coggeshall KM, Cambier JC. B cell activation. VIII. Membrane immunoglobulins transduce signals via activation of phosphatidylinositol hydrolysis. Journal of immunology. 1984;133(6):3382-6.
84. Penna A, Demuro A, Yeromin AV, Zhang SL, Safrina O, Parker I, et al. The CRAC channel consists of a tetramer formed by Stim-induced dimerization of Orai dimers. Nature. 2008;456(7218):116-20.

85. Hogan PG, Lewis RS, Rao A. Molecular basis of calcium signaling in lymphocytes: STIM and ORAI. *Annual review of immunology*. 2010;28:491-533.
86. Roozendaal R, Carroll MC. Complement receptors CD21 and CD35 in humoral immunity. *Immunological reviews*. 2007;219:157-66.
87. Carter RH, Fearon DT. CD19: lowering the threshold for antigen receptor stimulation of B lymphocytes. *Science*. 1992;256(5053):105-7.
88. Basten A, Silveira PA. B-cell tolerance: mechanisms and implications. *Current opinion in immunology*. 2010;22(5):566-74.
89. Nemazee D, Buerki K. Clonal deletion of autoreactive B lymphocytes in bone marrow chimeras. *Proceedings of the National Academy of Sciences of the United States of America*. 1989;86(20):8039-43.
90. Halverson R, Torres RM, Pelanda R. Receptor editing is the main mechanism of B cell tolerance toward membrane antigens. *Nature immunology*. 2004;5(6):645-50.
91. Rui L, Vinuesa CG, Blasioli J, Goodnow CC. Resistance to CpG DNA-induced autoimmunity through tolerogenic B cell antigen receptor ERK signaling. *Nature immunology*. 2003;4(6):594-600.
92. Pasare C, Medzhitov R. Toll-like receptors: linking innate and adaptive immunity. *Advances in experimental medicine and biology*. 2005;560:11-8.
93. Fischer MB, Ma M, Goerg S, Zhou X, Xia J, Finco O, et al. Regulation of the B cell response to T-dependent antigens by classical pathway complement. *Journal of immunology*. 1996;157(2):549-56.
94. Parsons RF, Vivek K, Redfield RR, 3rd, Migone TS, Cancro MP, Naji A, et al. B-lymphocyte homeostasis and BlyS-directed immunotherapy in transplantation. *Transplantation reviews*. 2010;24(4):207-21.
95. Scholz JL, Crowley JE, Tomayko MM, Steinel N, O'Neill PJ, Quinn WJ, 3rd, et al. BlyS inhibition eliminates primary B cells but leaves natural and acquired humoral immunity intact. *Proceedings of the National Academy of Sciences of the United States of America*. 2008;105(40):15517-22.
96. Neron S, Lemieux R. CD5+ B cell-dependent regulation of the murine T-cell independent immune response against the human blood group A antigen. *Immunological investigations*. 1997;26(5-7):631-47.

97. Irei T, Ohdan H, Zhou W, Ishiyama K, Tanaka Y, Ide K, et al. The persistent elimination of B cells responding to blood group A carbohydrates by synthetic group A carbohydrates and B-1 cell differentiation blockade: novel concept in preventing antibody-mediated rejection in ABO-incompatible transplantation. *Blood*. 2007;110(13):4567-75.
98. Samardzic T, Marinkovic D, Danzer CP, Gerlach J, Nitschke L, Wirth T. Reduction of marginal zone B cells in CD22-deficient mice. *Eur J Immunol*. 2002;32(2):561-7.
99. Ghosh S, Bandulet C, Nitschke L. Regulation of B cell development and B cell signalling by CD22 and its ligands alpha2,6-linked sialic acids. *Int Immunol*. 2006;18(4):603-11.
100. von Gunten S, Bochner BS. Basic and clinical immunology of Siglecs. *Ann N Y Acad Sci*. 2008;1143:61-82.
101. Crocker PR, Paulson JC, Varki A. Siglecs and their roles in the immune system. *Nat Rev Immunol*. 2007;7(4):255-66.
102. Paulson JC, Macauley MS, Kawasaki N. Siglecs as sensors of self in innate and adaptive immune responses. *Ann N Y Acad Sci*. 2012;1253:37-48.
103. Poe JC, Fujimoto Y, Hasegawa M, Haas KM, Miller AS, Sanford IG, et al. CD22 regulates B lymphocyte function in vivo through both ligand-dependent and ligand-independent mechanisms. *Nat Immunol*. 2004;5(10):1078-87.
104. Tedder TF, Tuscano J, Sato S, Kehrl JH. CD22, a B lymphocyte-specific adhesion molecule that regulates antigen receptor signaling. *Annual review of immunology*. 1997;15:481-504.
105. Erickson LD, Tygrett LT, Bhatia SK, Grabstein KH, Waldschmidt TJ. Differential expression of CD22 (Lyb8) on murine B cells. *International immunology*. 1996;8(7):1121-9.
106. Sherbina NV, Linsley PS, Myrdal S, Grosmaire LS, Ledbetter JA, Schieven GL. Intracellular CD22 rapidly moves to the cell surface in a tyrosine kinase-dependent manner following antigen receptor stimulation. *J Immunol*. 1996;157(10):4390-8.
107. Chaouchi N, Vazquez A, Galanaud P, Leprince C. B cell antigen receptor-mediated apoptosis. Importance of accessory molecules CD19 and CD22, and of surface IgM cross-linking. *J Immunol*. 1995;154(7):3096-104.

108. Torres RM, Law CL, Santos-Argumedo L, Kirkham PA, Grabstein K, Parkhouse RM, et al. Identification and characterization of the murine homologue of CD22, a B lymphocyte-restricted adhesion molecule. *Journal of immunology*. 1992;149(8):2641-9.
109. Stoddart A, Ray RJ, Paige CJ. Analysis of murine CD22 during B cell development: CD22 is expressed on B cell progenitors prior to IgM. *International immunology*. 1997;9(10):1571-9.
110. Hoffmann A, Kerr S, Jellusova J, Zhang J, Weisel F, Wellmann U, et al. Siglec-G is a B1 cell-inhibitory receptor that controls expansion and calcium signaling of the B1 cell population. *Nat Immunol*. 2007;8(7):695-704.
111. Ding C, Liu Y, Wang Y, Park BK, Wang CY, Zheng P. SiglecG limits the size of B1a B cell lineage by down-regulating NFkappaB activation. *PLoS One*. 2007;2(10):e997.
112. Munday J, Kerr S, Ni J, Cornish AL, Zhang JQ, Nicoll G, et al. Identification, characterization and leucocyte expression of Siglec-10, a novel human sialic acid-binding receptor. *Biochem J*. 2001;355(Pt 2):489-97.
113. Pfrenge F, Macauley MS, Kawasaki N, Paulson JC. Copresentation of antigen and ligands of Siglec-G induces B cell tolerance independent of CD22. *J Immunol*. 2013;191(4):1724-31.
114. Collins BE, Blixt O, Han S, Duong B, Li H, Nathan JK, et al. High-affinity ligand probes of CD22 overcome the threshold set by cis ligands to allow for binding, endocytosis, and killing of B cells. *J Immunol*. 2006;177(5):2994-3003.
115. Kelm S, Pelz A, Schauer R, Filbin MT, Tang S, de Bellard ME, et al. Sialoadhesin, myelin-associated glycoprotein and CD22 define a new family of sialic acid-dependent adhesion molecules of the immunoglobulin superfamily. *Curr Biol*. 1994;4(11):965-72.
116. Powell LD, SgROI D, Sjoberg ER, Stamenkovic I, Varki A. Natural ligands of the B cell adhesion molecule CD22 beta carry N-linked oligosaccharides with alpha-2,6-linked sialic acids that are required for recognition. *J Biol Chem*. 1993;268(10):7019-27.
117. Powell LD, Varki A. The oligosaccharide binding specificities of CD22 beta, a sialic acid-specific lectin of B cells. *J Biol Chem*. 1994;269(14):10628-36.
118. Hanasaki K, Powell LD, Varki A. Binding of human plasma sialoglycoproteins by the B cell-specific lectin CD22. Selective recognition of immunoglobulin M and haptoglobin. *J Biol Chem*. 1995;270(13):7543-50.

119. Adachi T, Harumiya S, Takematsu H, Kozutsumi Y, Wabl M, Fujimoto M, et al. CD22 serves as a receptor for soluble IgM. *Eur J Immunol.* 2012;42(1):241-7.
120. Kashani-Sabet M, Venna S, Nosrati M, Rangel J, Sucker A, Egberts F, et al. A multimarker prognostic assay for primary cutaneous melanoma. *Clinical cancer research : an official journal of the American Association for Cancer Research.* 2009;15(22):6987-92.
121. Hanasaki K, Varki A, Stamenkovic I, Bevilacqua MP. Cytokine-induced beta-galactoside alpha-2,6-sialyltransferase in human endothelial cells mediates alpha 2,6-sialylation of adhesion molecules and CD22 ligands. *J Biol Chem.* 1994;269(14):10637-43.
122. Stamatou NM, Curreli S, Zella D, Cross AS. Desialylation of glycoconjugates on the surface of monocytes activates the extracellular signal-related kinases ERK 1/2 and results in enhanced production of specific cytokines. *J Leukoc Biol.* 2004;75(2):307-13.
123. Aminoff D, Bruegge WF, Bell WC, Sarpolis K, Williams R. Role of sialic acid in survival of erythrocytes in the circulation: interaction of neuraminidase-treated and untreated erythrocytes with spleen and liver at the cellular level. *Proc Natl Acad Sci U S A.* 1977;74(4):1521-4.
124. Collins BE, Blixt O, DeSieno AR, Bovin N, Marth JD, Paulson JC. Masking of CD22 by cis ligands does not prevent redistribution of CD22 to sites of cell contact. *Proc Natl Acad Sci U S A.* 2004;101(16):6104-9.
125. Kitagawa H, Paulson JC. Differential expression of five sialyltransferase genes in human tissues. *J Biol Chem.* 1994;269(27):17872-8.
126. Muller J, Obermeier I, Wohner M, Brandl C, Mrotzek S, Angermuller S, et al. CD22 ligand-binding and signaling domains reciprocally regulate B-cell Ca²⁺ signaling. *Proceedings of the National Academy of Sciences of the United States of America.* 2013;110(30):12402-7.
127. Walker JA, Smith KG. CD22: an inhibitory enigma. *Immunology.* 2008;123(3):314-25.
128. Danzer CP, Collins BE, Blixt O, Paulson JC, Nitschke L. Transitional and marginal zone B cells have a high proportion of unmasked CD22: implications for BCR signaling. *Int Immunol.* 2003;15(10):1137-47.

129. Courtney AH, Puffer EB, Pontrello JK, Yang ZQ, Kiessling LL. Sialylated multivalent antigens engage CD22 in trans and inhibit B cell activation. *Proceedings of the National Academy of Sciences of the United States of America*. 2009;106(8):2500-5.
130. Nitschke L, Carsetti R, Ocker B, Kohler G, Lamers MC. CD22 is a negative regulator of B-cell receptor signalling. *Curr Biol*. 1997;7(2):133-43.
131. O'Keefe TL, Williams GT, Davies SL, Neuberger MS. Hyperresponsive B cells in CD22-deficient mice. *Science*. 1996;274(5288):798-801.
132. Otipoby KL, Andersson KB, Draves KE, Klaus SJ, Farr AG, Kerner JD, et al. CD22 regulates thymus-independent responses and the lifespan of B cells. *Nature*. 1996;384(6610):634-7.
133. Sato S, Miller AS, Inaoki M, Bock CB, Jansen PJ, Tang ML, et al. CD22 is both a positive and negative regulator of B lymphocyte antigen receptor signal transduction: altered signaling in CD22-deficient mice. *Immunity*. 1996;5(6):551-62.
134. Peaker CJ, Neuberger MS. Association of CD22 with the B cell antigen receptor. *European journal of immunology*. 1993;23(6):1358-63.
135. Nitschke L. CD22 and Siglec-G: B-cell inhibitory receptors with distinct functions. *Immunol Rev*. 2009;230(1):128-43.
136. Smith KG, Tarlinton DM, Doody GM, Hibbs ML, Fearon DT. Inhibition of the B cell by CD22: a requirement for Lyn. *J Exp Med*. 1998;187(5):807-11.
137. Blasioli J, Paust S, Thomas ML. Definition of the sites of interaction between the protein tyrosine phosphatase SHP-1 and CD22. *J Biol Chem*. 1999;274(4):2303-7.
138. Gagneux P, Varki A. Evolutionary considerations in relating oligosaccharide diversity to biological function. *Glycobiology*. 1999;9(8):747-55.
139. Poe JC, Tedder TF. CD22 and Siglec-G in B cell function and tolerance. *Trends Immunol*. 2012;33(8):413-20.
140. Severi E, Hood DW, Thomas GH. Sialic acid utilization by bacterial pathogens. *Microbiology*. 2007;153(Pt 9):2817-22.
141. O'Keefe TL, Williams GT, Batista FD, Neuberger MS. Deficiency in CD22, a B cell-specific inhibitory receptor, is sufficient to predispose to development of high affinity autoantibodies. *J Exp Med*. 1999;189(8):1307-13.

142. Mary C, Laporte C, Parzy D, Santiago ML, Stefani F, Lajaunias F, et al. Dysregulated expression of the Cd22 gene as a result of a short interspersed nucleotide element insertion in Cd22a lupus-prone mice. *J Immunol.* 2000;165(6):2987-96.
143. Law CL, Torres RM, Sundberg HA, Parkhouse RM, Brannan CI, Copeland NG, et al. Organization of the murine Cd22 locus. Mapping to chromosome 7 and characterization of two alleles. *J Immunol.* 1993;151(1):175-87.
144. Nitschke L, Lajaunias F, Moll T, Ho L, Martinez-Soria E, Kikuchi S, et al. Expression of aberrant forms of CD22 on B lymphocytes in Cd22a lupus-prone mice affects ligand binding. *Int Immunol.* 2006;18(1):59-68.
145. Chan VW, Meng F, Soriano P, DeFranco AL, Lowell CA. Characterization of the B lymphocyte populations in Lyn-deficient mice and the role of Lyn in signal initiation and down-regulation. *Immunity.* 1997;7(1):69-81.
146. Sjoberg ER, Powell LD, Klein A, Varki A. Natural ligands of the B cell adhesion molecule CD22 beta can be masked by 9-O-acetylation of sialic acids. *J Cell Biol.* 1994;126(2):549-62.
147. Cariappa A, Takematsu H, Liu H, Diaz S, Haider K, Boboila C, et al. B cell antigen receptor signal strength and peripheral B cell development are regulated by a 9-O-acetyl sialic acid esterase. *J Exp Med.* 2009;206(1):125-38.
148. Klein G, Zeuthen J, Terasaki P, Billing R, Honig R, Jondal M, et al. Inducibility of the Epstein-Barr virus (EBV) cycle and surface marker properties of EBV-negative lymphoma lines and their in vitro EBV-converted sublines. *Int J Cancer.* 1976;18(5):639-52.
149. Klein G, Giovanella B, Westman A, Stehlin JS, Mumford D. An EBV-genome-negative cell line established from an American Burkitt lymphoma; receptor characteristics. EBV infectibility and permanent conversion into EBV-positive sublines by in vitro infection. *Intervirology.* 1975;5(6):319-34.
150. Morbach H, Eichhorn EM, Liese JG, Girschick HJ. Reference values for B cell subpopulations from infancy to adulthood. *Clin Exp Immunol.* 2010;162(2):271-9.
151. Sims GP, Ettinger R, Shirota Y, Yarboro CH, Illei GG, Lipsky PE. Identification and characterization of circulating human transitional B cells. *Blood.* 2005;105(11):4390-8.

152. Huggins J, Pellegrin T, Felgar RE, Wei C, Brown M, Zheng B, et al. CpG DNA activation and plasma-cell differentiation of CD27- naive human B cells. *Blood*. 2007;109(4):1611-9.
153. Henn AD, Laski M, Yang H, Welle S, Qiu X, Miao H, et al. Functionally Distinct Subpopulations of CpG-Activated Memory B Cells. *Scientific reports*. 2012;2:345.
154. Blixt O, Han S, Liao L, Zeng Y, Hoffmann J, Futakawa S, et al. Sialoside analogue arrays for rapid identification of high affinity siglec ligands. *Journal of the American Chemical Society*. 2008;130(21):6680-1.
155. Piatosa B, Wolska-Kusnierz B, Pac M, Siewiera K, Galkowska E, Bernatowska E. B cell subsets in healthy children: reference values for evaluation of B cell maturation process in peripheral blood. *Cytometry Part B, Clinical cytometry*. 2010;78(6):372-81.
156. Osmond DG. Population dynamics of bone marrow B lymphocytes. *Immunol Rev*. 1986;93:103-24.
157. Caraux A, Klein B, Paiva B, Bret C, Schmitz A, Fuhler GM, et al. Circulating human B and plasma cells. Age-associated changes in counts and detailed characterization of circulating normal CD138- and CD138+ plasma cells. *Haematologica*. 2010;95(6):1016-20.
158. Amanna IJ, Slifka MK. Quantitation of rare memory B cell populations by two independent and complementary approaches. *Journal of immunological methods*. 2006;317(1-2):175-85.
159. Galili U. Anti-Gal: an abundant human natural antibody of multiple pathogeneses and clinical benefits. *Immunology*. 2013;140(1):1-11.
160. Krutzik PO, Irish JM, Nolan GP, Perez OD. Analysis of protein phosphorylation and cellular signaling events by flow cytometry: techniques and clinical applications. *Clinical immunology*. 2004;110(3):206-21.
161. Azuma Y, Sakanashi M, Matsumoto K. The effect of alpha2,6-linked sialic acid on anti-IgM antibody-induced apoptosis in Ramos cells. *Glycoconj J*. 2001;18(5):419-24.
162. Kitanaka A, Mano H, Conley ME, Campana D. Expression and activation of the nonreceptor tyrosine kinase Tec in human B cells. *Blood*. 1998;91(3):940-8.
163. Oksvold MP, Kullmann A, Forfang L, Kierulf B, Li M, Brech A, et al. Expression of B-cell surface antigens in subpopulations of exosomes released from B-cell lymphoma cells. *Clin Ther*. 2014;36(6):847-62 e1.

164. Prasad KV, Ao Z, Yoon Y, Wu MX, Rizk M, Jacquot S, et al. CD27, a member of the tumor necrosis factor receptor family, induces apoptosis and binds to Siva, a proapoptotic protein. *Proc Natl Acad Sci U S A*. 1997;94(12):6346-51.
165. Irish JM, Czerwinski DK, Nolan GP, Levy R. Kinetics of B cell receptor signaling in human B cell subsets mapped by phosphospecific flow cytometry. *J Immunol*. 2006;177(3):1581-9.
166. Irish JM, Myklebust JH, Alizadeh AA, Houot R, Sharman JP, Czerwinski DK, et al. B-cell signaling networks reveal a negative prognostic human lymphoma cell subset that emerges during tumor progression. *Proc Natl Acad Sci U S A*. 2010;107(29):12747-54.
167. Leprince C, Draves KE, Geahlen RL, Ledbetter JA, Clark EA. CD22 associates with the human surface IgM-B-cell antigen receptor complex. *Proc Natl Acad Sci U S A*. 1993;90(8):3236-40.
168. Sanjuan MA, Rao N, Lai KT, Gu Y, Sun S, Fuchs A, et al. CpG-induced tyrosine phosphorylation occurs via a TLR9-independent mechanism and is required for cytokine secretion. *The Journal of cell biology*. 2006;172(7):1057-68.
169. Kelm S, Gerlach J, Brossmer R, Danzer CP, Nitschke L. The ligand-binding domain of CD22 is needed for inhibition of the B cell receptor signal, as demonstrated by a novel human CD22-specific inhibitor compound. *J Exp Med*. 2002;195(9):1207-13.
170. Muller J, Nitschke L. The role of CD22 and Siglec-G in B-cell tolerance and autoimmune disease. *Nat Rev Rheumatol*. 2014;10(7):422-8.
171. Mihaylova N, Voynova E, Tchorbanov A, Dolashka-Angelova P, Bayry J, Devreese B, et al. Simultaneous engagement of FcγIIb and CD22 inhibitory receptors silences targeted B cells and suppresses autoimmune disease activity. *Mol Immunol*. 2009;47(1):123-30.
172. Weill JC, Weller S, Reynaud CA. Human marginal zone B cells. *Annu Rev Immunol*. 2009;27:267-85.
173. Wirths S, Lanzavecchia A. ABCB1 transporter discriminates human resting naive B cells from cycling transitional and memory B cells. *Eur J Immunol*. 2005;35(12):3433-41.
174. Viemann D, Schlenke P, Hammers HJ, Kirchner H, Kruse A. Differential expression of the B cell-restricted molecule CD22 on neonatal B lymphocytes depending upon antigen stimulation. *Eur J Immunol*. 2000;30(2):550-9.

175. Crotty S, Aubert RD, Glidewell J, Ahmed R. Tracking human antigen-specific memory B cells: a sensitive and generalized ELISPOT system. *J Immunol Methods*. 2004;286(1-2):111-22.
176. Zhang W, Caspell R, Karulin AY, Ahmad M, Haicheur N, Abdelsalam A, et al. ELISPOT assays provide reproducible results among different laboratories for T-cell immune monitoring--even in hands of ELISPOT-inexperienced investigators. *J Immunotoxicol*. 2009;6(4):227-34.
177. Ruprecht CR, Lanzavecchia A. Toll-like receptor stimulation as a third signal required for activation of human naive B cells. *Eur J Immunol*. 2006;36(4):810-6.
178. Dolmetsch RE, Lewis RS, Goodnow CC, Healy JI. Differential activation of transcription factors induced by Ca²⁺ response amplitude and duration. *Nature*. 1997;386(6627):855-8.
179. Razi N, Varki A. Cryptic sialic acid binding lectins on human blood leukocytes can be unmasked by sialidase treatment or cellular activation. *Glycobiology*. 1999;9(11):1225-34.
180. Nitschke L, Floyd H, Ferguson DJ, Crocker PR. Identification of CD22 ligands on bone marrow sinusoidal endothelium implicated in CD22-dependent homing of recirculating B cells. *The Journal of experimental medicine*. 1999;189(9):1513-8.
181. Chen WC, Sigal DS, Saven A, Paulson JC. Targeting B lymphoma with nanoparticles bearing glycan ligands of CD22. *Leuk Lymphoma*. 2012;53(2):208-10.

APPENDIX A

PPF assays in isolated splenic CD27⁺IgM⁺ and CD27-IgM⁺ B cells

The PPF assay was performed on adult CD27⁺IgM⁺ and CD27-IgM⁺ B cells following isolation by FACS and overnight culture at 37°C. Our findings show that the PPF assay can be successfully performed on primary isolated human B cells. However, further studies are necessary to directly compare the differences in the signaling kinetics between infant and adult B cells.

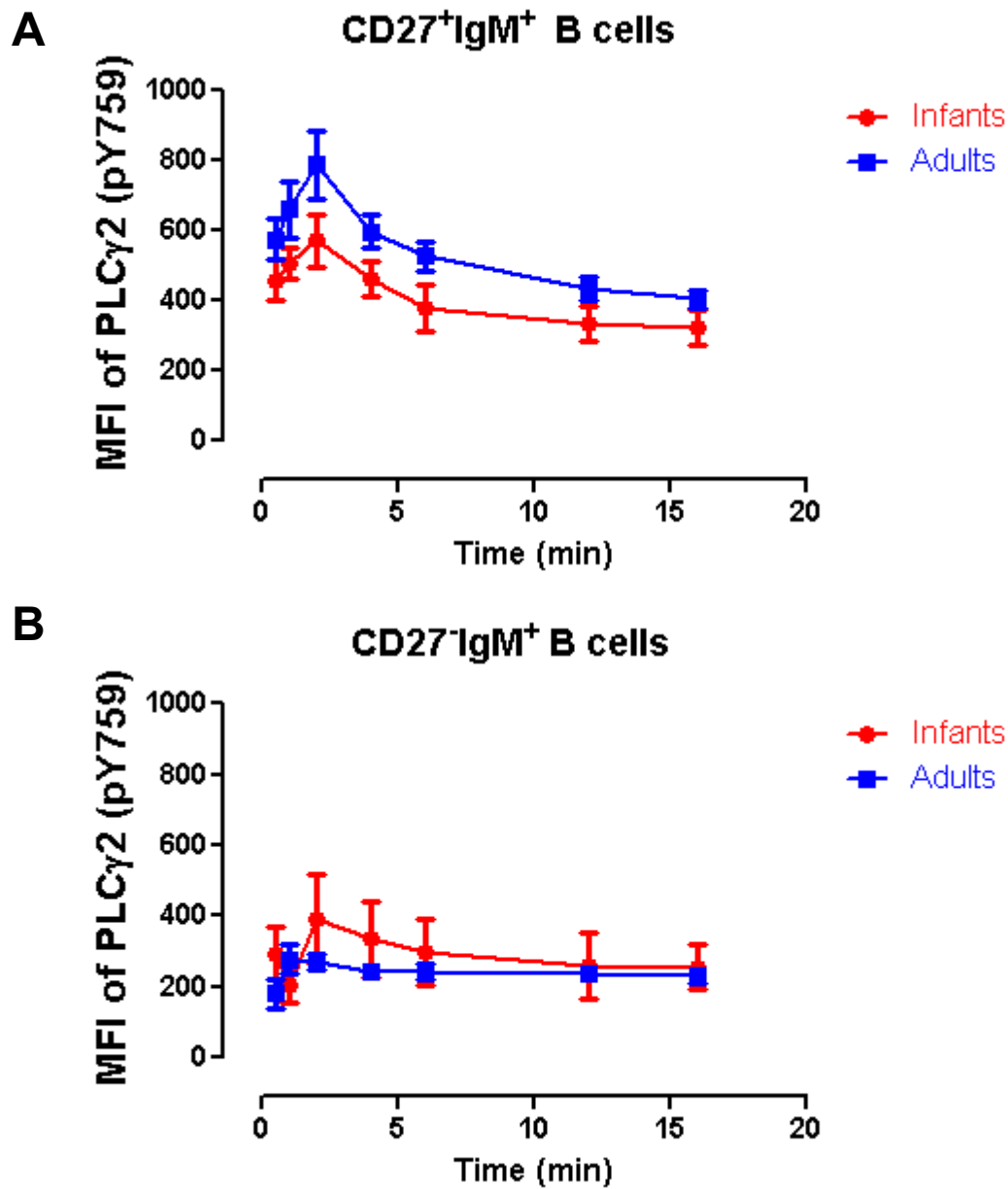


Figure A-1. PPF assay in primary CD27⁺IgM⁺ and CD27-IgM⁺ B cells. Primary cells were stimulated with 10 μ g/ml anti-IgM (affinipure F(ab')₂ fragment goat-anti human IgM) for the duration of the indicated time points (section 2.7.2). The signaling kinetics of primary cells is presented as the MFI of PLC γ 2 (pY759). Median and standard error are shown. Data represent six experiments (3 infant samples and 3 adult samples).

APPENDIX B

Proposed model for engaging CD22 in *trans* using CD22L and anti-IgM coated SaV

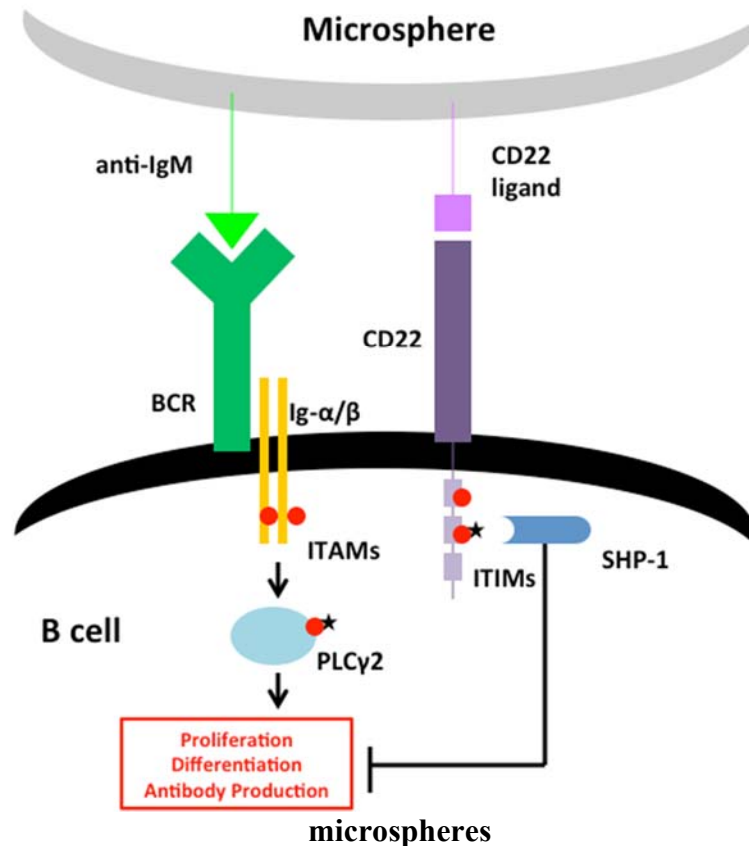


Figure B-1. A proposed model for the inhibition of the B cell signal by the engagement of CD22L and anti-IgM coated microspheres. BCR signaling is initiated by binding of anti-IgM and subsequent phosphorylation of immunoreceptor tyrosine-based activation motifs (ITAMs) located within the cytoplasmic tails of Ig α and Ig β . As CD22L is in close association with anti-IgM Ab on the microsphere this results in the binding of the BCR to anti-IgM Ab and also CD22 to its ligand resulting in diminished B cell activation (including decreased proliferation, differentiation and antibody production). Red circles represent phosphorylation. Phosphorylated proteins to be assessed in PPF assays are PLC γ 2 and pCD22, represented by black stars.